**Republic of Iraq**
**Ministry of Higher Education & Scientific Research**
**University of Babylon**
**College of Education for Pure Sciences**
**Department of Physics**

# Effect of Copper Nanowire on Structural and Optical Properties of PVA-PAAm Blend

A Thesis
Submitted to the Council of the College of Education for Pure Sciences, University of Babylon in Partial Fulfillment of the Requirements for the Degree of Master in Education / Physics

By

**Zainab Mohammed Jawad Jawad kadhim**

B. E. Sc. ( Physics)
(University of Babylon 2014)

Supervised by

**Prof. Khalid Haneen Abass, (Ph.D.)**

**2022 A.D.** **1443 A.H.**

بسم الله الرحمن الرحيم

﴿ آتُونِي زُبَرَ الْحَدِيدِ ۖ حَتَّىٰ إِذَا سَاوَىٰ بَيْنَ الصَّدَفَيْنِ قَالَ انفُخُوا ۖ حَتَّىٰ إِذَا جَعَلَهُ نَارًا قَالَ آتُونِي أُفْرِغْ عَلَيْهِ قِطْرًا ﴾

صدق الله العلي العظيم

سورة الكهف ٩٦

# Dedication

***To who gave me the endurance to complete my road my father***

***To the best woman in the universe my mother***

***To my brother and sister***

***To my supervisor, Prof. Khaled Haneen Abbas***

***To my close friends***

***and***

***Everyone who has helped me …***

***With my Respect***

*Zainab ..✍*

# Acknowledgements

*In the name of Allah the Merciful. I thank God, Lord of Earth and Heaven, for completing my research. I would like to express my thanks and gratitude to my supervisor (**Dr. Khalid Haneen Abass** ) for suggesting this topic to me and for his distinguished efforts, advice and sound guidance that helped alleviate all the difficulties I encountered during my work.*

*Thank you to the Deanship of the College of Education for Pure Sciences / University of Babylon and the Department of Physics for giving me this opportunity to complete my research. I also would like to express my grateful thanks to all lecturers, instructors, and students of the Department of Physics for their assistance.*

*Finally, many thanks go to those who support me and alleviate difficulties I have faced during my work and to everyone who helped me in a way or another during my preparation of this thesis, especially Mohammed Abd-ALKadhim and Yousif H. Abdul Hussain. Apologize for whom I miss mentioning. I wish success to all.*

*Zainab ..✍*

# Summary

The nanocomposites PVA-PAAm:CuNW were prepared by casting method with different thicknesses (120, 90) μm and different weight percentages (0.5, 1, 2) of CuNW additive at a temperature of 70 $^{o}$C. The morphology and structural, optical properties, also dispersion parameters of nanocomposites were studied. The results of the optical microscopy photos show the good distribution of CuNW inside the polymer blends for all nanocomposite films. Scanning electron microscopy (SEM) showed uniform morphology revealing a rather soft surface, and the increase of the ratio of CuNW in a polymer matrix for the PVA-PAAm:CuNW nanocomposites led to changes in the morphology of the surface and increase the roughness. The results of the FTIR spectrum of the nanostructure showed a change in the peak position as well as a change in the shape and density compared to a PVA-PAAm blend. The results of the optical properties of PVA-PAAm:CuNW nanocomposites showed that the absorbance, absorption coefficient, extinction coefficient, refractive index, optical conductivity, real and imaginary dielectric constants increase with the increased concentrations of CuNW, while the transmittance and optical energy gap of allowed indirect transition decreased. The PVA-PAAm:CuNW nanocomposites have high absorbance in the UV-region.

The dispersion parameters such as; $E_o$, $E_d$, $n_o$, $\varepsilon_\infty$, $M_{-1}$, $M_{-3}$ were calculated using the Wemple–DiDomenico model. The value of the energy gap estimated by Wemple–DiDomenico calculations was consistent with the value of the optical energy gap obtained from the Tauc relation.

The effect of thickness change was also studied and the results showed that the change in film thickness had a slight effect on the structural and optical properties.

| List of symbols and Abbreviations | |
|---|---|
| Symbol | **Physical Meanings** |
| $\alpha$ | **Absorption Coefficient** |
| **A** | **Absorbance** |
| **C.B** | **Conduction Band** |
| **CuNW** | **Copper Nanowire** |
| **E** | **Energy** |
| $\varepsilon$ | **Complex Dielectric Constant** |
| $\varepsilon_1$ | **The Real Part of The Dielectric Constant** |
| $\varepsilon_2$ | **The Imaginary Part of The Dielectric Constant** |
| $E_d$ | **Dispersion Energy** |
| $E_g$ | **Energy Gap** |
| $E_o$ | **The Energy of The Effective Single Oscillator** |
| $E_{ph}$ | **Energy of Phonon** |
| $\varepsilon_\infty$ | **Static Dielectric Constant** |
| **FTIR** | **Fourier Transform Infrared Spectroscopy** |
| **h** | **Planck Constant** |
| **hν** | **The Photon Energy** |
| $I_o$ | **The Incident Intensity of Light** |
| $I_T$ | **The Intensity of Ray Transmittance** |
| $k_o$ | **Extinction Coefficient** |
| $(M_{-1}, M_{-3})$ | **Moments of Optical Spectra** |
| **MW** | **Molecular Weights** |
| **n** | **Refractive Index** |
| **N** | **Complex Refractive Index** |
| $n_o(0)$ | **Static Refractive Index** |
| **OM** | **Optical Microscopy** |
| **PAAm** | **Poly Acrylamide** |
| **PVA** | **Polyvinyl Alcohol** |

| | |
|---|---|
| **R** | **Reflectance** |
| **SEM** | **Scanning Electron Microscopy** |
| **T** | **Transmittance** |
| **t** | **The Thickness of The Film** |
| **$T_g$** | **Glass Transition Temperature** |
| **$T_m$** | **Melting Temperature** |
| **UV** | **Ultraviolet Spectrum** |
| **V.B** | **Valence Band** |
| **WDD** | **Wemple–DiDomenico** |
| **$\lambda$** | **The Wavelength** |
| **$\sigma_{op}$** | **Optical Conductivity** |

# Chapter One

## Introduction and Literature Review

## 1.1 Introduction

In recent years, the use of most polymers was limited to the manufacture of cheap products which were used for simple purposes. However, the speedy technical development has required the replacement of some materials being used in industry with others having better specifications; consequently, polymers have replaced iron and aluminum for some purposes that require high temperature and stress [1].

Polymer composites have unrivaled properties like light weight, high flexibility, and possibility to be produced at low temperature and low cost [2]. The polymers can be divided into two denominations: industrial and natural. The natural polymers include proteins, cellulose, starches and rubber, either the industrial polymers include poly(vinyl chloride), polypropylene, nylons polyethylene, Polyvinyl Alcohol, Polyacrylamide and polyesters polycarbonate, etc.[3]. Over the past few years, a little word with big potential has been rapidly insinuating itself into the world's consciousness, that word is "Nano". Nanotechnology is one of the leading scientific fields today since it combines knowledge from the fields of physics, chemistry, biology, medicine, informatics, and engineering. It is an emerging technological field with great potential to lead in great breakthroughs that can be applied in real life. Nanotechnology tools and techniques enable the fabrication and control of new nano and biomaterials, as well as nanodevices [4].

Nanotechnology, often known as nanoscale science, is the study of matter at the nanoscale, which is defined as the range of (1 to 100) nm. A breakthrough in academic and industrial interest in these nanomaterials over the past 10 years has been of interest due to the remarkable differences in solid-state properties. In Greek, "Nano" means little man,

while the SI unit "Nano" corresponds to ($10^{-9}$ m) magnitudes, such as nanometers, nanoliters, nanograms [5].

The nanosciences have attracted a lot of interest for a number of reasons. Among them, the very large surface to volume ratio showed by many nanoscaled materials opened novel possibilities in surface-based science, such as heterogeneous catalysis [6].

Moreover, it has been discovered that the properties of materials change as their size approaches the nanoscale, or when a portion of certain atoms on the material's surface becomes significant. For example, inert metals such as platinum can act as catalysts, semiconductors such as silicon can act as conductors that become conductive, etc., the applications of nanotechnology have only increased in recent years, and the highest potential application is in the field of materials, followed by electronics and medicine [7].

## 1.2 Polymer Structure

Polymers are large organic molecules (macromolecules) composed of small structural components (monomers) linked together in a polymerization process [8]. Each molecule is made up of thousands of atoms that are connected by covalent chemical bonds, and molecules in polymers are attracted to one another by forces that vary depending on the polymer type. Polymers with low temperatures have limited crystal connections because polymers are made up of big, linked molecules that are difficult to handle. A linear chain of molecules can only arrange itself in an orderly fashion in a few locations. In the solid state, polymers have crystalline and non-crystalline regions [9].

## 1.3 Classification of Polymers

### 1.3.1 Chemical classification of polymers

There are different kinds of polymers categorized according to their structure and as follows [10]:

#### 1.3.1.1 Linear polymers

Single molecular is the basic structural unit for polymers in a series of certain lengths that are connected in a linear form. Linear polymers may include totals twisted that are a part of monomer but without any branch, as revealed in figure (1.1a).

#### 1.3.1.2 Branched polymers

This type of polymers consists of several branches that could be a Ladder and Crusader or Comb, which is usually present with various lengths, as illustrated in figure (1.1 b).

#### 1.3.1.3 Cross linked polymers

This kind of polymers consists of chains from three dimensional linked together in more than one site and monomers bonding in effective totals that are chemical bonds, as displayed in figure (1.1 c).

#### 1.3.1.4 Network polymers

Three-dimensional (3D) networks are made of trifunctional. Examples: phenol-formaldehyde and epoxies, as in the figure, as in the figure (1.1d).

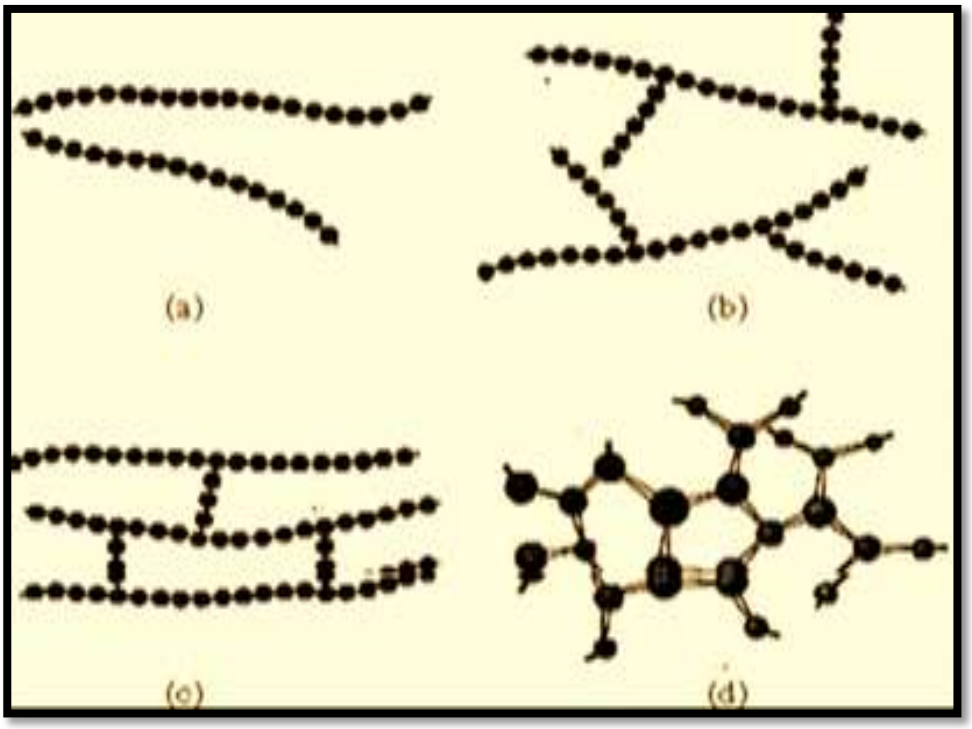


**Figure (1.1): Polymeric Chains Types (a) Linear, (b) Branched, (c) Cross-linked and (d) Network polymers [11].**

### 1.3.2 Classification of polymers dependent on homogeneity

Polymers are classified according on the homogeneity of the repeating units in

#### 1.3.2.1 Homopolymers

Materials made from one monomer are termed homopolymers [12].

#### 1.3.2.2 Copolymers

If there materials made from more than one type of monomer, they are termed copolymers [12] .

#### 1.3.2.3 Composite polymers

Composite polymers involve the addition of material to homogeneous polymers in order to alter some of their properties and introduce new properties [12].

### 1.3.3 Thermal classification of polymers

Polymers are classified according to the effect of temperature to:

#### 1.3.3.1 Thermoplastic polymers

The characteristics of these polymers change with the influence of temperature. When the temperature rises, it becomes elastic and sticky. These polymers recover to their original solid state when the temperature is lowered. This is due to the fact that the molecules of a thermoplastic polymer are held together by relatively weak intermolecular forces (Vander Vales forces). Polyethylene, poly vinyl alcohol, Polyacrylamide , and polypropylene are examples of molecules that can slide over each other when heated [13], as shown in figure (1.2).

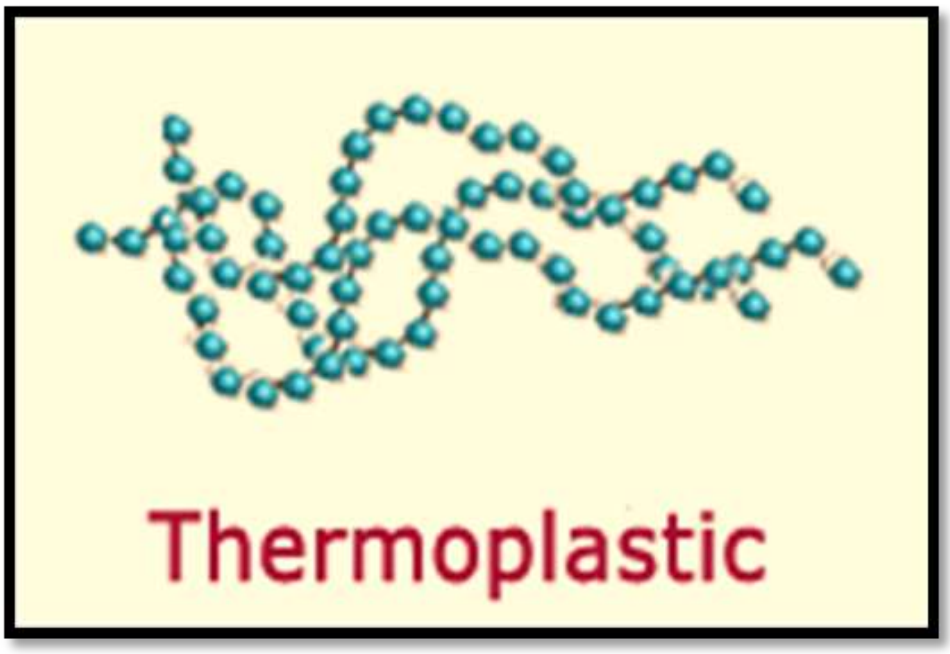


**Figure (1.2): Atomic configuration of thermoplastic polymers [13].**

### 1.3.3.2 Thermoset polymers

Some polymers undergo certain chemical changes on heating and convert themselves into an infusible mass. The curing or setting process involves chemical reaction leading to further growth and cross linking of the polymer chain molecules and producing giant molecules. For example, resins, Phenolic, epoxy resins, urea , diene rubbers, etc. [14], as shown in figure (1.3).

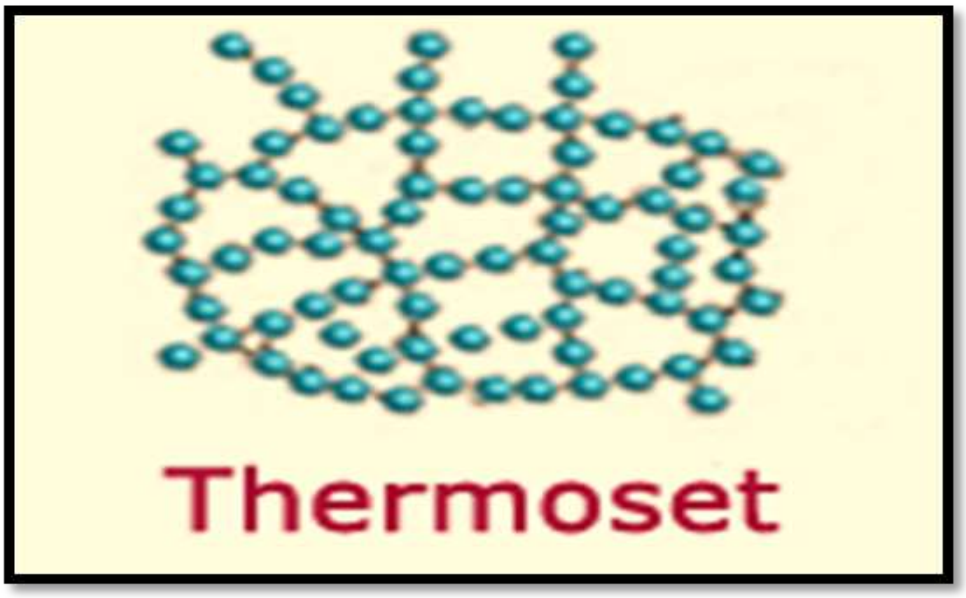


**Figure (1.3): Atomic configuration of thermoset polymers [13].**

## 1.4 Polymer Blends

A polymer blend is a mixture of two or more polymers that have been blended together to create a new material with different physical properties. Generally, there are five main types of polymer blend: thermoplastic–thermoplastic blends, thermoplastic–rubber blends, thermoplastic–thermosetting blends, rubber–thermosetting blends, and polymer–filler blends. Polymer blending has attracted much attention as an easy and cost-effective method of developing polymeric materials that have versatility for commercial applications. In other words, the properties of the blends can be manipulated according to their end use by correct selection of the component polymers [15].

## 1.5 Nanocomposites

Nanocomposites can be defined as a composite material in which at least one of the phases (mostly the filler) shows dimensions in the nanometer range. As the fillers size reaches the nanometer level, the interactions at the interfaces become considerably large with respect to the size of the inclusion and thus the final properties show significant changes [16].

A nanocomposite, like a traditional composite has two parts, filler and the matrix. A traditional composite typically uses a fiber such as carbon fiber or fiberglass as the filler, in a nanocomposite the filler is a nanomaterial. Some examples of nanomaterial are CNTs, carbon nanofiber, and nanoparticles such as gold, silver, diamond, copper and silicon. CNT nanocomposites are of particular interest because of the high strength and stiffness composites they produce at low CNT concentrations. [17, 18].

## 1.6 Materials Used in The Study

### 1.6.1 Polyvinyl Alcohol (PVA)

PVA (Poly-vinyl alcohol) is synthetic polymer employed since the early 1930s in a wide range of industrial, commercial, medical and food applications including resins , surgical threads, lacquers and food-contact applications [19]. Poly (vinyl alcohol) is a synthetic polymer that comes in the form of a granular powder that is odorless, transparent, tasteless, white, or cream-colored [20]. Polycarbonate (vinyl alcohol), which may be combined in water, has the benefit of being resistant to solvents and oils, as well as having outstanding characteristics [21]. PVA fiber has high tensile and compressive strengths, tensile modulus, and abrasion resistance due to its highest crystalline lattice modulus. Many researchers have looked at using PVA as a filler or in cross-linked products,

additionally, it has been widely employed as a thermoplastic polymer to make nontoxic, harmless, and living tissues, among other things [22,23]. It has been used in a wide range of applications and is also widely used in semiconductor applications [24]. Figure (1.4) shows the chemical structure of PVA, and the FTIR for pure PVA as shown in figure (1.5).

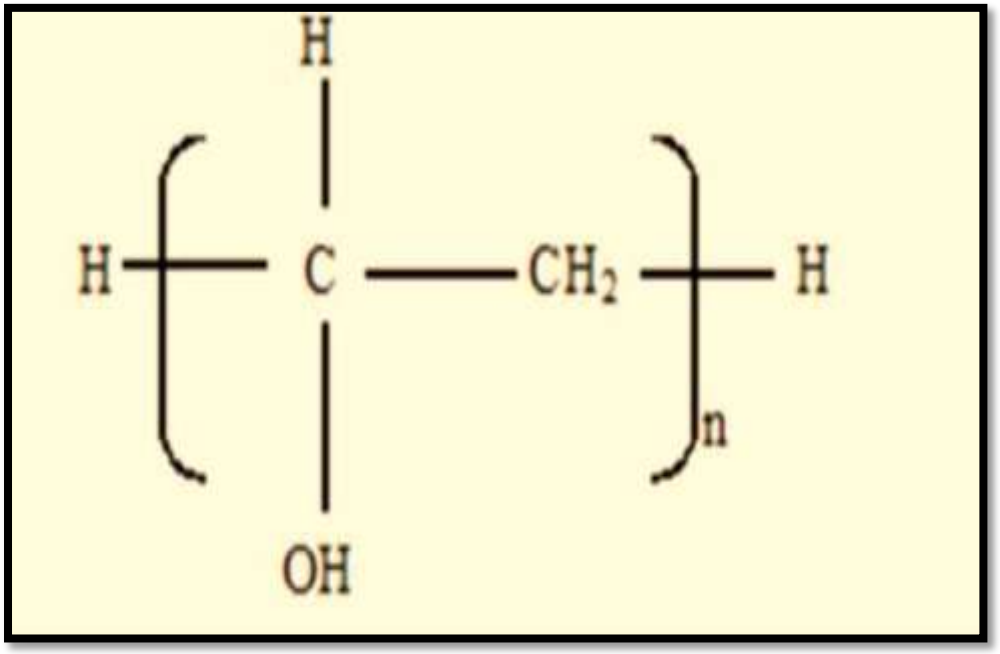


**Figure (1.4) The Chemical Structure of PVA [24].**

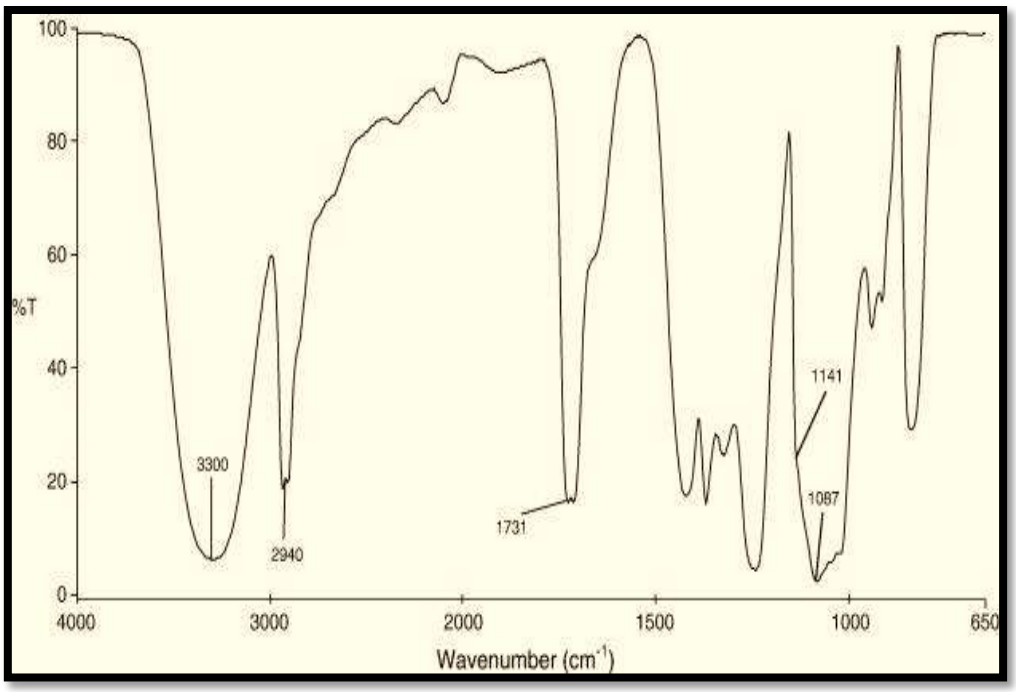


**Figure (1.5): FTIR spectra of pure PVA thin films [25].**

**Table (1.1): Physical and Chemical Properties of Poly(vinyl Alcohol) (PVA) [26].**

| Property | Description |
|---|---|
| **Appearance** | White to an ivory white granular powder |
| **Molecular formula** | $(C_2H_4O)_n$ |
| **Solution PH** | 5- 6.5 |
| **Density g/cm$^3$** | 1.3 g/cm$^3$ |
| **Refractive index** | 1.55 |
| **Glass transition temperature $T_g$ ºC** | 85 ºC |
| **Melting temperature $T_m$ ºC** | 230 ºC |

### 1.6.2 Poly Acrylamide (PAAm)

Polyacrylamide (PAAm) is another water-soluble polymer that has a wide range of industrial flocculant applications, rheology-control agents, drag-reducing polymers, andadhesives as in Table (1.2) [27], and has the formula (C3H5NO)n [28]. As shown in figure (1.6) and the FTIR for pure PAAm is shown in figure (1.7).

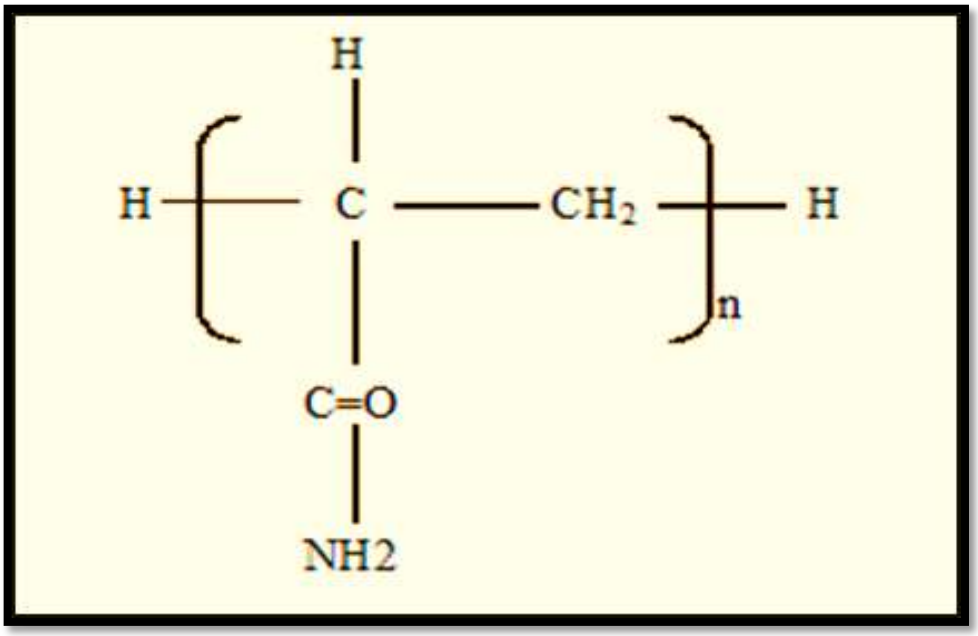


**Figure(1.6) Chemical formula of Polyacrylamide[29].**

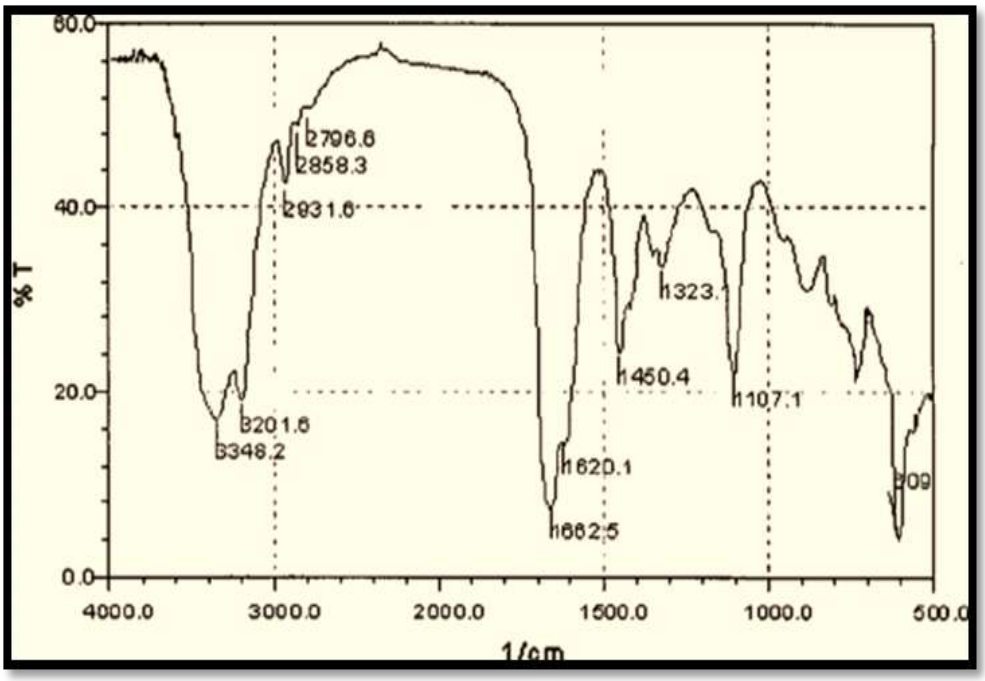


**Figure (1.7) ): FTIR spectra of pure PAAm thin films [30].**

PAAm and their derivatives increased attention during the past years and to the present time. This polymers dissolved in water which does not resemble al monomer and non-toxic because they contain nitrogen theoretically 19.7 % and the proportion of aggregates contains hydroxide 3.6% and the latter gives the polymer properties of multi-polarization

technique. The range for the PAAm at a temperature (25$^{o}$C) is (10-5000) x10$^{-3}$ (Poise).

PAAm is often used to increase the viscosity of water, polyamides and an acrylic material solid crystal is very stable. The presence of aggregates amine and carboxyl in the dry polymer chains lead to a severe reaction molecule when calculating the hydrogen bonds between chains and polyamides scores with very high melting relatively. Because bonded hydrogen molecular and differences in the hydrogen profile bonded poly amid and effectiveness increases strength and cohesion are used in the formation of fibers, called this kind nylons. The applications can be helpful as a result of mechanical characteristics of weak tensile strength of the weak and poor resistance to pressure and lack of lengthening her [31].

**Table (1.2): Physical and chemical properties of Polyacrylamide (PAAm) [32].**

| **Property** | **PAAm** |
|---|---|
| **Appearance** | white crystalline solid at room temperature |
| **Molecular formula** | $C_3H_5NO$ |
| **Solution PH** | 5 |
| **Density g/cm3** | 1.13 g/cm3 |
| **Refractive index** | 1.8 |
| **Glass transition temperature ($T_g$) $^{o}$C** | 84.5 |
| **Melting temperature ($T_m$) $^{o}$C** | 192.6 |

## 1.7 Nanomaterial Used in The Study

### 1.7.1 Copper Nanowire (CuNW)

Copper (Cu) NWs have recently garnered increasing attention as excellent candidates for TCFs. Because Cu has high intrinsic conductivity, it is a potential alternative to Indium tin oxide (ITO) and Ag NWs. Moreover, Cu is only 6% less conductive than Ag, very abundant (1000 times more abundant than Ag), and 100 times less expensive than Ag or ITO [33]. These reasons led to the promotion of copper to become an indispensable basic material in various fields and industrialization realized. Notably, the annual global production of copper is about 20 million tons in 2016, which is more than 740 times the production of Ag, next to iron (Fe) and aluminum (Al) in the metal [34]. There's no denying that the copper has attracted a lot of scientific and societal attention in recent decades. Due to the micron and even nanoscale device size, copper nanomaterials have been extensively explored to meet the needs of this development. Compared with bulk materials, the Cu nanomaterials exhibited unique properties, containing thermal, optics, electronics, mechanics and catalysis [35,36]. Coincidently, the next-generation devices require a superior performance and some Coincidently, the next-generation devices require a superior performance and some special features, which can adopt these nanomaterials. As a cost-effective and high- conductive candidate, the Cu nanomaterials are a promising attempt to solve the cost and scale issues for many future applications, which is impossible for Ag and Au. To date, various shapes of Cu nanomaterials have been successfully synthesized, including nanoparticles, nanorods, nanocubes, nanowires (NWs), nanorings and nanoplates [37-40]. Several studies have been reported, demonstrating how CuNW films can achieve high optical transmittance with high electric conductivity [41,42].

## 1.8 Literature Review

**Y. L. Luo, *et al.*, in (2012)** [43], fabricated well-dispersed copper nanoparticles were using poly(vinyl alcohol)/ polyacrylamide interpenetrating polymer networks (PVA/PAAm IPNs) as a nanoreactor template. The complexation of PVA in PVA/PAAm IPNs with $Cu^{2+}$ played an important role in avoiding the aggregation of copper nanoparticles and providing particle size and size distribution controllability and stability and FTIR spectra show these is no chemical reaction. The absorbance increases with increasing concentration of copper nanoparticles.

**A. Hashim, *et al.*, in (2013)** [44], prepared samples of composites consisting of polyvinyl alcohol-polyacrylamide and pomegranate peels using the casting method. The polymer composites which the prepared have many applications. The results showed that the optical properties of polymer matrix were changed with the increase of the pomegranate peel concentrations. the mechanical properties, ease of fabrication of thin films of desirable sizes and their ability to form proper electrode/electrolyte contact in electrochemical devices.

**M. A . Habeeb, *et al.*, in (2014)** [45], studied the effect of (CoO) nanoparticles on some optical properties of (PVA-PAAm) composite, using casting method, where many samples have been prepared by adding different weight percentages of cobalt oxide nanoparticles (3, 6, 9, and 12)wt.% in the wavelength range (200-1100) nm. The results of the work showed a good improvement in both calculated energy gap of the indirect allowed and forbidden transition as well as optical constant such as (refractive index, extinction coefficient and read and imaginary dielectric constants.

**M. A. Habeeb in (2014)** [46], preparated of (PVA-PAAm-Ti) nanocomposites and study their structural and mechanical properties to use it in many applications. The nanocomposites was tested by different methods such as Fourier transformation infrared ray (FTIR) and optical microscope. The results (FTIR) show that increasing of the value of the absorbance of (PVA-PAAm-Ti) nanocomposites with increases of concentration of titanium nanoparticles. The morphology of the nanocomposites was studied using optical microscope, which showed grain distribution at surface morphology and grain aggregates increases with increasing of titanium nanoparticles. There results showed that the mechanical properties for (PVA-PAAm-Ti) nanocomposites were increases with increasing of concentration of titanium nanoparticles except compressibility decreased under effect addition.

**M. M. El-Toony in (2017)** [47], studied casting of polyacrylamide/poly (vinyl alcohol) reinforced by carbon Nano-Wire for using into proton exchange membrane fuel cell. Characterizations of the casted membranes were carried out using Fourier transformer infra-red (FTIR), thermal gravimetric analysis (TGA) and scanning electron microscopy (SEM) for their investigations chemically, thermally and morphologically respectively. Studying the properties of the membranes was performed using ion exchange capacity (IEC), water uptake and tensile strength for testifying their availability into the proton exchange membrane fuel cell (PEMFC). Proton conductivity was measured (maximum value was $8.1 \times 10^{-2}$ S/cm) and free volumes sizes were evaluated using positron annihilation lifetime spectroscopy (PALS).

**X. Ren, *et al.*, in (2018)** [48], modified a fish slime-like coating by poly vinyl alcohol/polyacrylamide (PVA/PAAm) hydrogel which is the semi-interpenetrating network polymer was designed. A physical blending method loading PVA/PAAm hydrogels powder into the organic silicon resin was employed to prepare the coating. The oil-resistance of the coating was performed by time-sequence images of washing dyed beef tallow stain away. The results showed that the PVA/PAAm hydrogels modified coating had the greater ability of stain removal. The biomass of a marine microalgae species, Nitzschia closterium and f. minutissima attached on the coating were investigated using UV-Visible Spectrophotometer (UV) and Scanning electron microscopy (SEM). The results showed that the microalgaes showed a significantly lower numbers attached on PVA/PAAm hydrogels modified coating in comparison with on the organic silicon coating.

**N. F. Habubi, *et al.*, in (2018)** [49], prepared films of polyvinyl alcohol polymer was dissolved in water in order with various concentration of Fe using the casting method. He optical characteristics were determined by recording the transmittance spectrum in the wavelength range (300-900) nm. The dispersion parameters were calculated using the Wemple–DiDomenico method. With increasing Fe concentration in the PVA-Fe films, the dispersion energy ($E_d$) and the single oscillator energy of electronic transition ($E_o$) decreased, while Urbach energy was increased. The energy gap decreased from 4.08 eV to 3.52 eV for PVA: 4% Fe film.

**S. M. A. Asadi, *et al.*, in (2019)** [50], studied the effect of MGO nanoparticles on structure and optical properties of PVA-PAAm blend by casting solution method. The films of PVA-PAAm-MgO were manufactured in various amounts of (0, 0.02, 0.04)wt.% of 30 nm particle size of MgO. The structure of PVA-PAAm-MgO composite was investigated using FTIR to determine the activation groups. The optical microscopy was used to investigate the diffusion of MgO nanoparticles within the preparation blend and also homogeneity. A UV-Visible spectrophotometer that records transmittance spectra in the 300-900 nm range. With increasing MgO nanoparticles content in the PVA-PAAm-MgO composite, the transmittance decreased, and the absorbance increased. The optical constants were calculated, and the optical energy gap in the PVA-PAAm-MgO composite decreased as the MgO nanoparticle content increased.

**S. El-Gamal and A. M. El Sayed in (2019)** [51], manufactured the magnesium oxide/polyvinyl alcohol/polyacrylamide (MgO/PVA/PAM) nanocom-posite films by a solution chemical method. The effect of loading PVA and MgO nanoparticles (NPs) on the physical properties of PAM is discussed. The melting temperature, glass transition, and equilibrium swelling ratio all depend on the composition of the films. PAM had 87% anpercent transmittance, which increased to 90% percent once PVA was added, but decreased to 74% after MgO loading. PVA blending and MgO addition cause significant variations in the extinction coefficient and indirect/direct band gap of PAM.

**H. M. Ragab and A. Rajeh in (2020)** [52], the chemical generation of silver nanoparticles was achieved by reducing the concentration of silver salt. To confirm the existence of nanoparticles, XRD, TEM, and UV–VIS spectrophotometry were used to characterize the Ag NPs. The casting technique contributed to the creation of novel Ag/PAM/PVA nanocomposites films. Analytical tests using XRD and FTIR confirmed the interaction between the polymer blend and the Ag nanoparticles. The FTIR signal intensity variations with increasing dopant concentration imply a rise in the basicity of the major functional groups, indicating the carbonyl group's potential to behave as a powerful electron donor when interacting with the Ag+ cation. The high conductivity accompanied by the high concentration of $Ag^{+}$ was explained in terms of the amorphicity increase. Therefore, these alterations show that these films are highly sensitive to doping, indicating that they are suitable for use in optical and/or electrical devices.

**O. K. Abdali and K. H Abass in (2021)** [53], studied the effect of silver nano-particles on structural, optical and electrical properties of casted (polyvinyl alcohol/ polyacrylamide/polyethylene oxide) composites for antibacterial applications by solution casting method. The diffusion of nanoparticles (NPs) in the blends was examined using an optical microscopy and a scanning electron microscopy (SEM). The aggregation of NPs was clearly visible in the high-weight additives. Optical microscopy, SEM, and FTIR were used to examine the materials. The absorption spectrum records in the wavelength scope (190-1100) nm. The optical parameters directly proportional to Ag nanoparticle additions except for the transmittance and the energy gap were lowered. The optical parameters show that Ag doping clearly effects on the films characteristics, the optical constants enhanced.

**A. K. Al-Shammari and E. Al-Bermany in (2021)** [54], studied the effect of the functional group of the polymers have the same mainstay of the polymer chain but with a different end functional group in addition to the influence of graphene oxide (GO) nanosheets. These polymers mixed with Poly (vinyl alcohol) (PVA) separately after dissolved in distilled water (DW) then reinforced with GO applying the developed acoustic-sonication-casting method. The new nanocomposites exhibited homogeneous combinations with an acceptable dispersal of GO in the polymers matrix as presented in the visual microscopy (OM). Coupled with the strong interplay between polymers in the matrix and the polymer with GO nanoparticles as nanocomposites, Fourier transform infrared coefficient, compressibility and Bulk modulus, etc. (FTIR) verified the successful preparation of GO. Interestingly, the PAA-PVA/GO nanocomposites presented a smoother surface and better mechanical results in comparison with PAAm-PVA/GO that showed rough surface and soften behavior.

## 1.9 The Aims of Study

1. Preparation of PVA-PAAm:CuNW nanocomposites by casting method with high homogeneity.

2. Studying of some physical properties (morphology and structure, optical) of PVA-PAAm:CuNW nanocomposites to find out the appropriate application for these films.

3. Studying the dispersion Parameters using the Wemple–DiDomenico model of PVA-PAAm:CuNW nanocomposites to find its potential for use in optical communications and in the design of optical devices.

# Chapter tow

# Theoretical part

## 2.1 Introduction

This chapter includes a general description of the theoretical part of this study, physical concepts, relationships, scientific clarifications, and laws used to interpret the study results of morphology and structural, optical, and dispersion parameters. Morphology and structural properties used in this work are given by (optical microscopic, scanning electron microscope, and Fourier transform infrared spectrometer (FTIR), optical properties of nanocomposite (the optical constants, fundamental absorption edge, electronic transitions). This explanation can be considered as an entryway to admission to scientific knowledge of polymer nanocomposite.

## 2.2 Morphology and Structural Properties

### 2.2.1 Optical microscope (OM)

The optical microscope is known to be a compound optical instrument, which makes use of visible light for producing a magnified sample image that is projected on an imaging device or onto the retina of the eye. The term compound refers to the fact that the final image is created through two lenses: the objective lens and the eye-piece or ocular lens, which together perform the magnification of the image. The microscope is most commonly used for minute light-diffracting specimens such as diatoms, bacteria and bacterial flagella, isolated organelles and polymers such as cilia, microtubules, flagella, and actin filaments, and silver grains and gold particles in his to chemically labeled cells and tissues. The number of scattering objects in the specimen is an important factor, because the scattering of light from too many objects may brighten the background and obscure fine [55], as shown in figure (2.1).

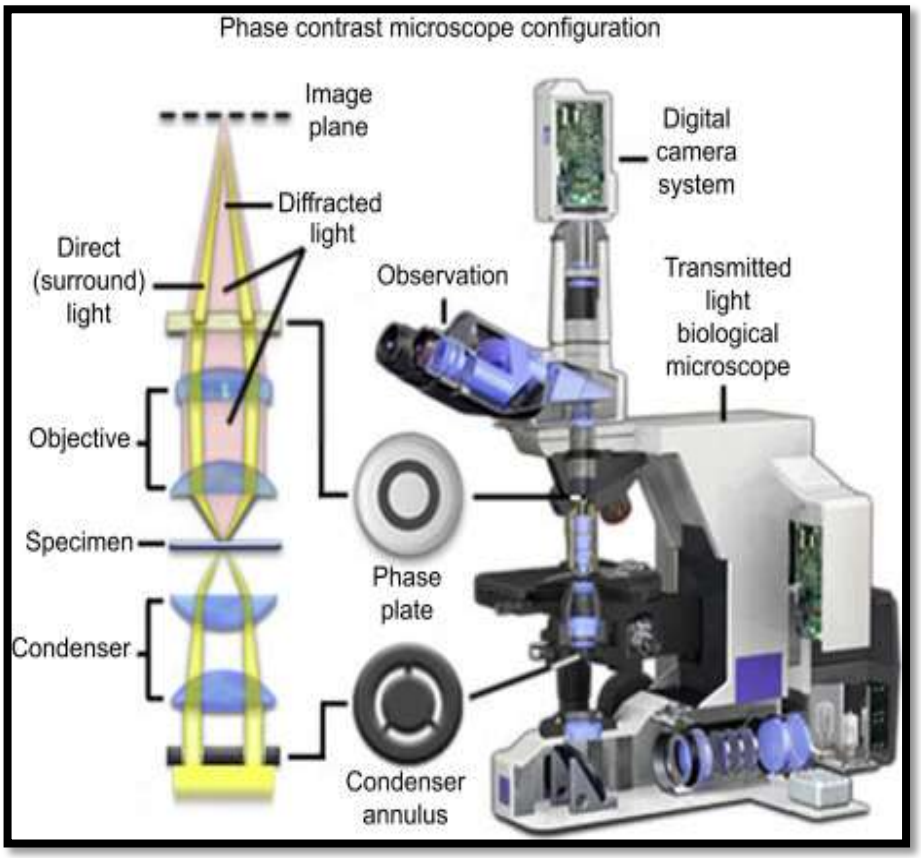


**Figure (2.1): Optical Microscope [56].**

### 2.2.2 Scanning electron microscope (SEM)

The scanning electron microscope (SEM) is a vital research and manufacturing instrument that is widely utilized in many industries throughout the world. The instrument's appeal stems from the necessity to inspect and gather information about samples whose structure is deteriorating. The SEM provides a better level of resolution for examination and inspection than existing optical microscope techniques. In addition, unlike the optical microscope, the SEM has a range of analytical modes, each of which provides unique information on the physical, chemical, and electrical properties of a certain specimen, device, or circuit. Because of recent advances that eliminate or at least minimize sample degradation and contamination, allowing continuous nondestructive in-process inspection, the SEM is currently finding

increased uses in research and production quality control [57], as shown in figure (2.2).

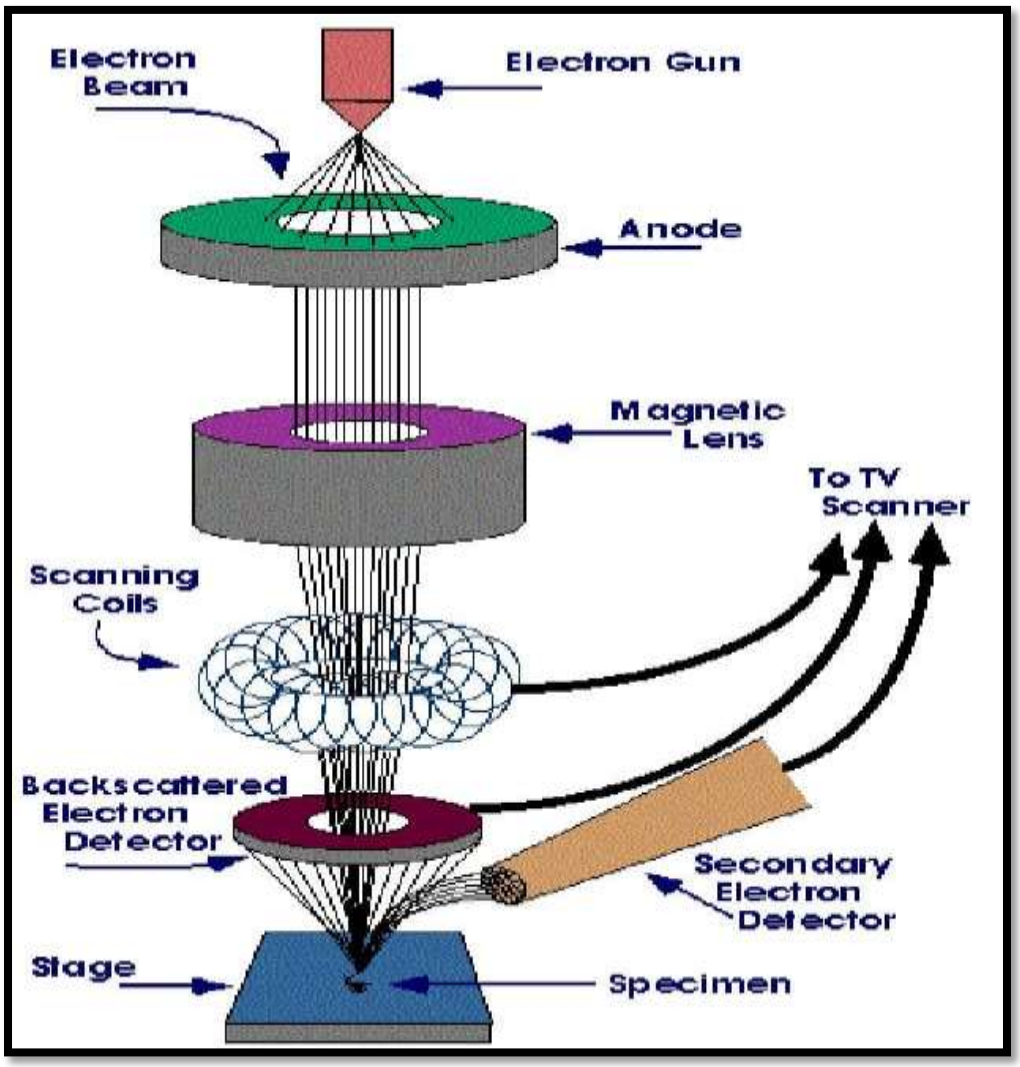


**Figure (2.2 ): Schematic diagram of scanning electron microscope (SEM) [58].**

### 2.2.3 Fourier transform infrared (FTIR) spectroscopy

Fourier Transforms Infrared (FTIR) is chemical investigative spectroscopy. This measures the infrared intensity with light wavenumber. The wavenumbers consist of infrared light that is divided into three regions, far-infrared, mid-infrared and near-infrared, which are between (4 ~ 400) $cm^{-1}$, between (400 ~ 4,000) $cm^{-1}$ and finally, between (4,000 ~ 14,000) $cm^{-1}$, respectively [59].

Infrared radiation is permitted to pass through a material in FTIR spectroscopy. Some of the infrared radiation is transmitted and some is absorbed by the sample. The resulting spectrum is similar to the sample's molecular fingerprint and contains information about the various chemical groups and chemical bonds present in the sample. Two molecular structures never generate the same infrared spectrum like fingerprints are unique for every person [60], as shown in figure (2.3).

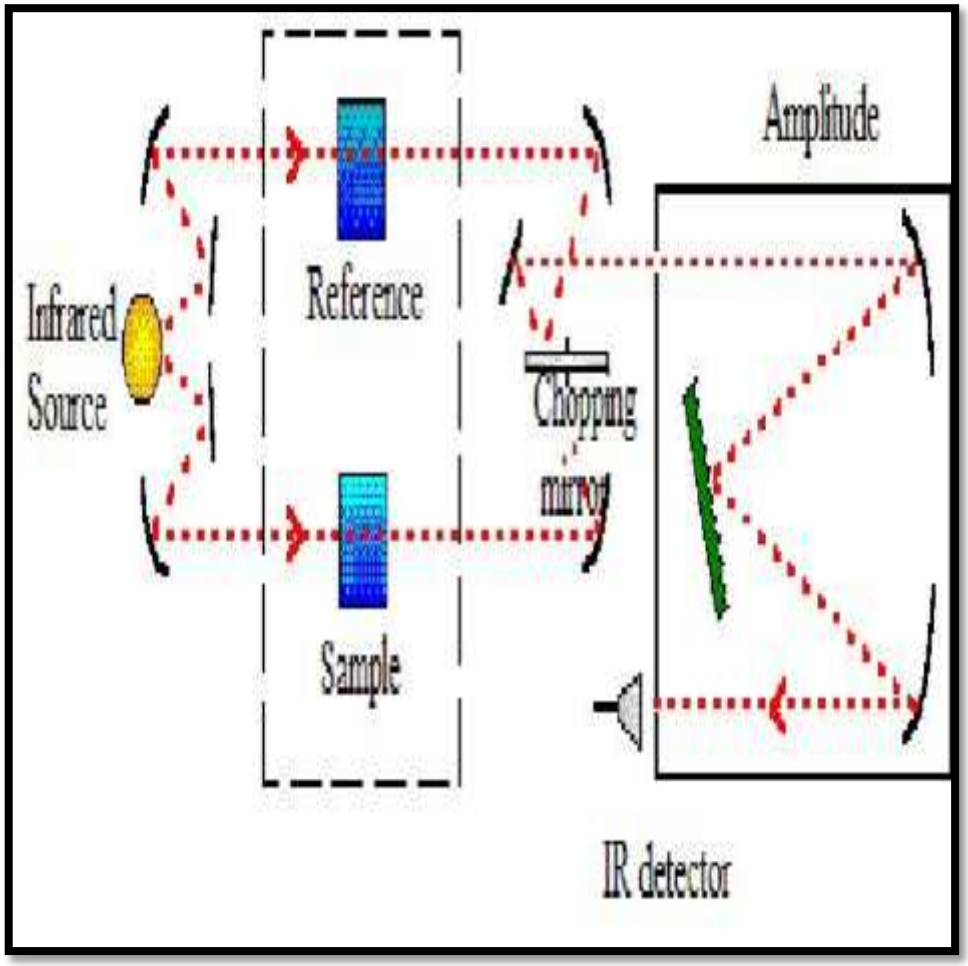


**Figure (2.3): A schematic diagram of the classical dispersive IR spectrophotometer [61].**

## 2.3 Optical Properties

The purpose of studying the optical properties of polymeric materials is to gain a better knowledge of the internal structure of the polymer and the nature of its bonds, in addition to broadening the scope of potential applications [62].

Knowing the spectrums of absorption and transmittance a polymer assist in identifying many optical properties in different ranges of wavelengths. Examining the ultraviolet spectrum enables us to determine the type of bonds, orbital and energy beams. The visible spectrum gives sufficient information about a substance's behavior for solar applications. The infrared range is essential for understanding the general structure of a polymer and the constituents that make up its chemical structure [63].

Optical properties represent one of the main factors in its results, which were based on a lot of analyzes about the nature of the atomic structure of the material or to the effect of the absorption material for photons of light in the incidence of the transfer of electronic within the installation packs. This shows the installation of power packs as well as the energy gap whether directly or indirectly. That is provided with information about the nature of the change constants visual such as, absorption coefficient, coefficient of refraction, extinction coefficient and others [64].

### 2.3.1 Light absorbance and electronics transitions

He aggregate molecular energy has been partitioned into the electronic energy ($E_{ele}$), vibration energy ($E_{vib}$), rotational energy ($E_{rot}$) and transitional energy ($E_{trans}$). Due to the change in the distinct energies, the absorbance of an electromagnetic wave results in a change in the total energy of the molecule [65].

$$\Delta E_{total} = \Delta E_{vib} + \Delta E_{rot} + \Delta E_{ele} + \Delta E_{trans} \quad (2.1)$$

The visible and ultraviolet spectrums are those of electronic absorbance, while the rest are those of other absorbance. In the absorbance spectrum, the $E_{ele}$ is the clearest. The photon's reaction with the molecule causes the photon's electrical field to agitate the electronic structure of the molecule to the point where The photon vanishes, and its energy is transferred to the molecule whose state has been changed to excited.[66]. As shown in figure (2.4) shows the energy regions and molecular energies.

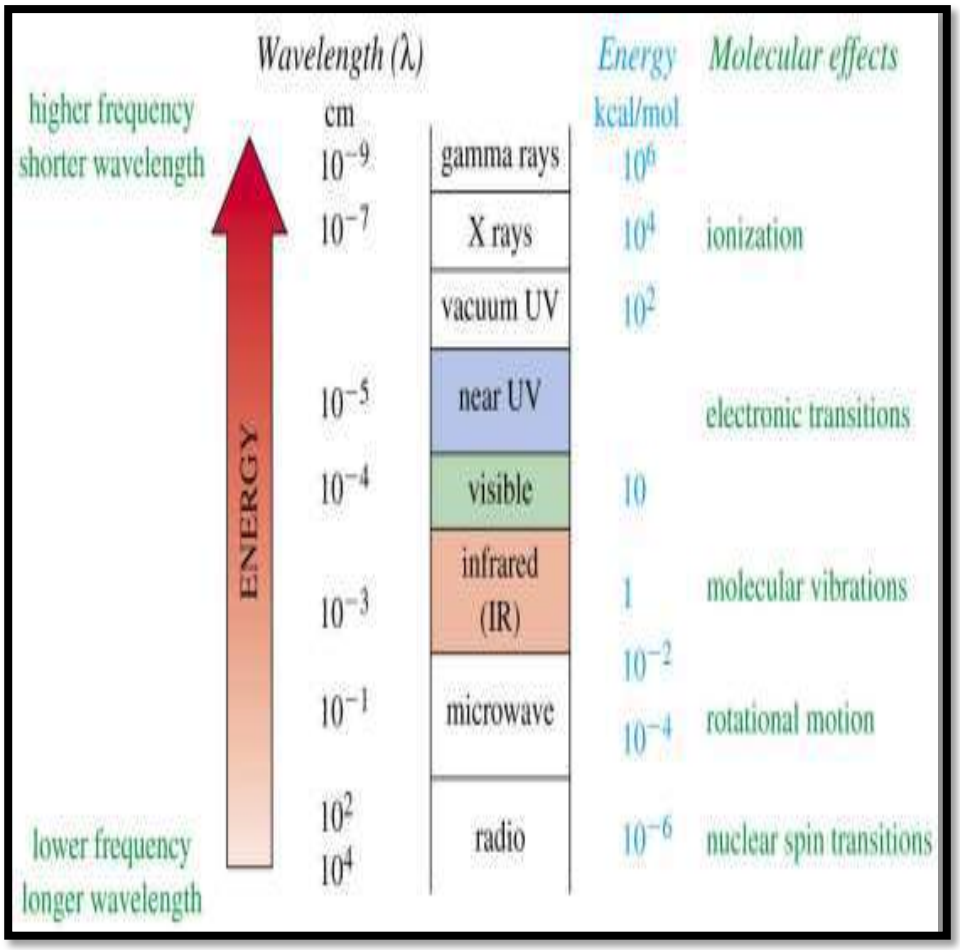


**Figure (2.4): The electromagnetic spectrum region [67].**

### 2.3.2 Optical properties of semiconductors

#### 2.3.2.1 Absorbance (A)

The absorbance occurs when light passes through a material and the intensity is reduced based on the colors that are absorbed.

It can be defined as the ratio between absorbed light intensity ($I_A$) by material and the incident intensity of light ( $I_o$) [68]:

$$\mathbf{A = \frac{I_A}{I_o}} \qquad \textbf{(2.2)}$$

#### 2.3.2.2 Transmittance (T)

The intensity of transmitted rays from the film ($I_T$) over the intensity of incident rays on the film ($I_o$) is called the transmittance (T), and can be obtained as follows [69]:

$$\mathbf{T = \frac{I_T}{I_o}} \qquad \textbf{(2.3)}$$

#### 2.3.2.3 Optical constants

There are many ways to find the optical constants of refractive index, extinction coefficient, optical conductivity, dielectric constant, and absorption coefficient

##### 2.3.2.3.1 Refractive index (n)

The refractive index can be defined as the ratio of the velocity of light in vacuum (c) to the velocity of light in the medium (υ) according to [70]:

$$\mathbf{n = \frac{c}{\upsilon}} \qquad \textbf{(2.4)}$$

The following equation describes the relationship between reflectance and refractive index [70,71]:

$$\mathbf{R = \frac{(n-1)^2 + k^2}{(n+1)^2 + k^2}} \qquad \mathbf{(2.5)}$$

where: ($k$) is the extinction coefficient.

R: is the reflectance.

The relation can be used to calculate reflectance from absorption A and transmission T spectra in accordance with the conservation of energy law [72]:

$$\mathbf{R + A + T = 1} \qquad \mathbf{(2.6)}$$

where:

The following equation can be used to calculate the refractive index [58]:

$$\mathbf{n = \sqrt{\frac{4R - k^2}{(R-1)^2}} - \frac{(R+1)}{(R-1)}} \qquad \mathbf{(2.7)}$$

### 2.3.2.3.2 Extinction coefficient ($k_o$)

The electrical coefficient the amount of photons absorbed by the membrane, that is, the energy absorbed by the electrons of the material, and expresses the following relationship [73]:

$$\mathbf{k_o = \alpha\lambda/4\pi} \qquad \mathbf{(2.8)}$$

Where (λ) is the wavelength of the incident light and (α) absorption coefficient.

### 2.3.2.3.3 Optical conductivity

The optical conductivity ($\sigma_{op}$) has been determined from the following equation:

$$\mathbf{\sigma_{op} = \alpha_{op} \frac{nc}{4\pi}} \qquad \mathbf{(2.9)}$$

$\sigma_{op}$ is the absorption coefficient [74].

### 2.3.2.3.4 Dielectric constant

The dielectric constant expresses a material's polarization ability, whose expression [75], is computed using the following equation:

$$\varepsilon = \varepsilon_1 - i\varepsilon_2 \quad \textbf{(2.10)}$$

$$\varepsilon = N^2 \quad \textbf{(2.11)}$$

$$(n - ik_o)^2 = \varepsilon_1 - i\varepsilon_2 \quad \textbf{(2.12)}$$

$$\varepsilon = (n^2 - k_o^2) - i(2nk_o) \quad \textbf{(2.13)}$$

The dielectric coefficient (ε) can be determined using the refractive index (n), join complex dielectric coefficient (ε) with complex refractive index (N).

From equation (2.12) and (2.13) real and imaginary complex dielectric coefficient can be written as in following equation:

$$\varepsilon_1 = (n^2 - k_o^2) \quad \textbf{(2.14)}$$

$$\varepsilon_2 = (2nk_o) \quad \textbf{(2.15)}$$

### 2.3.2.3.5 The absorption coefficient

It is defined as a ratio decrement in incident ray energy flux relative to distance unit in the direction of incident wave diffusion. The absorption coefficient (α) depends by the incident photon energy (hυ) as well as the properties of the sample, where electronic transitions type (n) or (p), and forbidden energy gap, photon energy give the following equation [76]:

$$E = h\upsilon \quad \textbf{(2.16)}$$

When the incident photon energy is lower than the forbidden energy gap, the photon is transmitted, and the transmittance equation is as follows. [77].

$$\mathbf{T = (1 - R)^2 \, . e^{-\alpha t}} \qquad \textbf{(2.17)}$$

If the incident ray intensity ($I_o$) that incident on blend film material of thickness (t), the intensity of transmittance ray (I) is determined by the beer Lambert law [78].

$$\mathbf{I = I_o \, e^{(-\alpha t)}} \qquad \textbf{(2.18)}$$

*a* means the absorption coefficient ($cm^{-1}$).

$$\mathbf{\alpha t = 2.303 \log \frac{I}{I_o}} \qquad \textbf{(2.19)}$$

Where the quantity of log ($I/I_o$) indicates the absorbance (A) The following equation can be used to compute the absorption coefficient.:[79]

$$\mathbf{\alpha = 2.303 \left(\frac{A}{t}\right)} \qquad \textbf{(2.20)}$$

Where (t) represent a thickness of sample.

### 2.3.2.4 Fundamental absorption edge

The fundamental absorption edge can be characterized as the quick increase in absorbance when the amount of energy absorbed is nearly equal to the band energy gap; Thus, the fundamental absorption edge denotes the less difference in the energy between up point in valance band to bottom point in conduction band [80].

### 2.3.2.5 Absorption regions

There are three different types of absorption regions [75]:

**A) High absorption region**

This region is shown in figure (2.5). In part (A), the absorption coefficient's magnitude (α) is greater than or equal to ($10^4$ $cm^{-1}$). The magnitude of the forbidden optical energy gap ($E_g^{opt}$) can be introduced from this region.

**B) Exponential region**

This region is shown as in figure (2.5). In part (B) The absorption coefficient (α) equals ($1\ cm^{-1} < \alpha < 10^4\ cm^{-1}$). It describes the transition from extensive levels in the Valens band (V.B.) to local levels in the conductive band (C.B.) and vice versa, transitioned from local levels in (V.B.) to extended levels at the conductive band's bottom (C.B.).

**C) Low absorption region**

The absorption coefficient (α) is extremely small in this region. it is about ($\alpha < 1\ cm^{-1}$). The transition occurs in this region as a result of state density inside space motion caused by structural faults [81]. As in figure (2.5), the part (C).

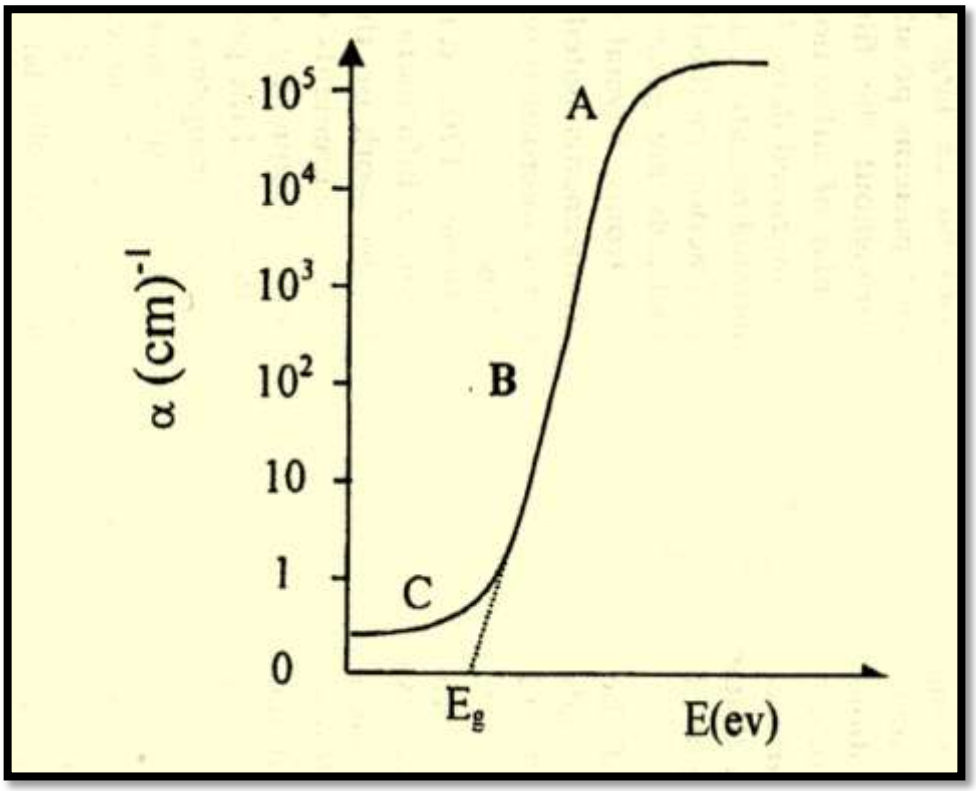


**Figure.(2.5): The variation of absorption edge with absorption regions [81].**

### 2.3.2.6 The electronic transitions

There are two basic forms of electronic transition: direct and indirect transition.

#### 1. Direct transitions

This kind of transitions occurs in semi-conductors, where the bottom of the conduction is precisely above the top of the valance band, thus implying that they share similar wave vector values i.e. ($\Delta K = 0$). In such a case, the absorption would occur at ($h\upsilon = E_g^{opt}$.). Therefore, the phonons do not take part in direct transition since the phonon's wave vector (K) is much greater than that of the photons. This transition type requires the laws of conservation in momentum and energy. The direct photon transition to the energy of the minimum gap reaches no satisfaction of the demand for conserving the wave vector, as the photon

wave vectors could be neglected in the given energy range [82]. There are two kinds of direct transitions [83].

**a. Direct allowed transition**

This transition occurs from the top points in the (V.B.) and the bottom point in the (C.B.), as shown in figure(2.6 a) [70].

**b. Direct forbidden transitions**

This transition occurs from near top points of (V.B.) and the bottom points of (C.B.),as shown in figure (2.6 b).

The absorption coefficient for this type of transition is equal to [70] :

$$\alpha h\upsilon = B(h\upsilon E_g^{opt})^r \qquad (2.21)$$

Where $E_g$ energy gap between direct transition .

B: the constant depended on the type of material

r: the exponential constant, its value depended on type of transition.

r =1/2 for the allowed direct transition.

r =3/2 for the forbidden direct transition.

**2. Indirect transitions**

In these transitions type, the bottom of (C.B.) is not over the top of (V.B.), in curve (E-K). The electron transits from (V.B.) to (C.B.) is not perpendicularly when the value of the electron's wave vector before and after the transition is not equal ($\Delta K \neq 0$), this transition type occurs with the help of a particle named Phonon. For conservation of the energy and momentum law. Indirect transitions are classified into two types. [84], they are:

**a. Allowed indirect transitions:**

This type of transition occurs in a different region of K-space that is the electrons transmitted between the V.B. top and the C.B. bottom, as exposed in figure (2.6 c).

**b. Forbidden indirect transitions:**

Forbidden indirect transitions are displayed between the nearest points in the top and the bottom of the valance and conductive bands respectively, as shown in figure (2.6 d).

The equation (2.22) giving the transition absorption coefficient and the phonon absorption [80]:

$$\boldsymbol{\alpha h\upsilon = B(h\upsilon - E_g^{\,opt} \pm E_{ph})^r} \qquad \textbf{(2.22)}$$

$E_{ph}$. is the phonon energy, where the sing (-) applied when phonon absorption, whereas the sing (+), used when phonon mission. The exponential constant is represented as r in the equation, in which its value is determined by the transition r=2 and r=3 for the allowed indirect, and forbidden indirect transitions, respectively.

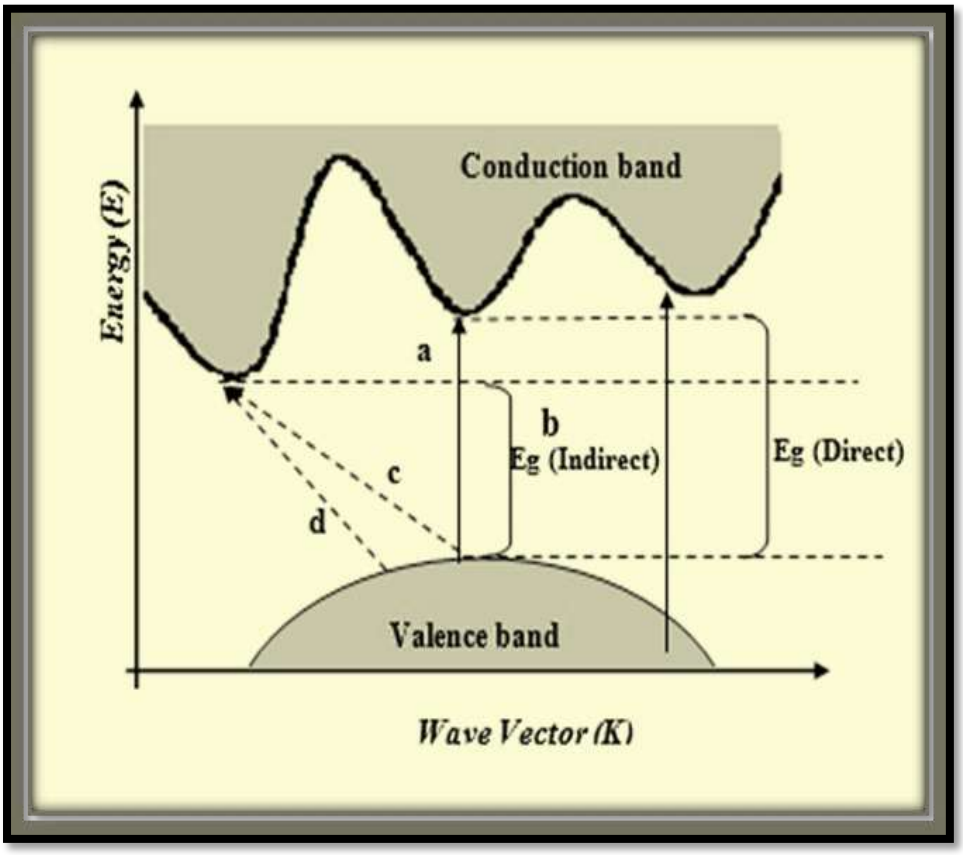


**Figure (2.6): The Electronic Transitions Types**
**(a) Allowed direct transition (b) Forbidden direct transition,**
**(c) Allowed indirect transition and (d) Forbidden indirect transition [80].**

## 2.4 Dispersion Parameters

The dispersion parameters are very important in many applications such as optical communications and in the design of optical devices [85]. The Wemple–DiDomenico (WDD) single effective oscillator model accurately describes the refractive index dispersion [86]. This model provides an understandable physical interpretation for the observed parameters, which aids in fitting the experimental results [87]. The energy of the effective single oscillator ($E_o$) and the dispersion energy ($E_d$) are the model's primary outputs.

The energy ($E_o$), or average energy gap, provides quantitative information about the material's overall band structure. It must be

considered that the information gained through ($E_o$) is completely different from to that obtained from the optical energy gap ($E_g$). The optical energy gap is related to the material's optical characteristics near its basic absorption edge. In spite of the difference be showing that the oscillator energy, ($E_o$) is often twice the optical energy gap, ($E_g$) i.e. ($E_o \approx 2E_g$) [86]. On the other hand, the dispersion energy ($E_d$), which is a measure of oscillator strength, quantifies the average energy of interband optical transitions and is associated to the sample's structural order, i.e, it is related to the ionicity, anion valency and coordination number of the material. It's worth noting at this point that the dispersion energy ($E_d$) is almost completely independent of the effective single oscillator energy, ($E_o$). This is because $E_d$ is proportional to the dielectric loss, whereas ($E_o$) is independent of the dielectric loss, either close or from afar. The relationship between ($E_o$, $E_d$) and incident photon energy (hυ) is as follows according to the (WDD) model [88,86].

$$(\mathbf{n^2 - 1}) = \frac{\mathbf{E_d\, E_o}}{\mathbf{E_o{}^2 - (h\nu)^2}} \qquad \textbf{(2.23)}$$

Where:

n: refractive index

$E_o$: the energy of the effective single oscillator

$E_d$ : the dispersion energy

hυ :incident photon energy

The static refractive index $n_o(0)$ and the static dielectric constant can be obtained from the following relations [89]

$$\mathbf{n^2(0) = 1 + \frac{E_d}{E_o}} \qquad \textbf{(2.24)}$$

$$\varepsilon_\infty = \mathbf{n^2(0)} \qquad \textbf{(2.25)}$$

He $M_{-1}$ and $M_{-3}$ moments of the optical spectra can be obtained from the relationships [90]:

$$\mathbf{E_o^2 = \frac{M_{-1}}{M_{-3}}} \qquad \textbf{(2.26)}$$

$$\mathbf{E^2_d = \frac{M_{-1}^3}{M_{-3}}} \qquad \textbf{(2.27)}$$

The obtained values are given formula the $M_{-1}$ and $M_{-3}$ moments changed due to the formation coordination Wimple-DiDomenico.

# Chapter Three

# Experimental Part

## 3.1 Introduction

This chapter involves the preparation process, instrumentation and mensuration techniques. A general description of materials (Polyvinyl alcohol, Polyacrylamide and Copper Nanowire) used in this work are given by optical microscopic, Scanning Electron Microscope (SEM), Fourier Transform Infrared spectrometer (FTIR) and UV-Vis spectrophotometer, as shown in figure (3.1 ).

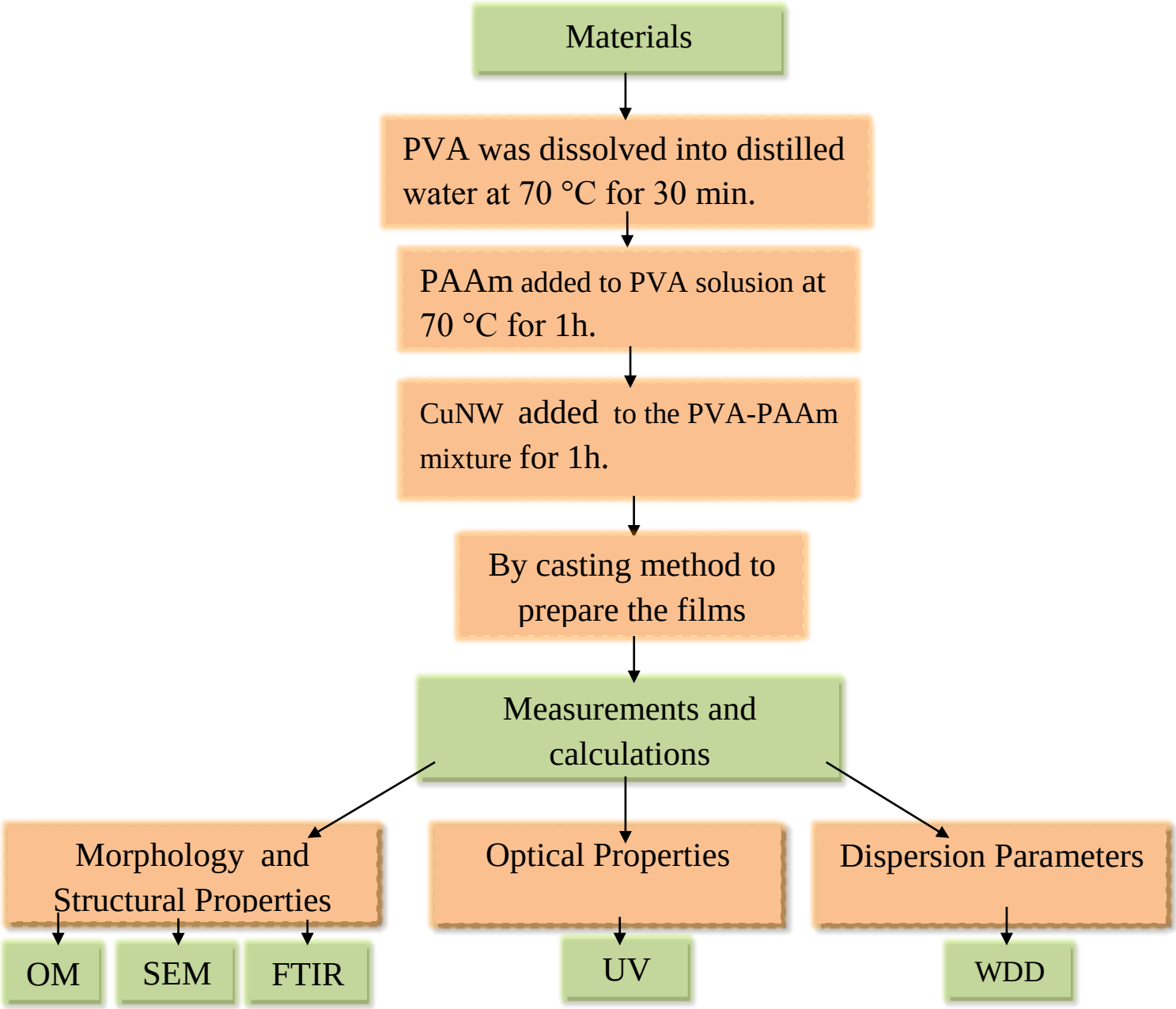


**Figure (3.1): Scheme of experimental part.**

## 3.2 The Utilized Materials

The utilized materials in this study are:

### 3.2.1 Matrix material

Two types of polymers were used in this work:

#### 3.2.1.1 Polyvinyl Alcohol (PVA)

The polymer was used as granular form, (PVA) was supplied from (Panreac\Spain, Lnc) Barcelona Espana (M.W = 18000-12000), with high purity (99.0%).

#### 3.2.1.2 Poly Acrylamide (PAAm)

The polymer was used in a white granular form soluble in water, and Its molecular weight was ($5\times10^6$ g/mol), with high purity (99.99 %). It is manufactured by a company (British Drug Houses (BDH)).

### 3.2.2 Additive nanomaterial

#### 3.2.2.1 Copper Nanowire (CuNW)

Copper Nanowire supplier Houston USA, (Purity 99.5%, Diameter 100 nm, Length 10 μm).

## 3.3 Preparation of Nanocomposites

### 3.3.1 Preparation of PVA-PAAm:CuNW nanocomposites

Polymers nanocomposites films have been prepared by mixing 80% PVA in 50 mL of distilled water, in a glass beaker equipped with a magnetic stirrer, the mixing process continued for 30 min to obtain more homogeneous solution with temperature of 70 $^{o}$C. Then 20% PAAm was added to the mixture under continuous stirring for 1h to get a mixture of more homogenous solution with temperature of 70 $^{o}$C. The adding three ratios (0.5, 1, 2) wt.% of CuNW for 1 h of each case to prepare PVA-PAAm:CuNW nanocomposite films as shown in Table (3.1). The mixture was left in the glass beaker for 24 hours. Each one of these ratios has been casted in a petri dish (5 cm and 9 cm in diameter). The entire set is placed in a dust-free room and the solvent is allowed to slowly evaporate into air at room temperature for 7 days. Then it is peeled of the petri dish gently. The thickness of these films was measured and found to be within (120, 90) µm. The steps of the composite preparation are shown in figure (3.2).

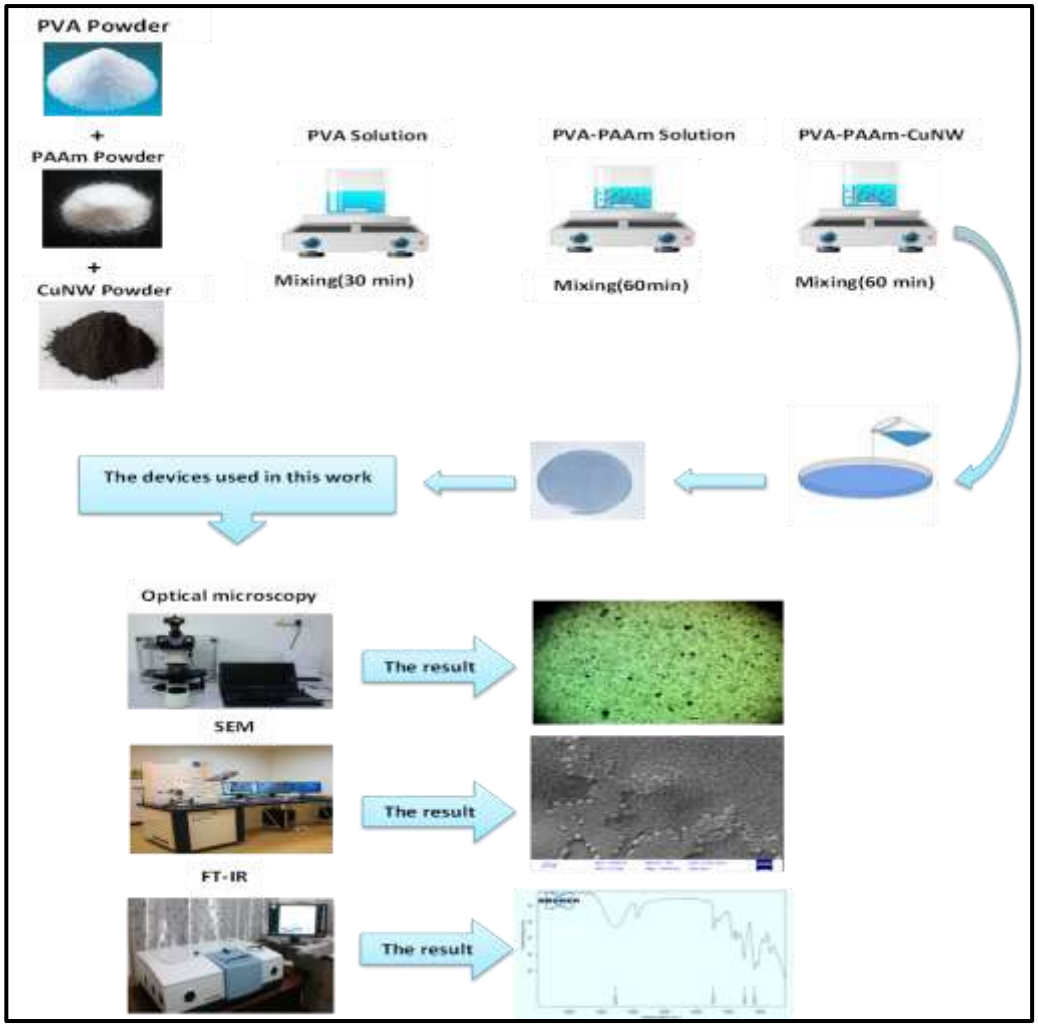


**Figure (3.2): The practical diagram.**

**Table (3.1)**: **Weight percentages of PVA-PAAm:CuNW Nanocomposites.**

| PVA (g) | PAAm (g) | CuNW (g) |
|---|---|---|
| 0.8 | 0.2 | 0.0 |
| 0.796 | 0.199 | 0.005 |
| 0.792 | 0.198 | 0.01 |
| 0.784 | 0.196 | 0.02 |

## 3.4 Measurements of Morphology and Structural Properties

### 3.4.1 Optical microscope (OM)

The samples of PVA-PAAm:CuNW nanocomposites were examined using the optical microscope, which was supplied from Olympus name (Top View) type (Nikon-73346), equipped with light intensity automatic controlled camera under magnification (100x), it is implemented in the university of Babylon /college of education for pure sciences/ department of physics.

### 3.4.2 Scanning electron microscope (SEM)

SEM is an electron microscope that uses a high-energy electron beam to photograph the surface of a sample in a raster scanning pattern. After sample preparation, the portion of each sample was cut out with dimensions (5 mm ×10 mm) and inserted into a SEM sample holder for examination. The surface morphology of the blended polymer PVA-PAAm and nanocomposites PVA- PAAm:CuNW was observed using model SEM details (Zeiss Sigma 300- HV) manufacturing and country GERMANY.

### 3.4.3 Fourier transform infrared spectroscopy (FTIR)

FTIR spectra were recorded by FTIR Fourier Transform Infrared spectrometer (Bruker) existed in Babylon University/College of Education for Pure Sciences /Department of Physics. The wave number range is (400- 4000) $cm^{-1}$. The sharply defined transmission peaks that corresponded with various vibrational modes of chemical bonds were determined for all the prepared films.

## 3.5 Optical properties measurements

### 3.5.1 UV-visible spectrophotometer

The double beam spectrophotometer (Shimadzu model UV-1800A$^{o}$ (JAPAN) was used to record the absorption spectrum of PVA-PAAm:CuNW nanocomposites in the wavelength range (200-1100) nm. It is located at the University of Babylon /College of Education for Pure Sciences/Department of Physics.

# Chapter Four

## Results and Discussio

## 4.1 Introduction

This chapter presents the results and discussion of the morphology and structural and optical properties of PVA-PAAm:CuNW nanocomposites (the disper-sion parameters were also investigated using Wemple-Didominco model) and compared with the results of previous studies of PVA-PAAm blend and PVA-PAAm:CuNW nanocomposites. The samples were diagnosed by OM, SEM, FTIR and UV.

## 4.2 The Morphology and Structural Properties

Morphology and structural Properties include the optical microscope (OM), Fourier Transform Infrared Spectrometer (FTIR) and Scanning Electron Microscope (SEM).

### 4.2.1 The optical microscopy (OM)

The morphological properties of the films have been showed using OM at magnification power (100x). Figures (4.1and 4.2) show the images microscopic of PVA-PAAm:CuNW nanocomposites with two different thicknesses and concentrations of CuNW. These images illustrated fine homogeneity of the matrix with a good distribution of CuNW into the blend-polymer composites. The OM images exhibited a successful preparation of the PVA-PAAm:CuNW nanocomposites using this method. In comparison among the polymers blending films with PVA-PAAm:CuNW nanocomposites films that were displayed a notable modification with increasing the ratio of the CuNW. The contribution of CuNW exposed many changes in all these films without any effect of the transparency of the films. Additionally, the fine distribution was considerably got better with increasing the ratio of the CuNW, as illustrated in figure (4.1d and 4.2d). When comparing the two thicknesses (120, 90) µm, it can be seen that films with thickness 120 µm has more

distribution and less aggregates than films with thickness 90 µm. The results agree with the results of the previous researchers [91, 53].

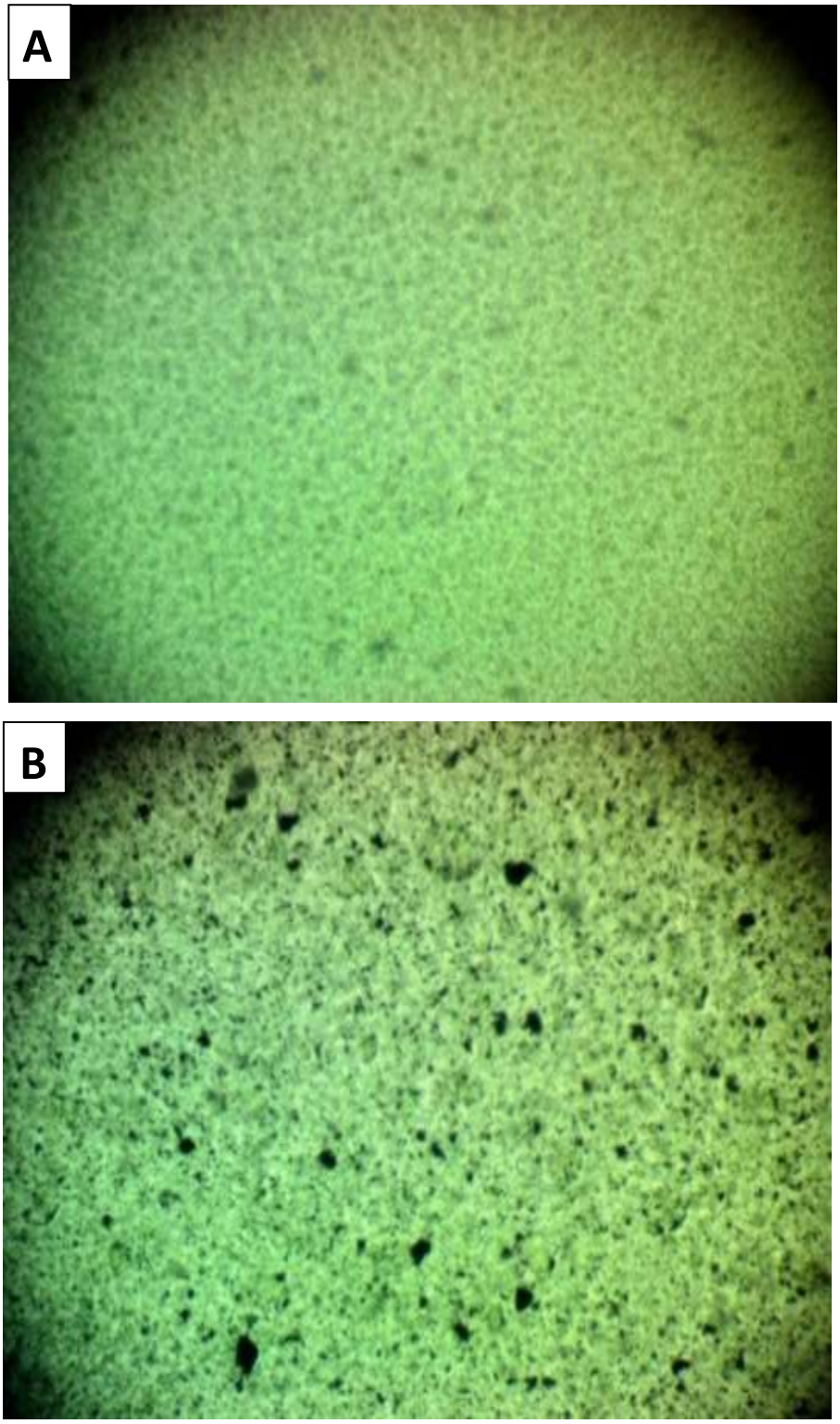

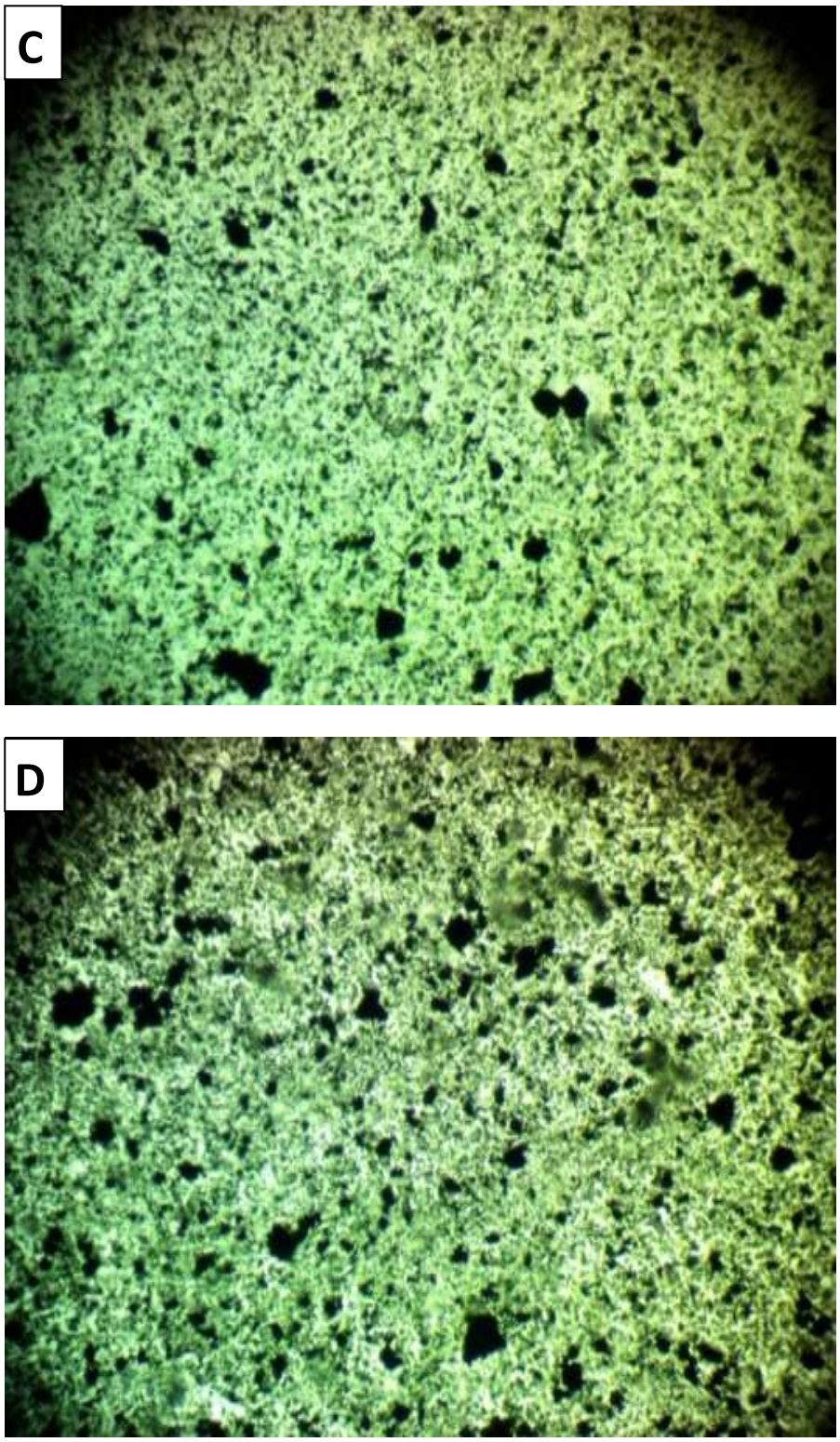


**Figure (4.1): Photomicrographs (100X) of PVA-PAAm with various content of CuNW: (A) 0 wt.% (B) 0.5 wt.% (C) 1 wt.% and (D) 2 wt.% with thickness of 120 µm.**

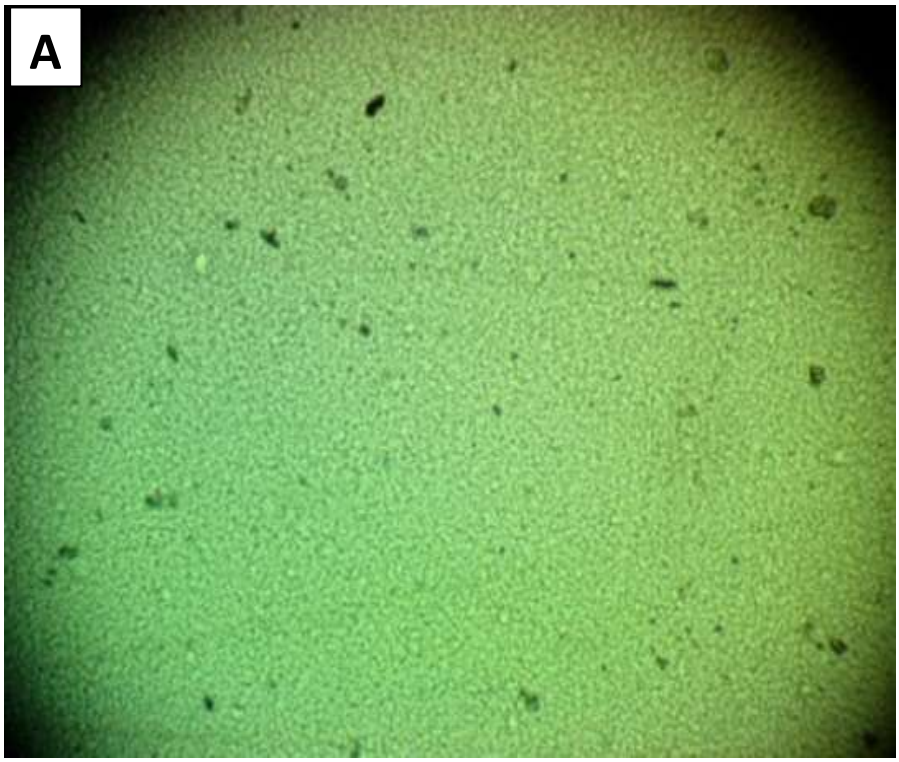
A

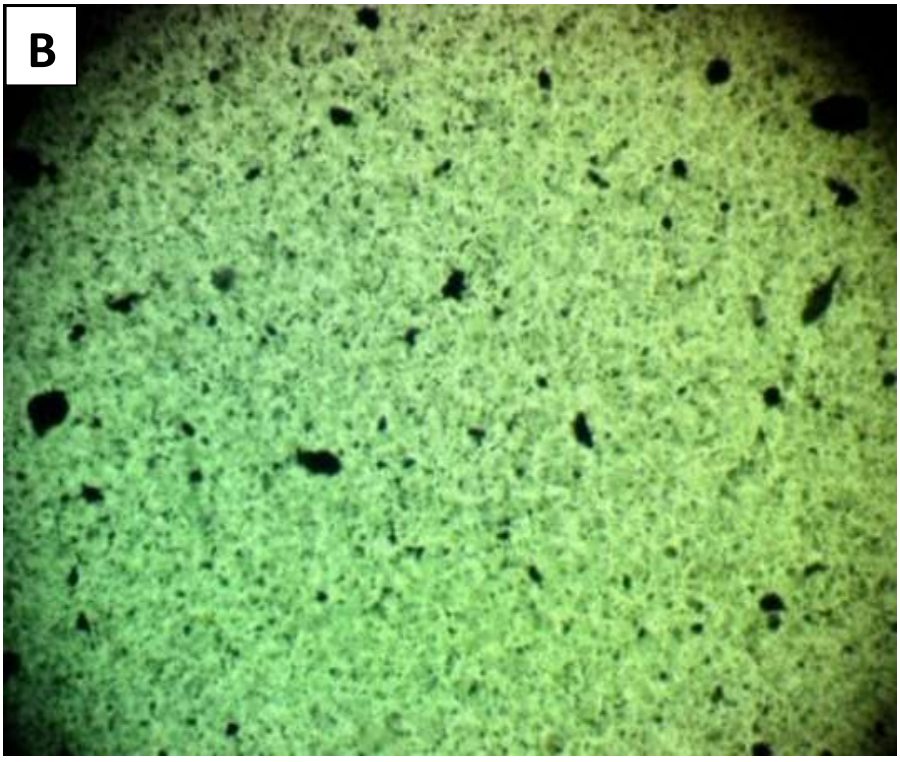
B

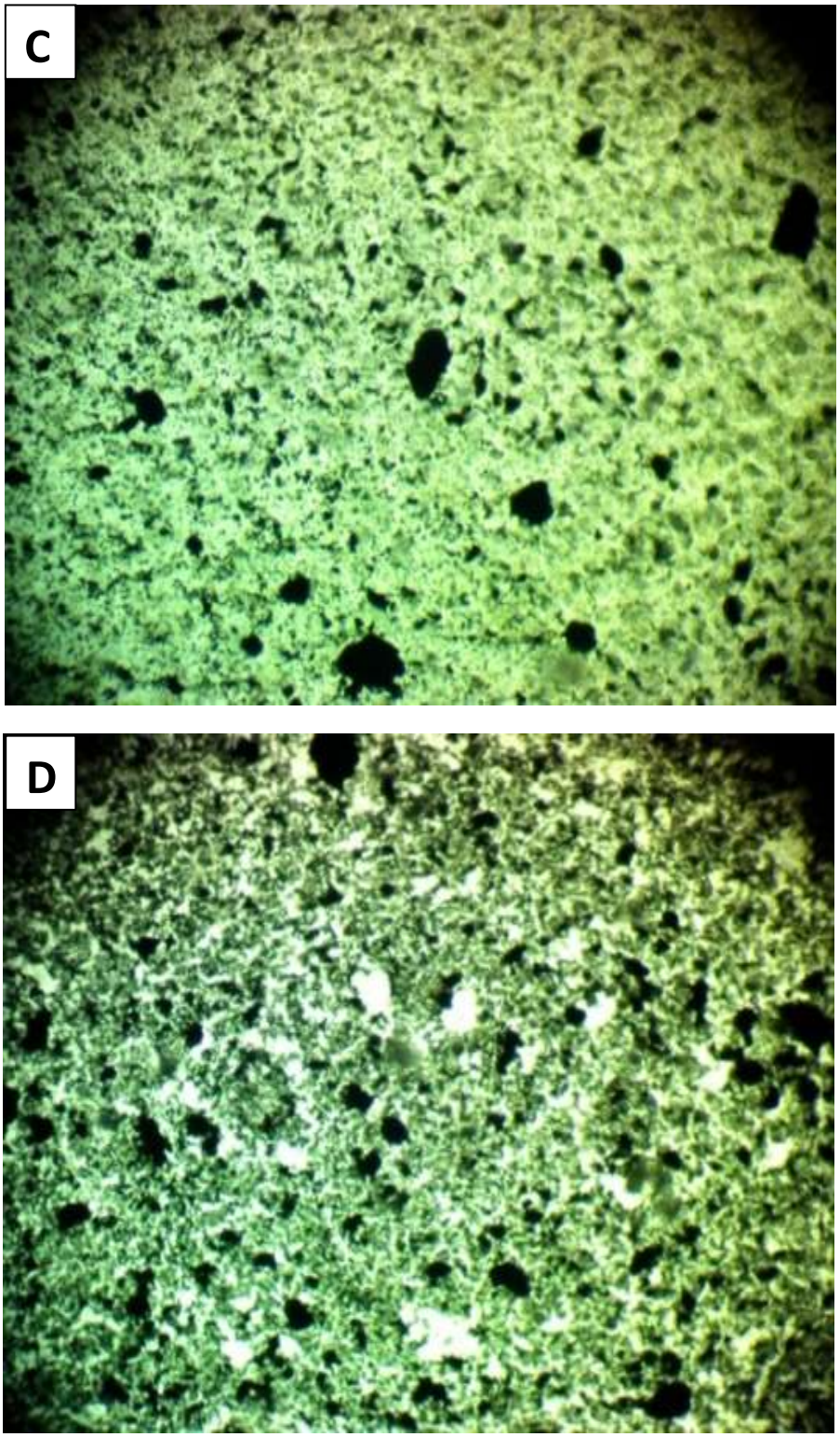


**Figure (4.2): Photomicrographs (100X) of PVA-PAAm with various content of CuNW: (A) 0 wt.% (B) 0.5 wt.% (C) 1 wt.% and (D) 2 wt.% with thickness of 90 µm.**

### 4.2.2 Scanning electron microscopy measurements (SEM)

Scanning Electron Microscopy was used to investigate the surface morphology of samples and the dispersion of CuNW in the polymers matrix. Figures (4.3 and 4.4) with two different thicknesses show an SEM micrograph of the surface of the PVA-PAAm blend and PVA-PAAm:CuNW nanocomposites films. From the images (A, B) in figure (4.3 and 4.4) uniform morphology revealing a rather soft surface. In figure (4.3 and 4.4) (C, D), the increase of the ratio of CuNW in a polymer matrix for the PVA-PAAm:CuNW nanocomposites led to changes in the morphology of the surface and increase the roughness. The nanocomposite films show many CuNW that were fine dispersion without aggregates with well-distributed and spread densely on the surface, this may be indicating the occurrence of a homogeneous growth mechanism. When comparing the two thicknesses (120, 90) µm, it can see that the increase the thickness, the decreases roughness. The results are consistent with optical microscopy, and the results of the previous researchers [92].

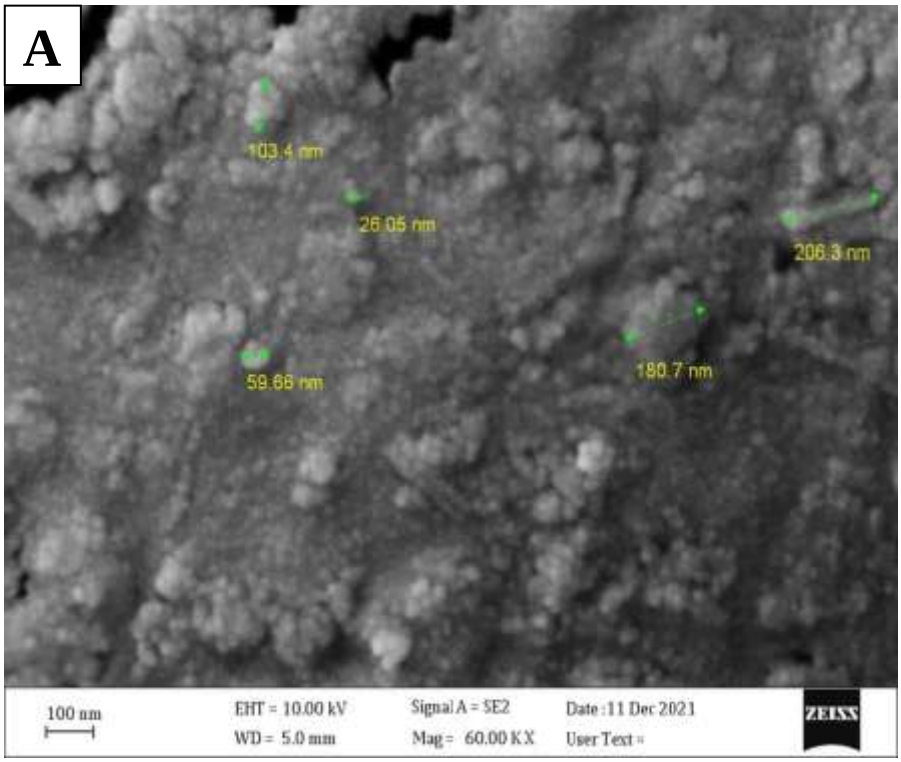
A
103.4 nm
26.05 nm
206.3 nm
59.66 nm
180.7 nm
100 nm
EHT = 10.00 kV
WD = 5.0 mm
Signal A = SE2
Mag = 60.00 K X
Date :11 Dec 2021
User Text =
ZEISS


B
104.0 nm
75.91 nm
22.33 nm
37.22 nm
51.74 nm
100 nm
EHT = 10.00 kV
WD = 5.0 mm
Signal A = SE2
Mag = 60.00 K X
Date :11 Dec 2021
User Text =
ZEISS

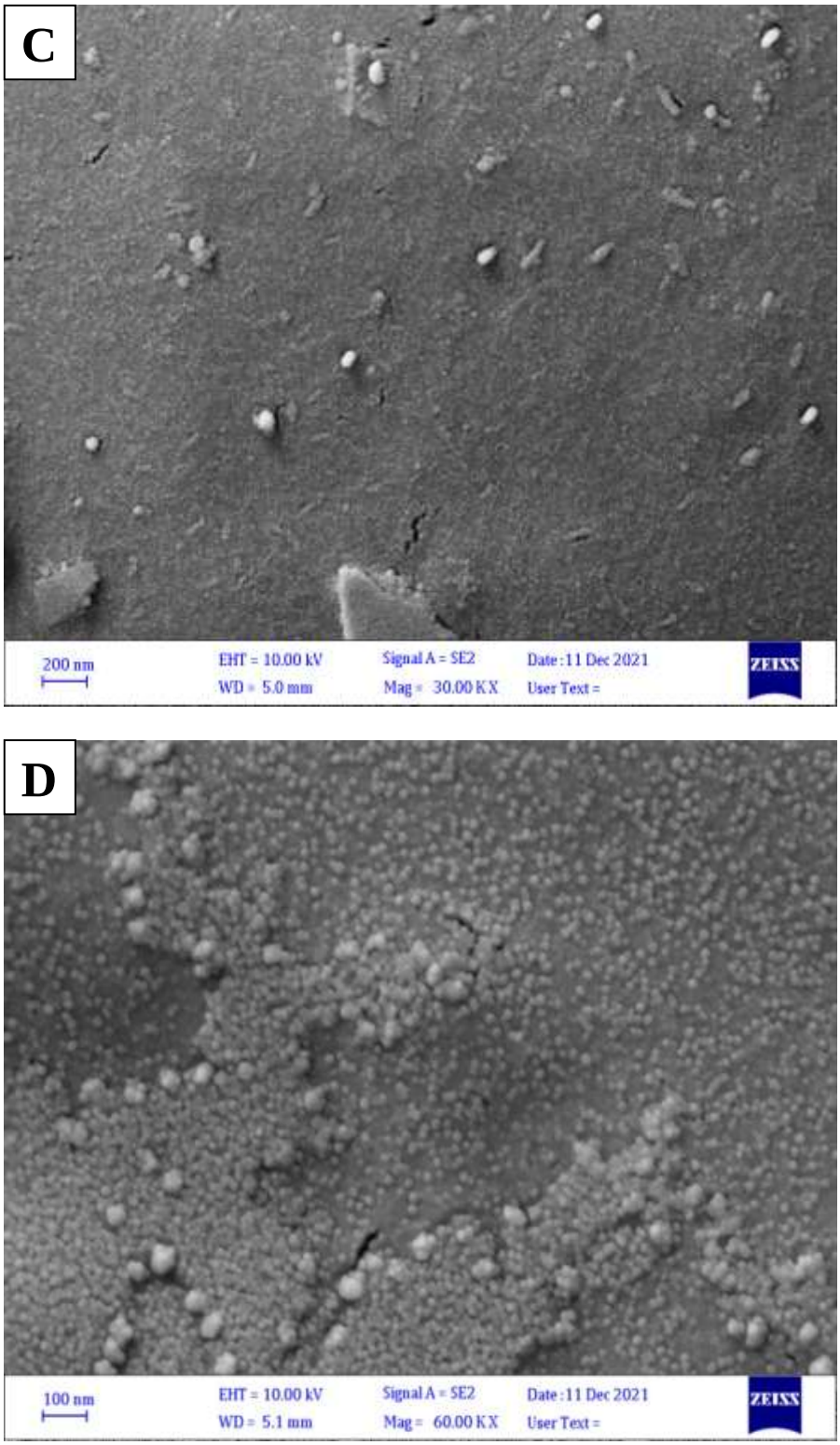


**Figure (4.3): SEM images of PVA-PAAm with various content of CuNW: (A) 0 wt.% (B) 0.5 wt.% (C) 1 wt.% and (D) 2 wt.% with thickness of 120 µm.**

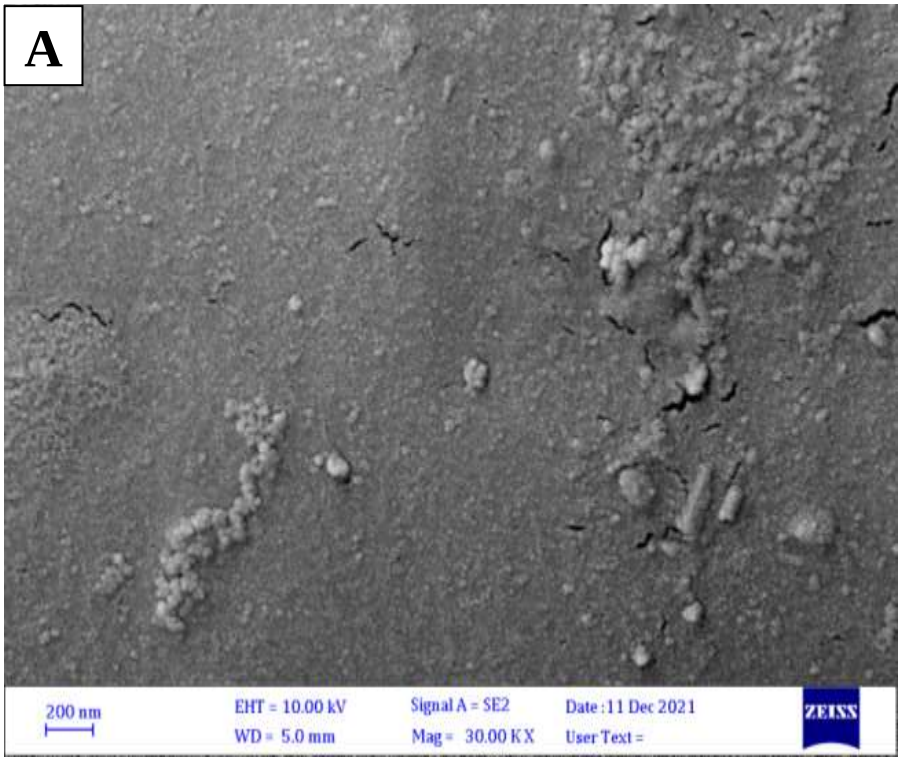
A
200 nm
EHT = 10.00 kV
WD = 5.0 mm
Signal A = SE2
Mag = 30.00 K X
Date :11 Dec 2021
User Text =
ZEISS


B
100 nm
EHT = 10.00 kV
WD = 5.0 mm
Signal A = SE2
Mag = 60.00 K X
Date :11 Dec 2021
User Text =
ZEISS

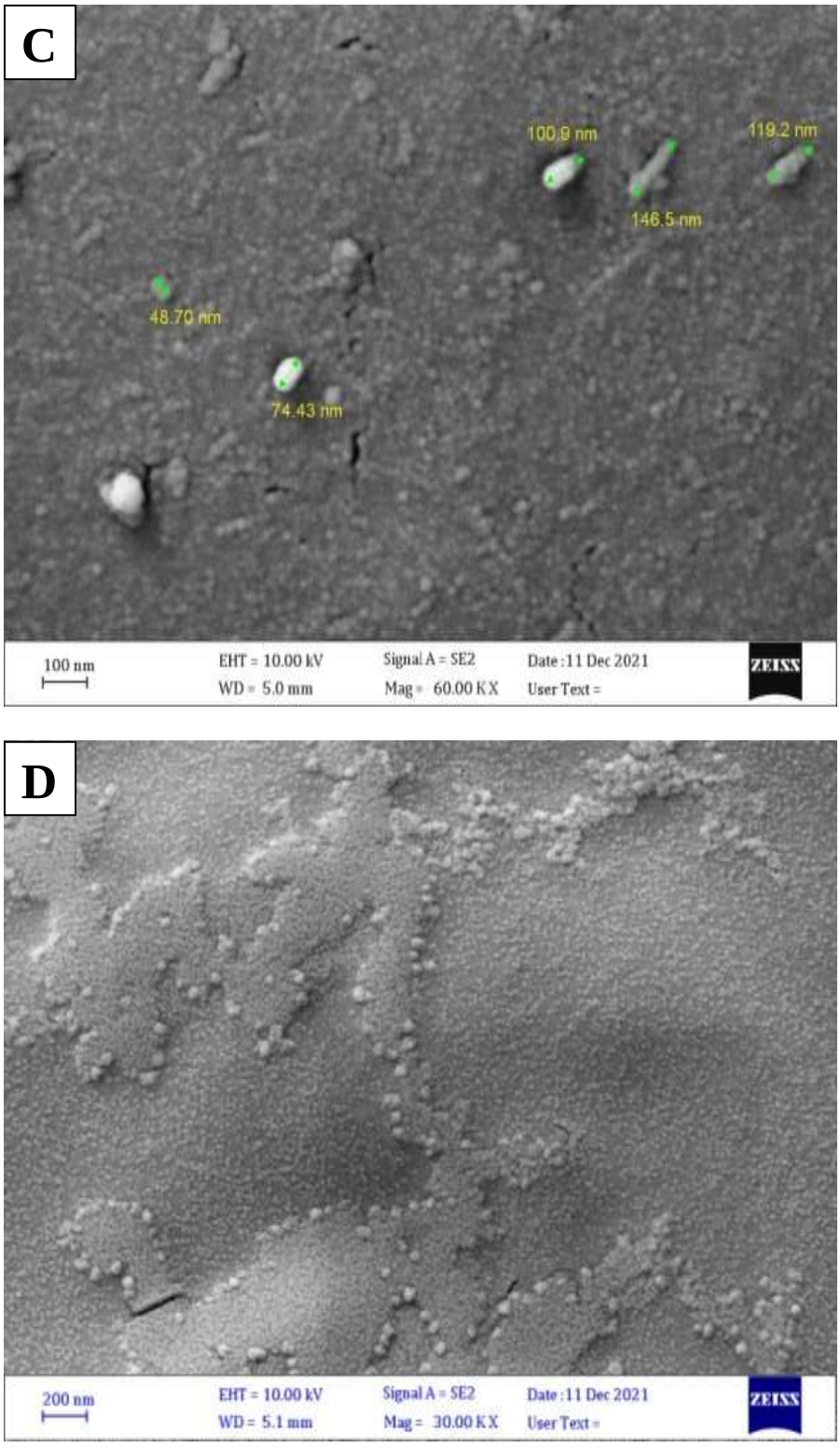


**Figure (4.4): SEM images of PVA-PAAm with various content of CuNW: (A) 0 wt.% (B) 0.5 wt.% (C) 1 wt.% and (D) 2 wt.% with thickness of 90 µm.**

### 4.2.3 Fourier transform infrared rays (FTIR)

The FTIR spectra of PVA-PAAm:CuNW nanocomposites with the different ratio of CuNW and different thicknesses were recorded at room temperature in the region (4000-500) $cm^{-1}$ as shown in figures (4.5 and 4.6). The spectra exhibited characteristic bands of stretching and bending vibrations of the functional groups formed in composites. From these spectra it can be noted that the absorption peaks at about (3280.78, 3284.93, and 3275.87) $cm^{-1}$ were attributed assigned to the stretching vibration of hydroxyl group (OH) in the polymer matrix chain [93]. As for the absorption peak at (2937.04) $cm^{-1}$ were attributed to methylene (C-H) stretching while the band (1732.54) $cm^{-1}$ were attributed to carboxyl acid (C=O) stretching [94]. Meanwhile, the functional groups at (1238.76, 1240.38, and 1242.67) $cm^{-1}$ of all them attributed to carbon dioxide (C-O) stretching [95]. At (1084.01) $cm^{-1}$, the peak is recognized as (C-C) stretching vibration [96]. FTIR spectra shows a shift in peak position as well as the change in shape and intensity comparing with pure PVA-PAAm films also it can be noticed that the peak at 3300 $cm^{-1}$ which belong to PVA polymer and represent the (OH) stretching vibration bond, did not appear in these peaks, while the peaks (3280.78, 3284.93, and 3275.87) $cm^{-1}$ that belonged to (OH) stretching vibration appeared. As well the peak at 1141 $cm^{-1}$ which belong to PVA polymer and represent the C-O stretching bond, while the peak 1323 $cm^{-1}$ that belongs to PAAm polymer did not appear in these peaks. Instead the peaks (1238.76, 1240.38, and 1242.67) $cm^{-1}$ that associated with C-O stretching appeared. There is a simple shift in the (C-H) stretching bond which represent PVA and PAAm polymer, that move and become at 2937.04 $cm^{-1}$, instead of the 2940 $cm^{-1}$ and 2931 bond for the same polymer which also goes back to (C-H) stretching. As well there is a simple shift in the (C=O) stretching bond, which represent

PVA polymer that move and become at 1732.54 $cm^{-1}$ instead of the 1731 $cm^{-1}$ bond for the same polymer which also goes back to (C=O) stretching, and there is a simple shift in the (C-C) stretching bond which represent PVA polymer that move and become at 1084.01 $cm^{-1}$ rather than the 1087 $cm^{-1}$ bond for the same polymer which also goes back to (C-C) stretching [25,30]. CuNW did not appear in the FTIR spectrum because it appears at the wave number less than 500 $cm^{-1}$. Also it can be noticed that there is a decrease in transmittance with increasing the proportion of CuNW. The increased density of the films means an increase of atoms and ions in the light path and increase the absorbance at UV invers the IR, as shown in figures (4.5 and 4.6) as in the images (B, C and D). When comparing the two thicknesses (120, 90) µm, the results showed that the change of films thickness had a slight effect. The results agree with the results of the previous researchers [43].

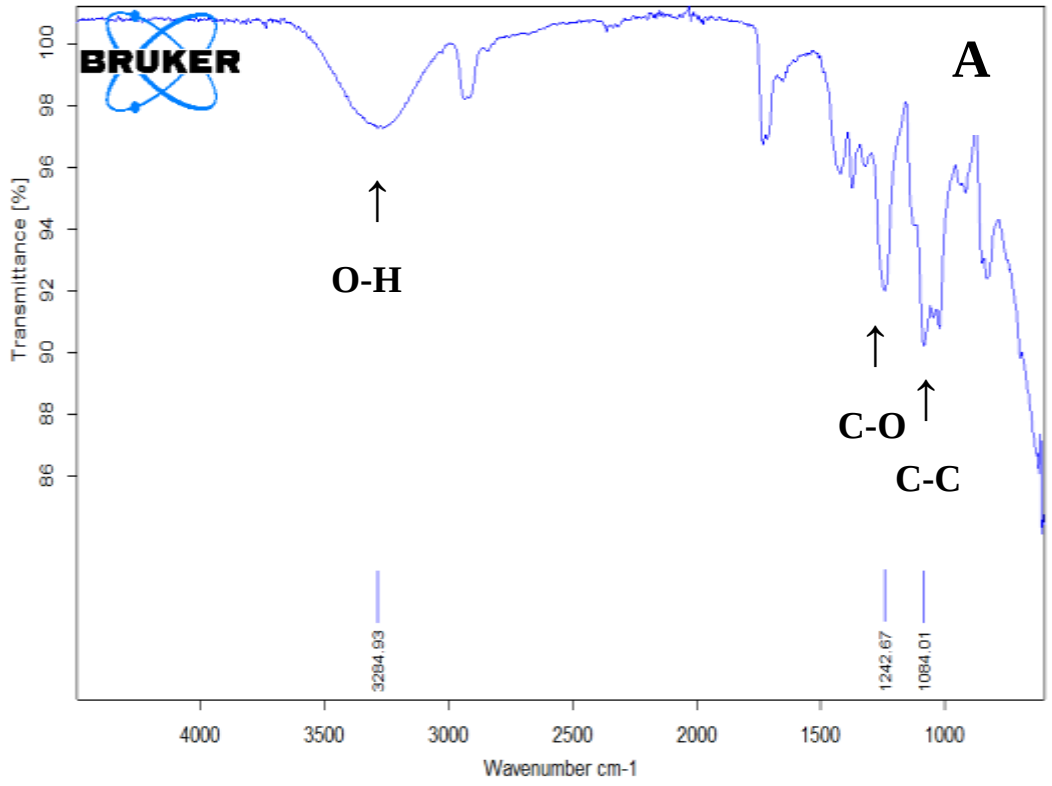
BRUKER
A
O-H
C-O
C-C
Transmittance [%]
100
98
96
94
92
90
88
86
3284.93
1242.67
1084.01
4000
3500
3000
2500
2000
1500
1000
Wavenumber cm-1

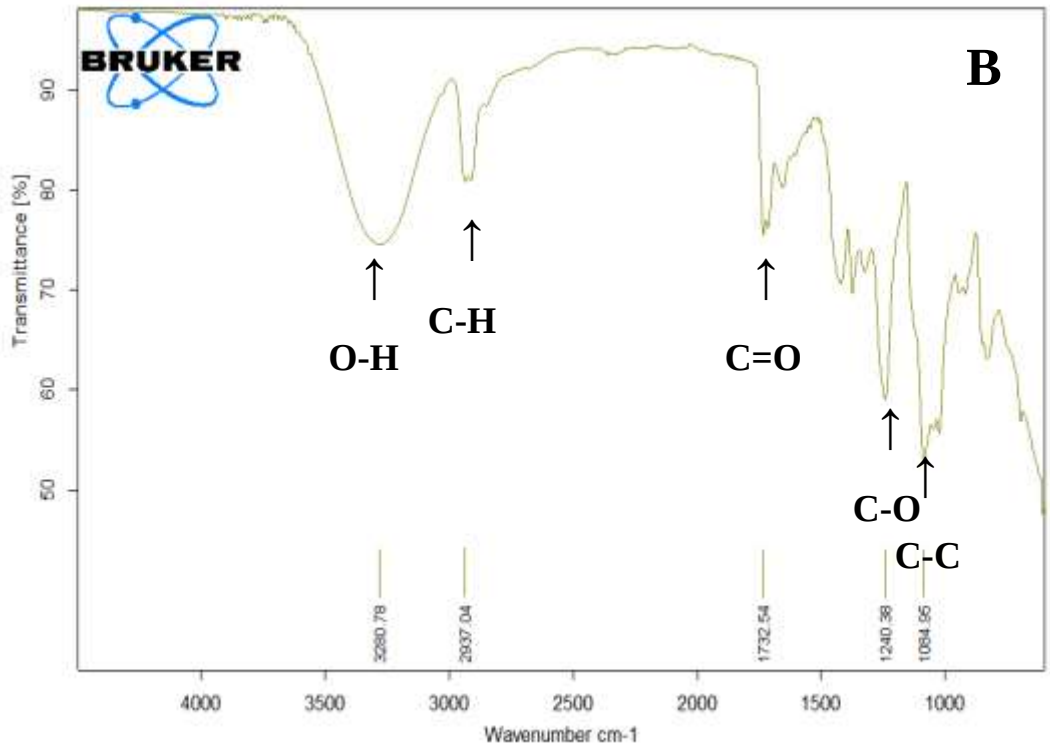
BRUKER
B
O-H
C-H
C=O
C-O
C-C
Transmittance [%]
90
80
70
60
50
3280.78
2937.04
1732.54
1240.38
1084.95
4000
3500
3000
2500
2000
1500
1000
Wavenumber cm-1

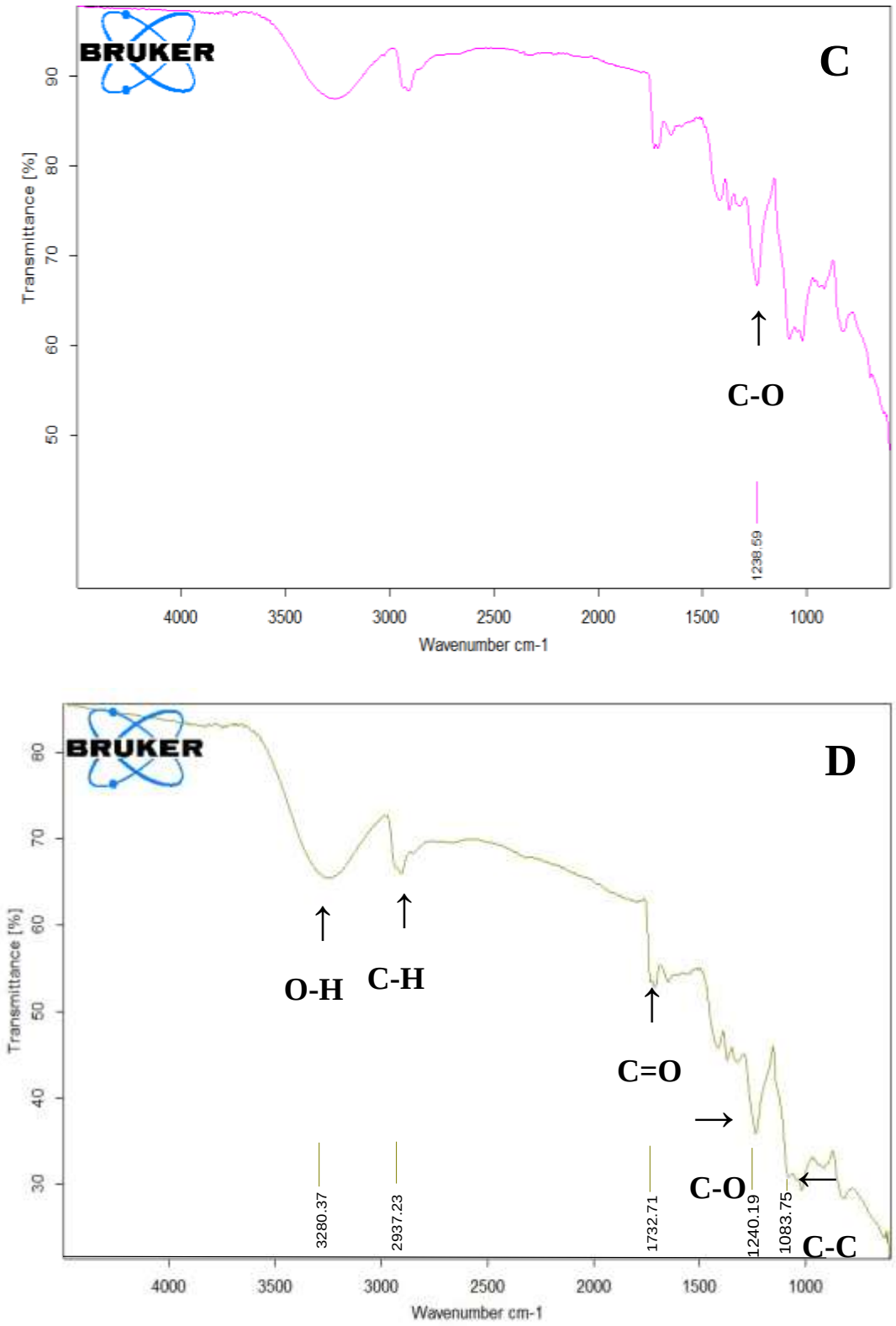


**Figure (4. 5) : FTIR spectra of PVA-PAAm with various content of CuNW: (A) 0 wt.% , (B) 0.5 wt.% (C) 1 wt.% and (D) 2 wt.% with thickness of 120 µm.**

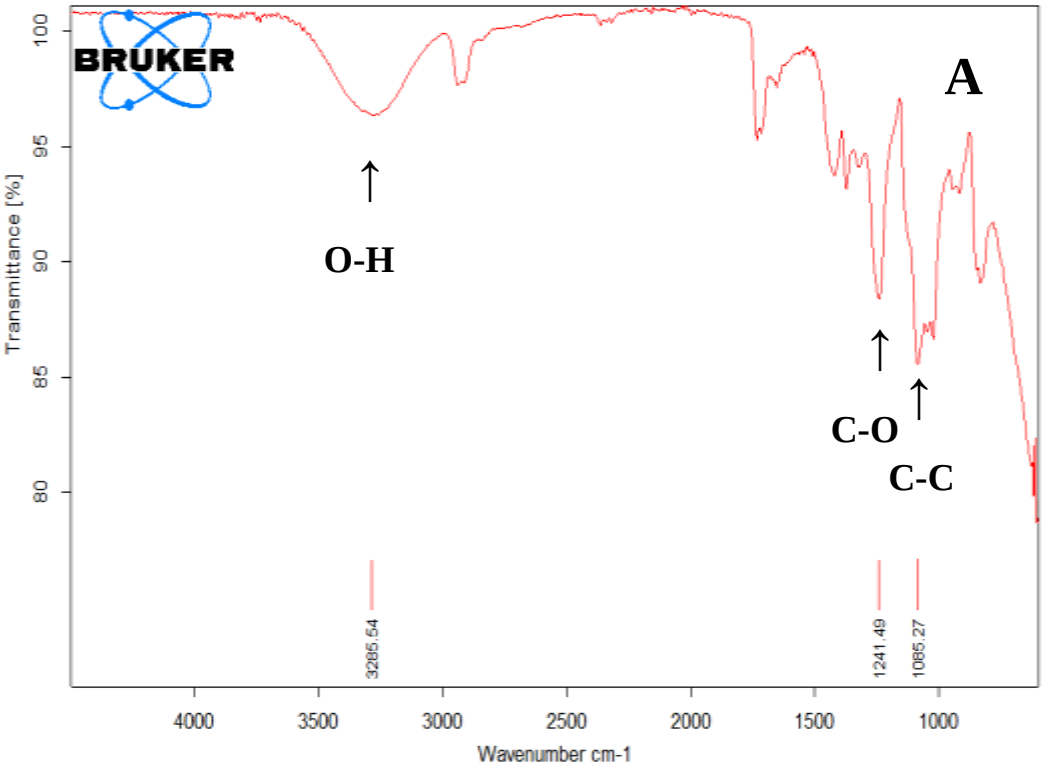
BRUKER
A
O-H
C-O
C-C
Transmittance [%]
100
95
90
85
80
3285.54
1241.49
1085.27
4000
3500
3000
2500
2000
1500
1000
Wavenumber cm-1

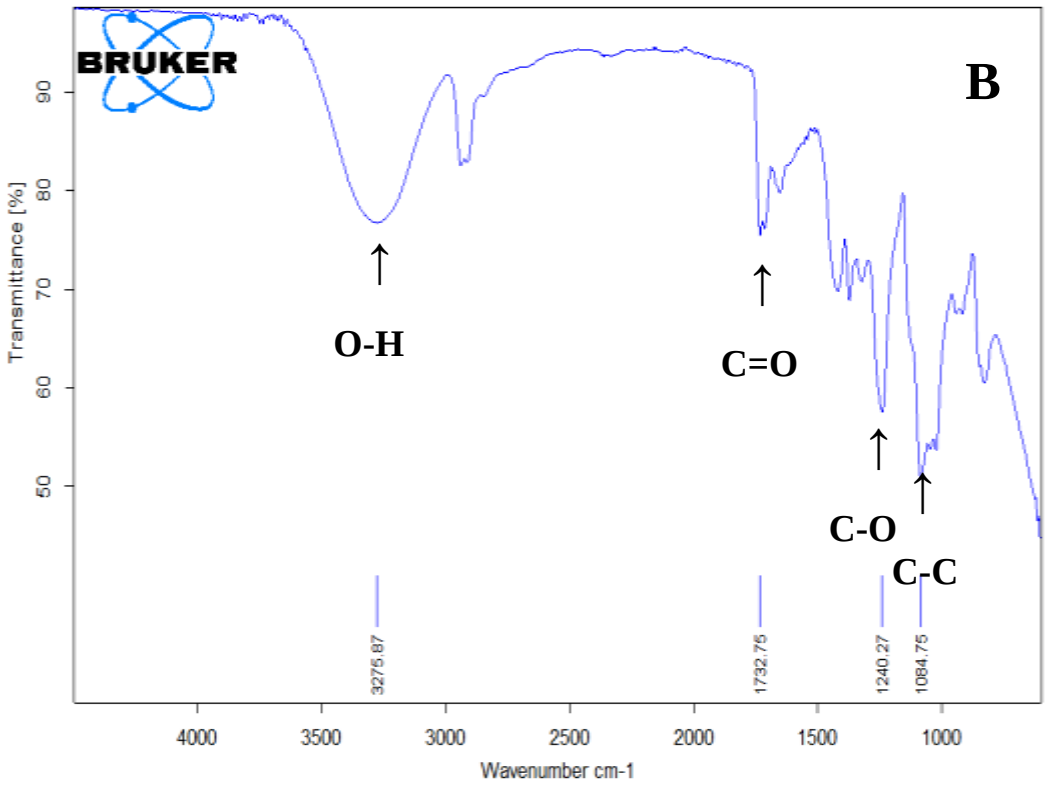
BRUKER
B
O-H
C=O
C-O
C-C
Transmittance [%]
90
80
70
60
50
3275.87
1732.75
1240.27
1084.75
4000
3500
3000
2500
2000
1500
1000
Wavenumber cm-1

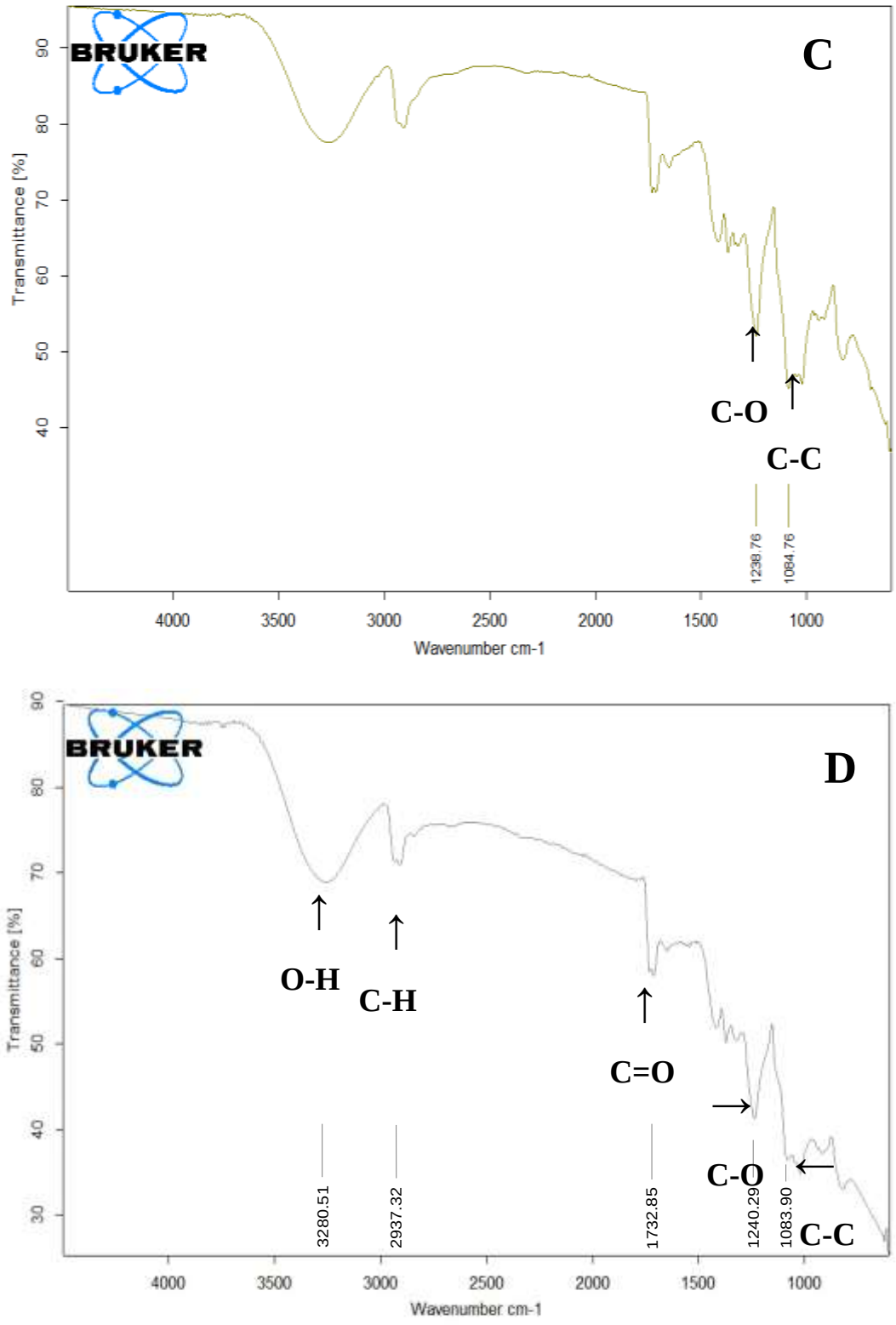


**Figure (4. 6) : FTIR spectra of PVA-PAAm with various content of CuNW: (A) 0 wt.% (B) 0.5 wt.% (C) 1 wt.% and (D) 2 wt.% with thickness of 90 µm.**

## 4.3 The Optical Properties

The main purpose of studying the optical properties of the PVA-PAAm:CuNW nanocomposites is to identify the effect of CuNW adding on the optical properties. The research covers the recording of the spectrum of absorbance of the PVA-PAAm:CuNW films at the room temperature and calculating the absorption coefficient, extinction coefficient and other optical constants, as well as identifying the types of electronic transitions and calculating energy gaps

### 4.3.1 Absorbance (A)

The absorbance of PVA-PAAm:CuNW nanocomposites with two different thicknesses with varies concentration of CuNW for wavelength range (200-1100) nm was recorded at room temperature. Figures (4.7and 4.8), display the variation of optical absorbance with wavelength of PVA-PAAm:CuNW nanocomposites. From these figures it can be noted that the spectra reveal that all the films show more absorbance in ultraviolet region. All nanocomposites show that low absorbance in the visible region, this behavior can be explained as follows: at high wavelength the incident photons doesn't have enough energy to interact with atoms and thus the photon will be transmitted. When the wavelength decreases (at the neighborhood of the fundamental absorption edge), the interaction between incident photon and material will occur, and the photon will be absorbance. The absorbance increases with the increasing of weight percentages of the nanomaterials. This is due to absorb the incident light by free electrons. When compare the absorbance of the two thicknesses (120, 90) μm, it can seen that films with thickness 120 μm has a slightly higher absorbance than films with thickness 90 μm. The results agree with the results of the previous researchers [44, 97].

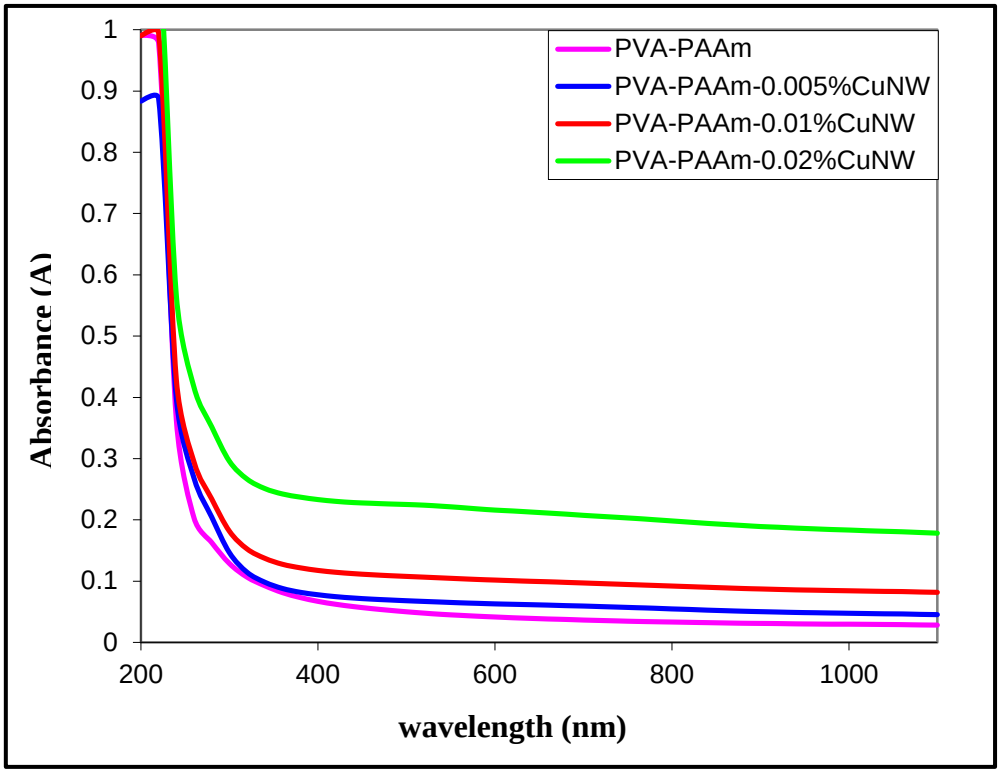


**Figure (4.7): The absorbance spectra as a function of wavelength of PVA-PAAm Blend and PVA PAAm:CuNW Nanocomposites with thickness of 120 µm.**

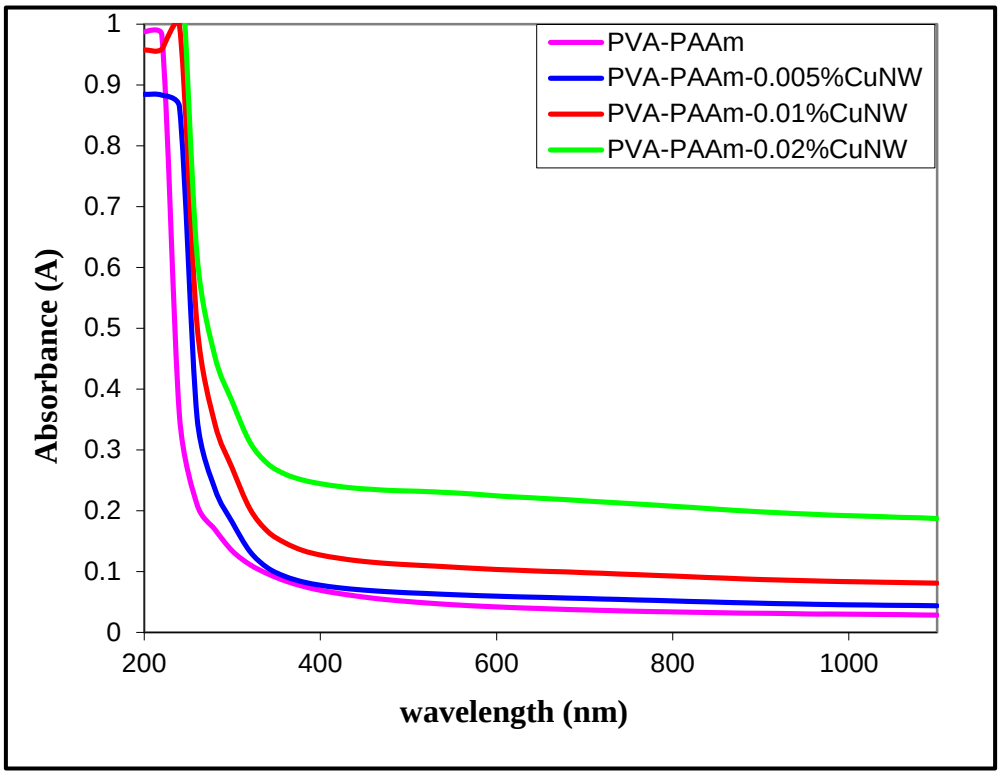


**Figure (4.8): The absorbance spectra as a function of wavelength of PVA-PAAm Blend and PVA-PAAm:CuNW Nanocomposites with thickness of 90 µm.**

### 4.3.2 Transmittance (T)

The transmittance (T) was calculated using equation (2.3). Figures (4.9 and 4.10) with two different thicknesses show that the transmittance spectrum as function of wavelength of PVA-PAAm:CuNW nanocom-posities. It can noticed the transmittance is increased with an increasing wavelength and the decreases in transmittance with increasing concentration of CuNW. This is caused by the added CuNW, that contain electrons which absorb electromagnetic energy and move to a higher level. As for (pure) film, it has high transmittance due to the absence of particles. It does not have free electrons and needs high energy to transition to break the bonds. When compare the transmittance of the two thicknesses (120, 90) µm, it can seen that films with thickness 120 µm has a slightly less transmittance than films with thickness 90 µm. The results agree with the results of the previous researchers [ 98].

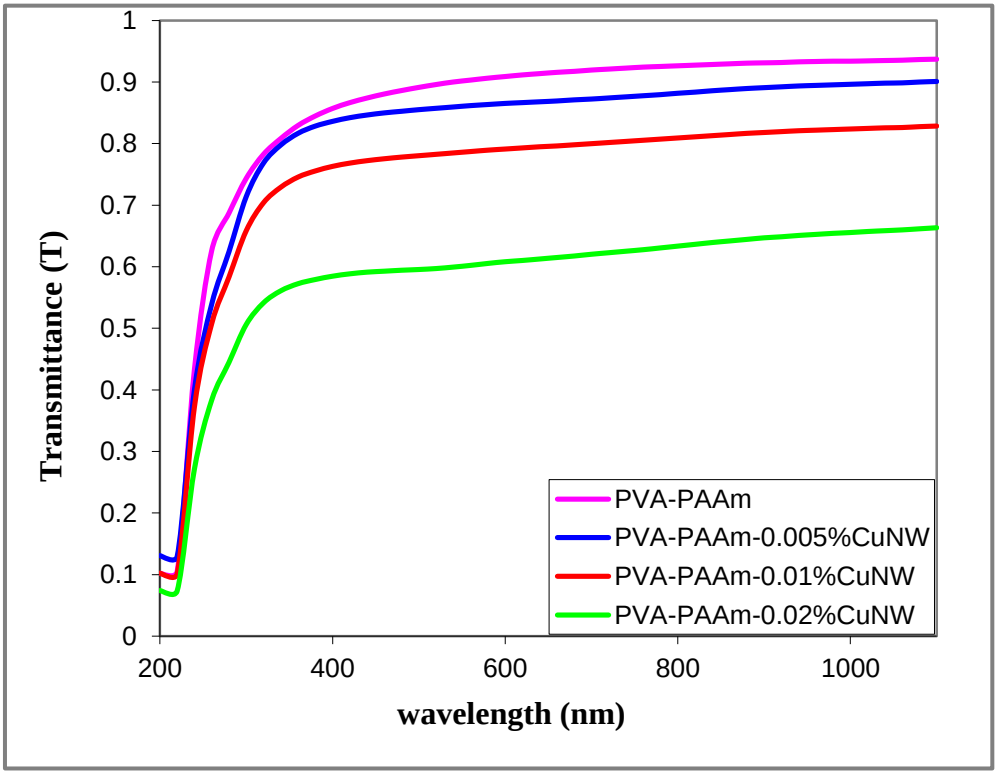


**Figure (4.9): The transmittance versus wavelength of PVA-PAAm Blend and PVA-PAAm:CuNW Nanocomposites with thickness of 120 µm.**

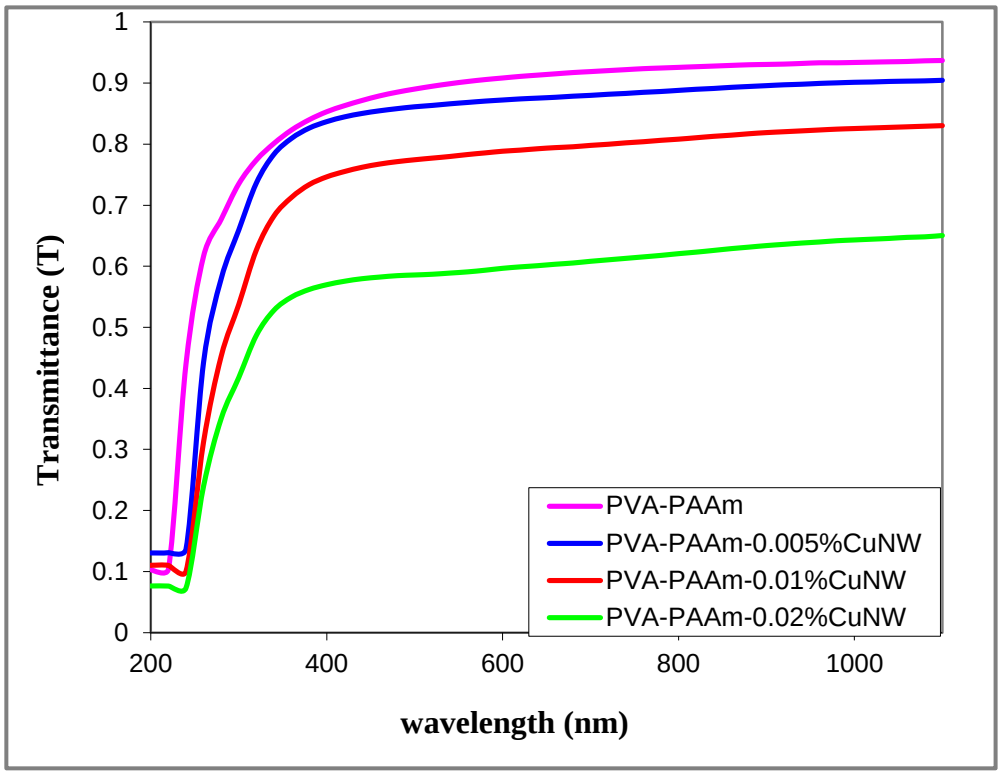


**Figure (4. 10): The transmittance versus wavelength of PVA-PAAm Blend and PVA-PAAm:CuNW Nanocomposites with thickness of 90 µm.**

### 4.3.3 Refractive index (n)

The refractive index was calculated from equation (2.7). Figures (4.11 and 4.12) with two different thicknesses show the change of refraction index of PVA-PAAm:CuNW nanocomposites as a function of wavelength. From the figures it can seen that the refractive index increases with increasing the weight percentages of the concentration of CuNW in the polymers, also it is decreased with the increase of the wavelength. This behavior attributed to the increase of the density of nanocomposites. When the incident light interacts with a sample has high refractivity at UV region, hence, the values of refractive index will be increased. When compare the refractive index of the two thicknesses (120, 90) µm, it can seen that films with thickness 120 µm has a slightly higher refractive

index than films with thickness 90 µm. The results agree with the results of the previous researchers [45, 99].

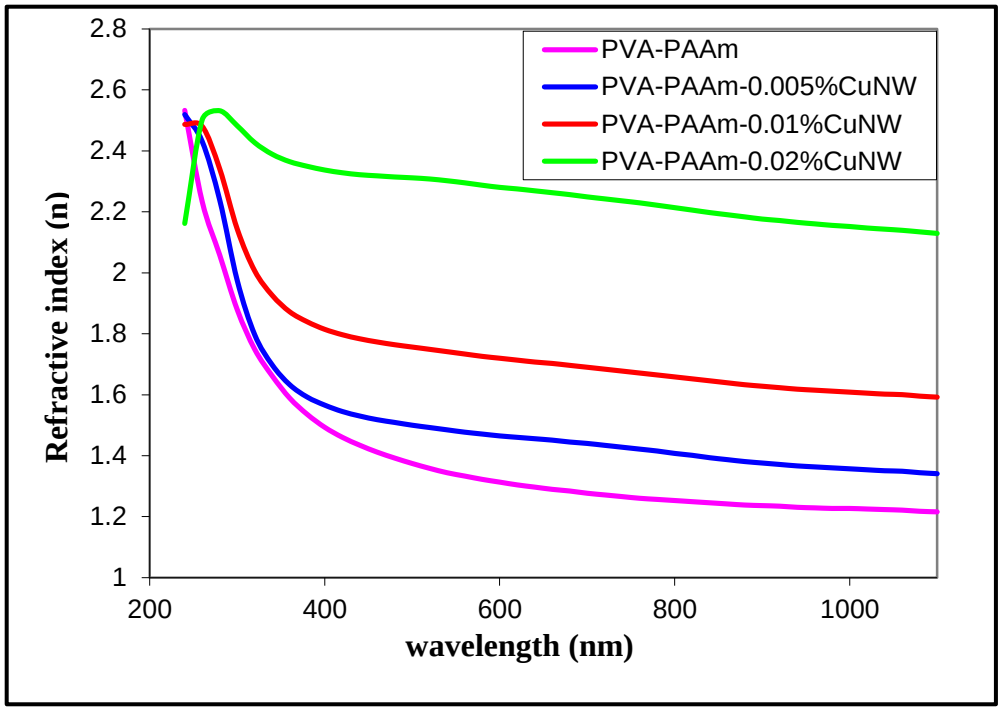


**Figure (4.11): The refractive index (n) as a function of wavelength of PVA-PAAm Blend and PVA-PAAm:CuNW Nanocomposites with thickness of 120µm.**

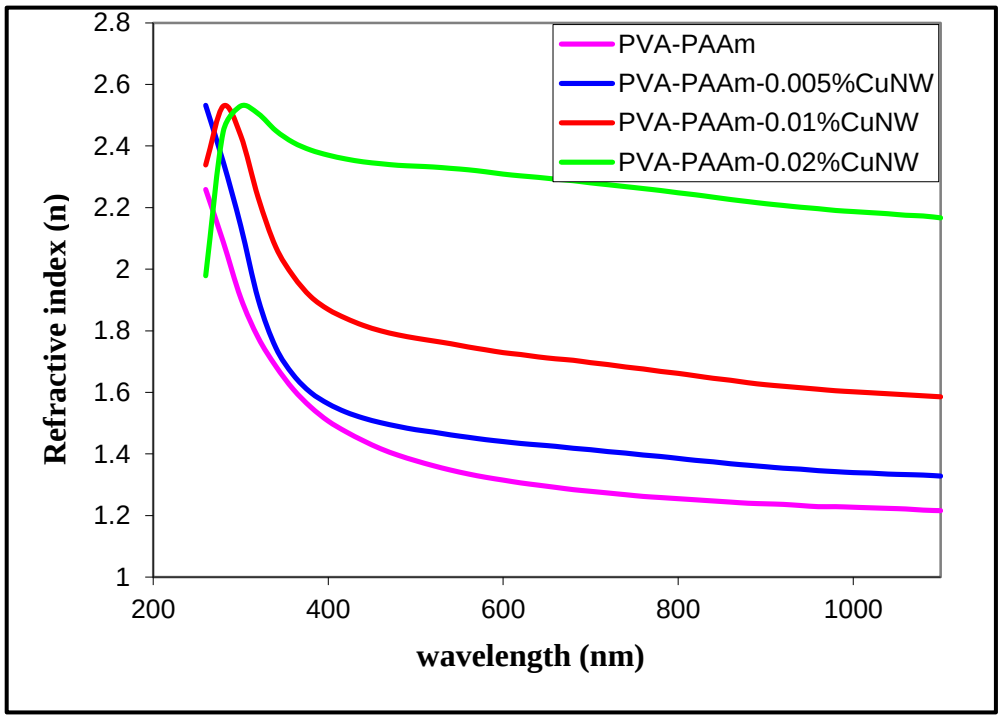


**Figure (4.12): The refractive index (n) as a function of wavelength of PVA-PAAm Blend and PVA-PAAm:CuNW Nanocomposites with thickness of 90µm.**

### 4.3.4 Extinction coefficient ($k_o$)

Extinction coefficient ($k_o$) was calculated using equation (2.8). The variation of the extinction coefficient of PVA-PAAm:CuNW nanocomposites as a function of wavelength shown in figure (4.13 and 4.14) with two different thicknesses. The figure shows that extinction coefficient increases with increasing the concentration of CuNW, this is due to the increase in optical absorption and photons dispersion in the PVA-PAAm polymer matrix. The extinction coefficient of nanocomposites has high values at UV region, this behavior attributed to high absorbance of the samples of nanocomposites. Also, extinction coefficient of nanocomposites increases with the increasing of the wavelength at visible and near infrared regions, which attributed to the absorption coefficient of nanocomposites that approximately constant at visible and near infrared region, hence, the extinction coefficient increases with the increasing of the wavelength. When we compare the extinction coefficient of the two thicknesses (120, 90) μm, it can seen that films with thickness 120 μm has a slightly higher extinction coefficient than films with thickness 90 μm. The results agree with the results of the previous researchers [100, 101].

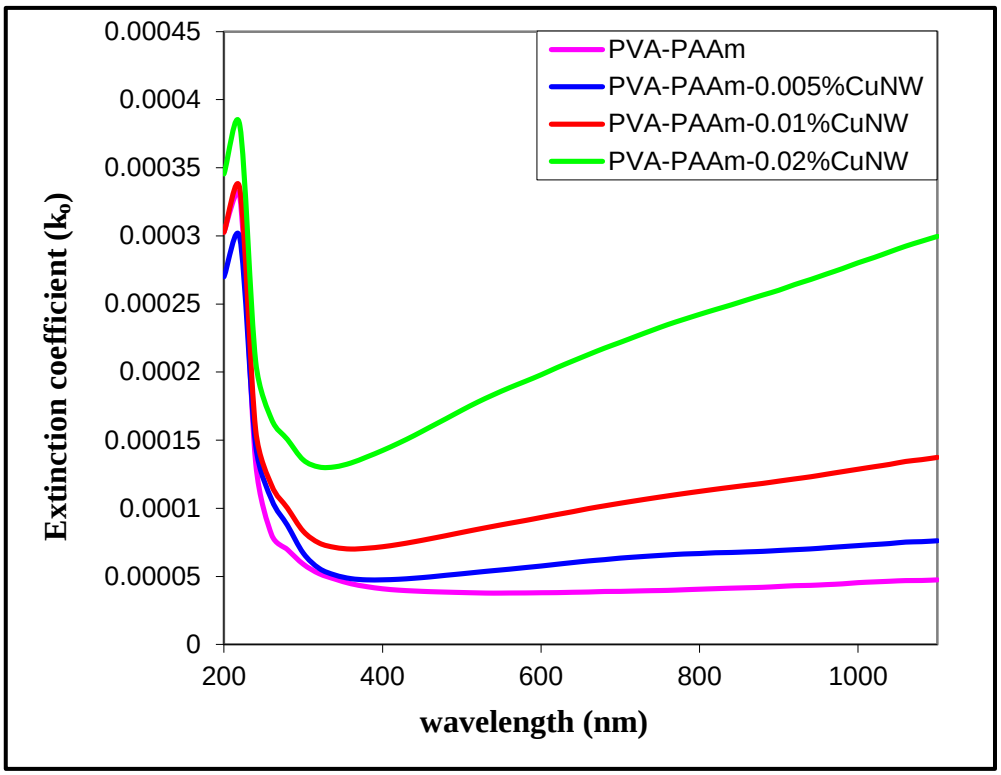


**Figure (4.13): Variation of Extinction coefficient with wavelength of PVA-PAAm Blend and PVA-PAAm:CuNW Nanocomposites with thickness of 120 µm.**

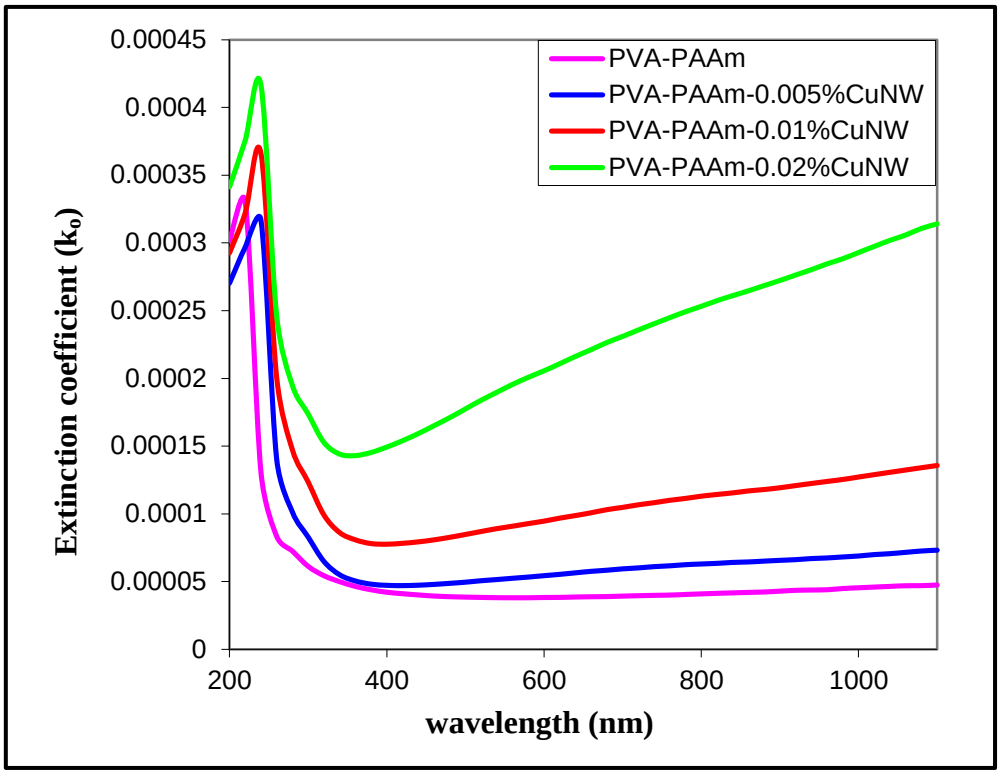


**Figure (4.14): Variation of Extinction coefficient with wavelength of PVA-PAAm Blend and PVA-PAAm:CuNW Nanocomposites with thickness of 90µm.**

### 4.3.5 The optical conductivity (σ)

The optical conductivity ($\sigma_{op}$) has been calculated using equation (2.9). As shown figures (4.15 and 4.16) with two different thicknesses show that the optical conductivity of the samples of composites that were decreases with the increasing of the wavelength, this behaviour, attributed to optical conductivity, was strongly dependent on the wavelength of the radiation incident on the composite samples; the increases in optical conductivity at low wavelengths of photon is due to high absorbance of all composite samples in this region, resulting in an increasing in charge transfer excitations. The optical conductivity spectra revealed that the samples transmit light in the visible and near-infrared ranges. Additionally, the optical conductivity of composites increases with the addition of CuNW this behavior is related to the formation of localized levels in the energy gap; an increases in the concentration of CuNW increasing the density of localized stages in the band structure. hence, increases of the absorption coefficient consequently increasing the optical conductivity of PVA-PAAm:CuNW composites. When compare the optical conductivity of the two thicknesses (120, 90) μm, it can seen than films with thickness 120 μm has a slightly higher the optical conductivity than films with thickness 90 μm. The results agree with the results of the previous researchers [102].

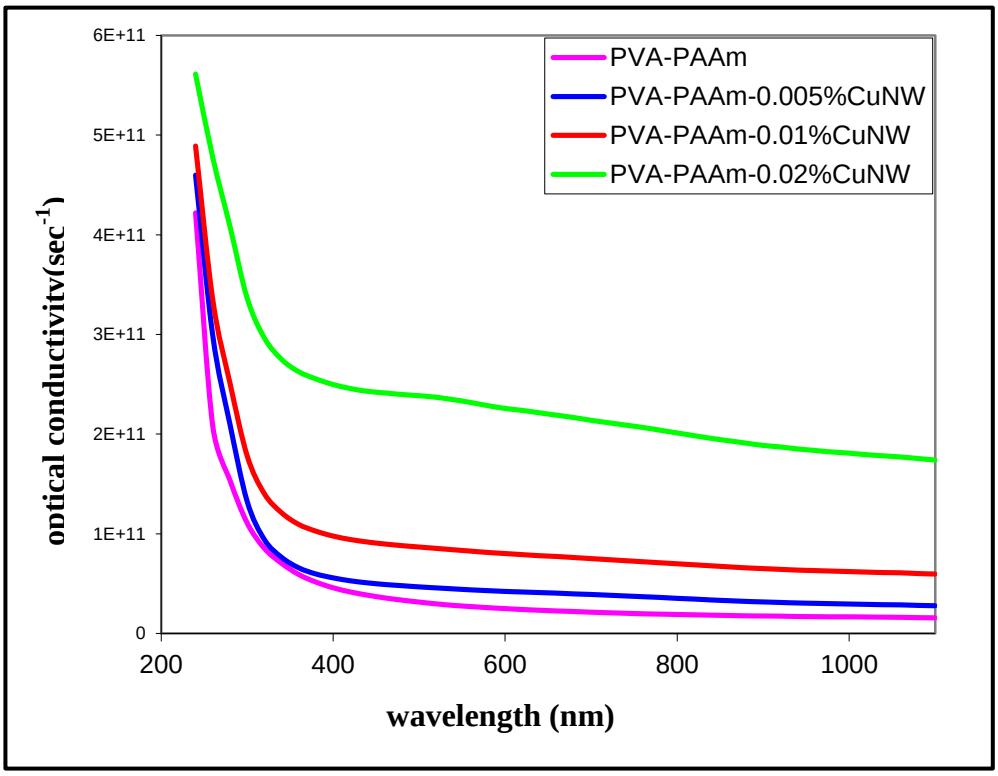


**Figure: (4.15): The optical conductivity versus wavelength of PVA-PAAm:CuNW Nanocomposites with various content of CuNW respectively wih thickness of 120 µm .**

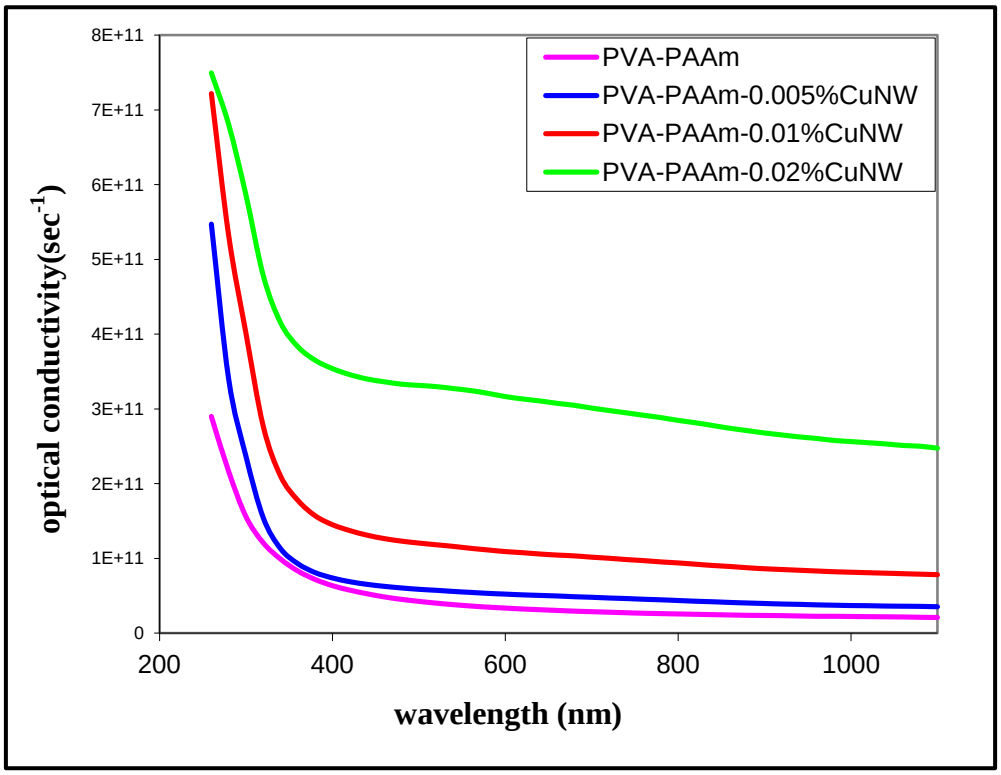


**Figure: (4.16): The optical conductivity versus wavelength of PVA-PAAm:CuNW Nanocomposites with various content of CuNW respectively with thickness of 90 µm.**

### 4.3.6 Real and imaginary parts of dielectric constant

The dielectric constant for two parts (real and imaginary) of PVA-PAAm:CuNW nanocomposites have been calculated from equation (2.14 and 2.15). The figures (4.17, 4.18, 4.19, and 4.20) with two different thicknesses show the variation dielectric constant for two parts (real and imaginary) as a function of the wavelength. These figures show that dielectric constant for two part real and imaginary were increased with the increasing of CuNW concentrations, this behavior attributed to the increase of electrical polarization due to contribution of concentration in the sample i.e., the increase in the dielectric constant of PVA-PAAm blends and PVA-PAAm:CuNW a fractional increase in charges within the polymers. As shown in the figures, the real and imaginary parts of dielectric constant of PVA-PAAm:CuNW and PVA-PAAm blends were changed with the wavelength, this was due to the real part of dielectric constant depends on refractive index because the effect of extinction coefficient is very small and the imaginary part of dielectric constant depends on extinction coefficient especially in the visible and near infrared regions of wavelength where the refractive index was approximately constant while extinction coefficient increases with the increase of the wavelength. When compare the dielectric constant of the two thicknesses (120, 90) μm, it can seen that the films with thickness 120μm has a slightly higher dielectric constant than films with thickness 90 μm. The results agree with the results of the previous researchers [103].

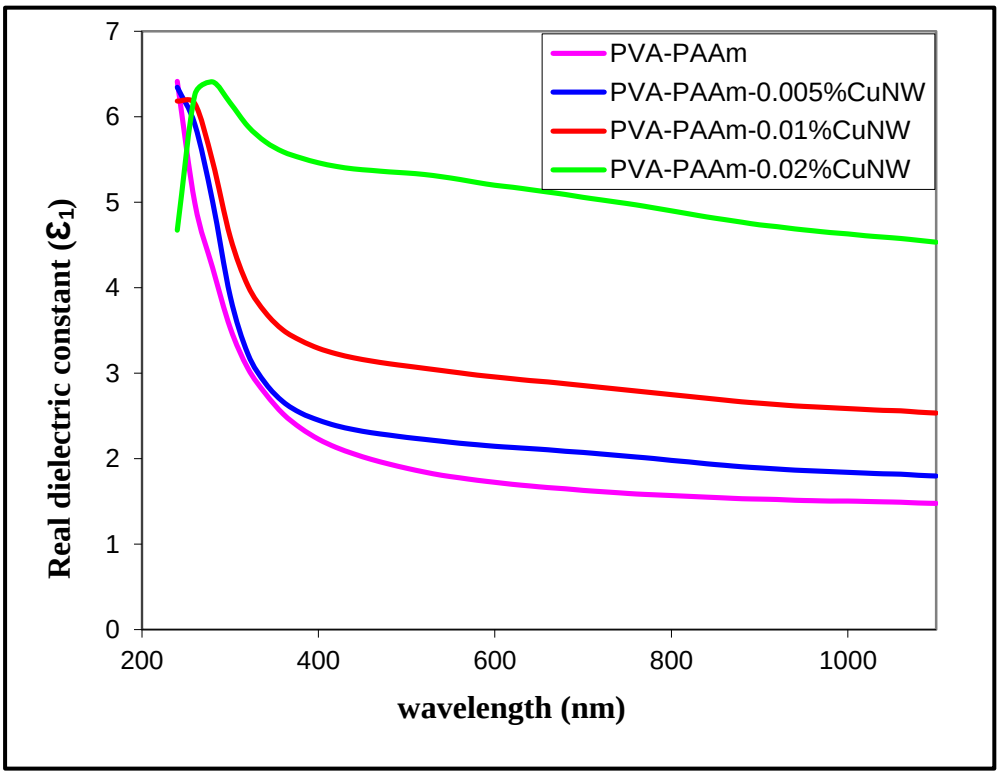


**Figure (4.17). The Real Dielectric Constant with the Wavelength of PVA-PAAm Blend and PVA-PAAm:CuNW Nanocomposite with thickness of 120 µm.**

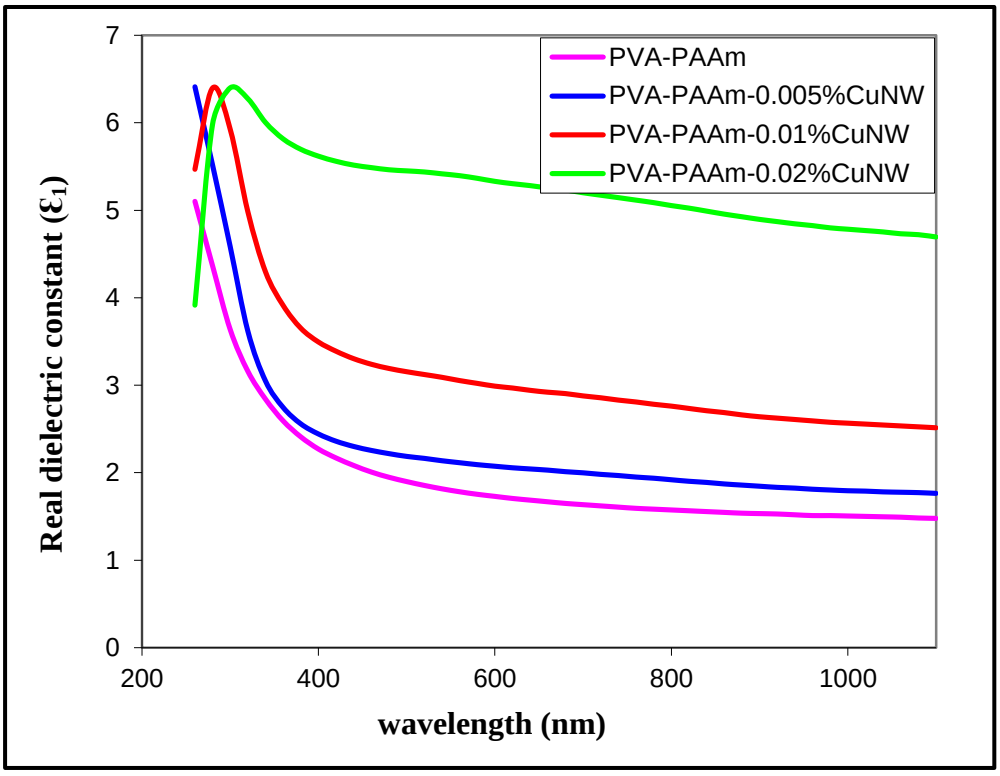


**Figure (4.18). The Real Dielectric Constant with the Wavelength of PVA-PAAm Blend and PVA-PAAm:CuNW Nanocomposite with thickness of 90 µm.**

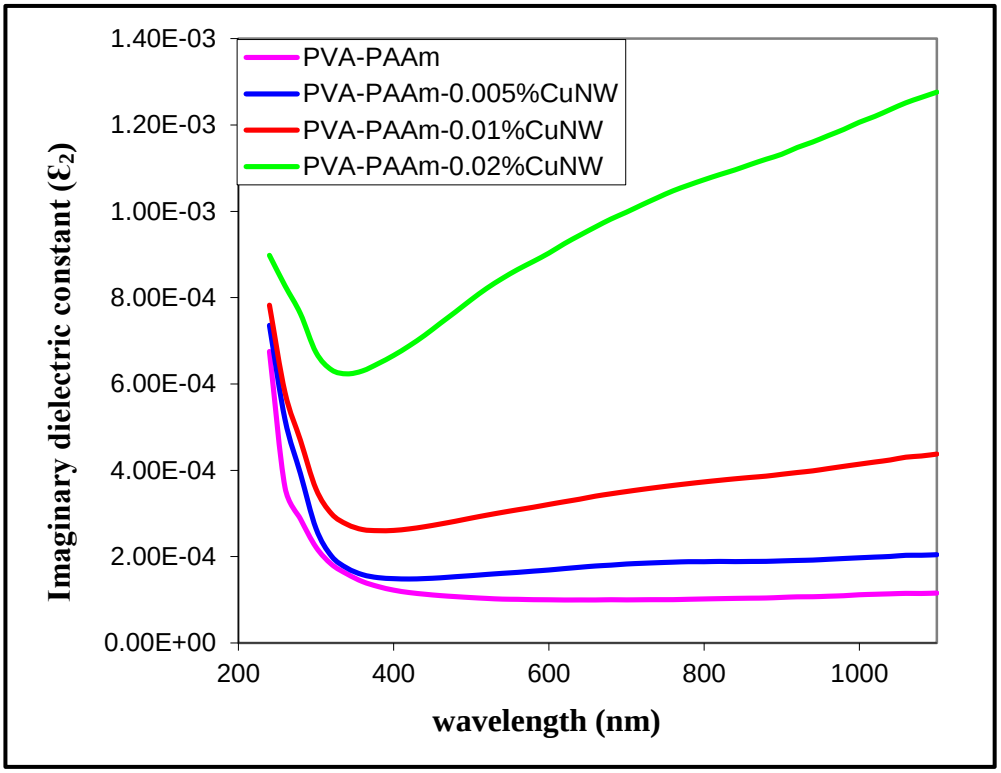


**Figure(4.19). The Imaginary Dielectric Constant with the Wavelength of PVA-PAAm Blend and PVA-PAAm:CuNW Nanocomposite with thickness of 120µm.**

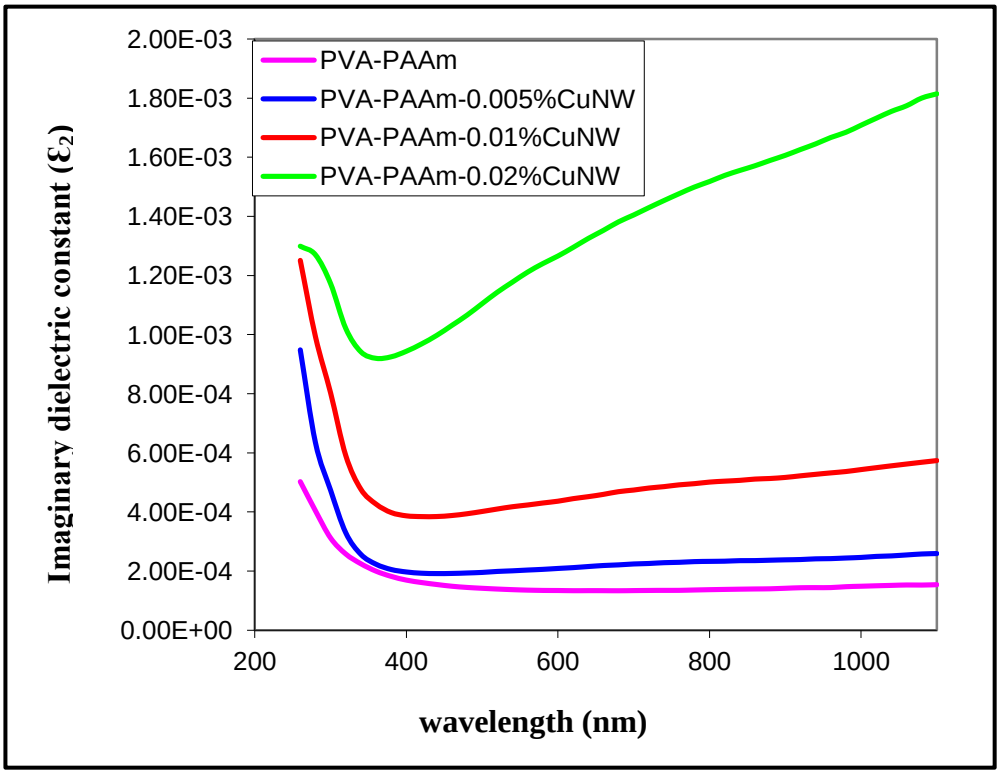


**Figure(4.20). The Imaginary Dielectric Constant with the Wavelength of PVA-PAAm Blend and PVA-PAAm:CuNW Nanocomposite with thickness of 90 µm.**

### 4.3.7 Absorption coefficient (α)

The absorption coefficient (α) was calculated using equation (2.20). Figures (4.21 and 4.22) with two different thicknesses as show the absorption coefficient (α) as a function of wavelength of PVA-PAAm:CuNW nanocomposites. It can be seen that the absorption coefficient is the smallest at high wavelength (low energy), this means that the possibility of electron transition is little because the energy of the incident photon is not sufficient to move the electron from the valence to the conduction band.

At high energies, absorption is greater; this means that a great possibility for electron transitions consequently, the energy of incident photon is enough to move the electron from the valence band to the conduction band. The energy of the incident photon is greater than the forbidden energy gap, this shows that the absorption coefficient assists in figuring out the nature of electron transition, when the values of the absorption coefficient are high ($\alpha > 10^4$ $cm^{-1}$) at high energies, It is expected that direct transition of electron occur, the energy and moment are maintained by the electrons and photons. While, when the values of the absorption coefficient are low ($\alpha < 10^4$ $cm^{-1}$) at low energies, it is expected that indirect transition of electron occurs, and the electronic momentum is maintained with the assistance of the phonon. When compare the absorption coefficient of the two thicknesses (120, 90) μm, it can seen that thickness 120 μm has a slightly higher the absorption coefficient than thickness 90 μm. The results agree with the results of the previous researchers [104].

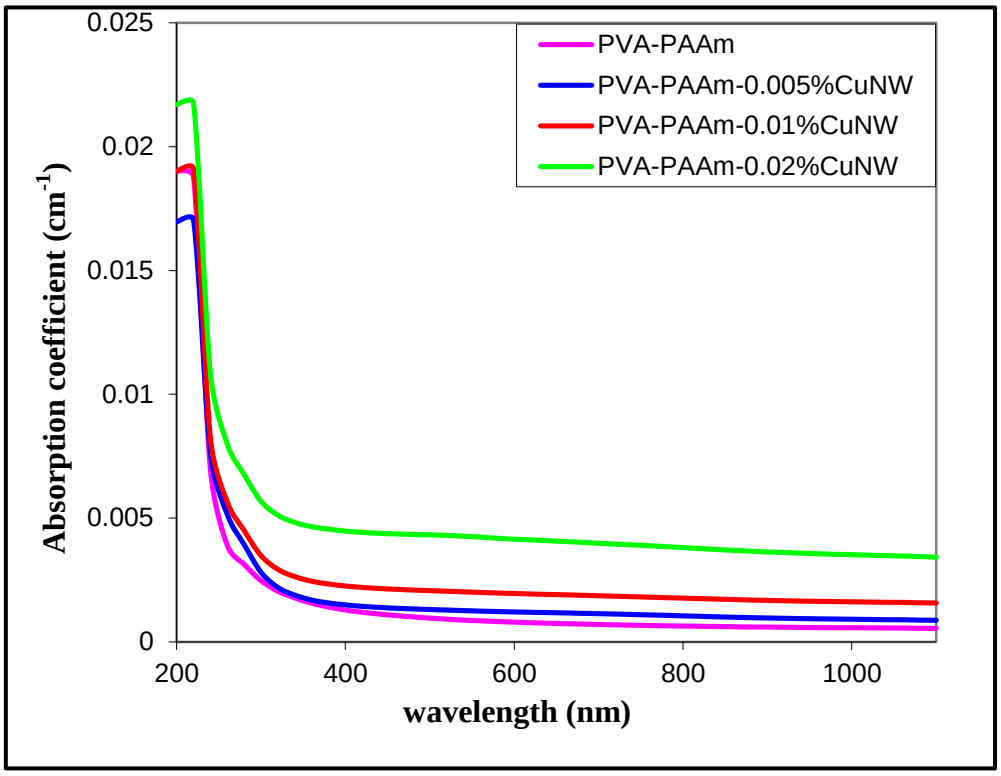


**Figure (4. 21): The absorption coefficient spectra as a function of with wavelength of PVA-PAAm Blend and PVA-PAAm:CuNW Nanocomposites with thickness of 120 µm.**

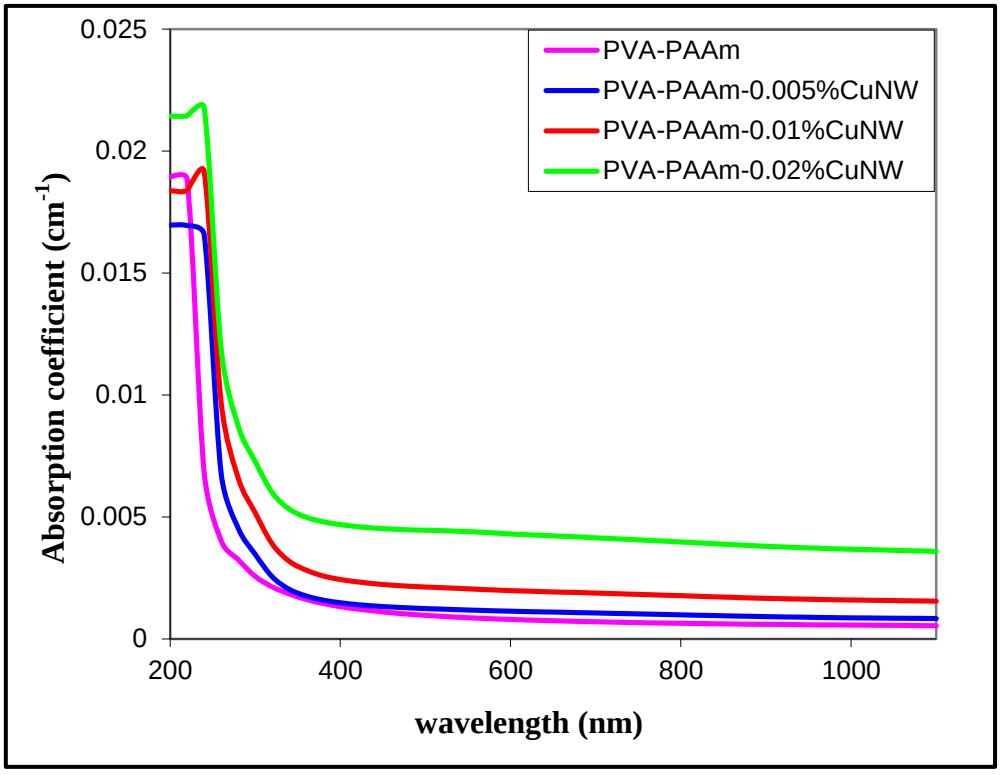


**Figure (4. 22): The absorption coefficient spectra as a function of with wavelength of PVA-PAAm Blend and PVA PAAm:CuNW Nanocomposites with thickness of 90 µm.**

### 4.3.8 Optical energy gaps of the allowed indirect transition

Both the allowed and forbidden indirect transition band energy gap have been calculated using equation (2.22). When the value of r =2, the allowed indirect transition band gap was calculated, but when the value of r=3, the forbidden indirect transition band gap was calculated. Figures (4.23 and 4.24) with two different thicknesses show the relation between absorption edge $(\alpha h\upsilon)^{1/2}$ of PVA-PAAm:CuNW nanocomposites as a function of photon energy on drawing straight line from the upper part of the curve toward the (x) axis at the value $(\alpha h\upsilon)^{1/2}=0$ we get the energy gap for the allowed indirect transition [105].

The obtained values are shown in tables (4.1). It can see that the values of energy gap decrease with the increasing of the weight percentages of CuNW . This attributed to the creation of site levels in the forbidden energy gap, the transition in this case was conducted in two stages that involve the transition of electron from the valence band to the local levels to the conduction band as a result of increasing the CuNW weight percentage. This behavior was attributed to the fact that nanocomposites were of heterogeneous type (i.e. the electronic conduction depends on added materials), the increase of the CuNW provides electronic paths in the polymer which facilitates the crossing of electron from the valance band to the conduction band, which explains the decrease of energy gap with the increase of the CuNW. When it compare the energy gap of the two thicknesses (120, 90) µm, it can seen that the films with thickness 120 µm has a slightly less the energy gap than films with thickness 90 µm. The results agree with the results of the previous researchers [50, 106].

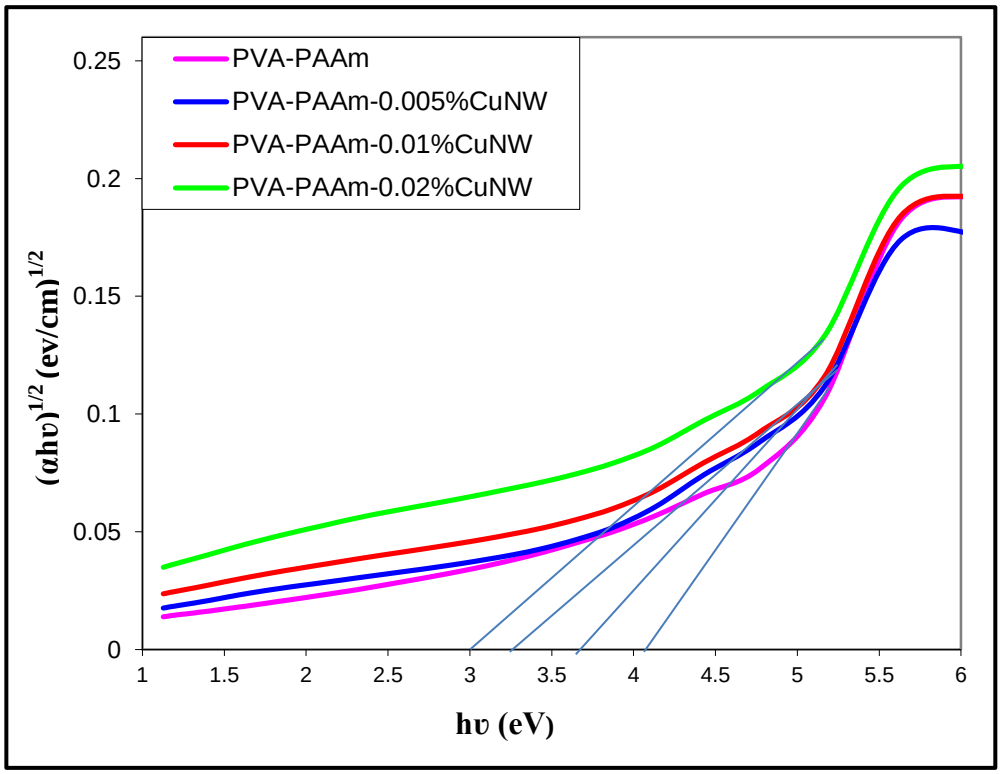


**Figure (4.23): A plots of $(\alpha h\upsilon)^{1/2}$ versus photon energy ($h\upsilon$) of PVA-PAAm:CuNW Nanocomposites respectively with thickness of 120 µm.**

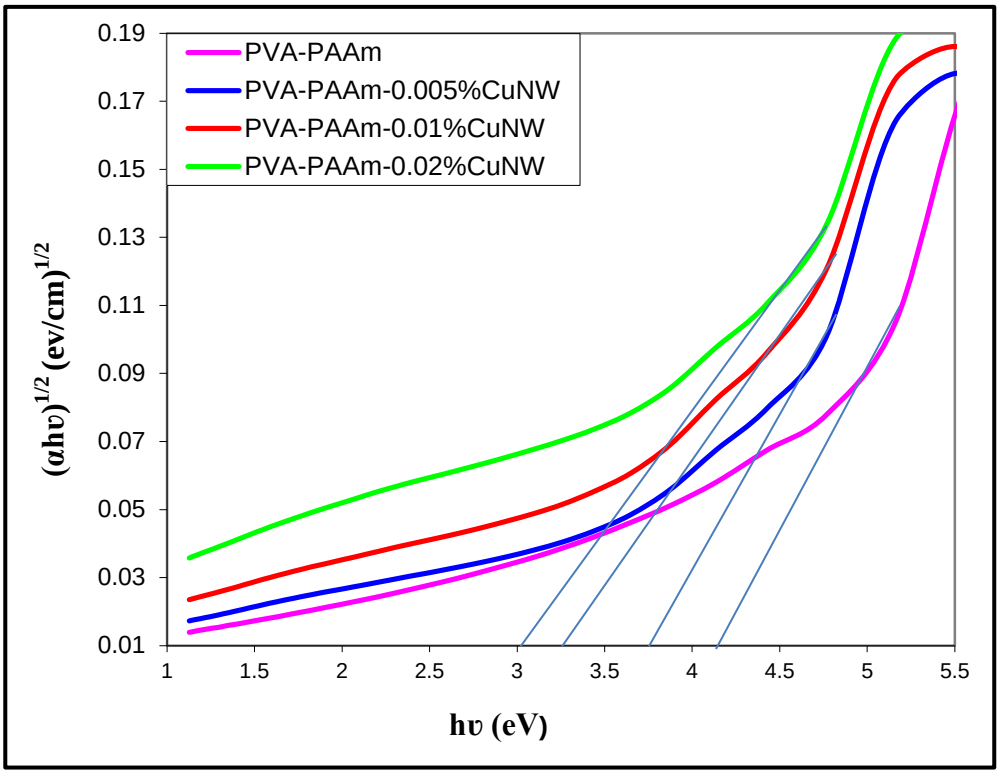


**Figure (4.24): A plots of $(\alpha h\upsilon)^{1/2}$ versus photon energy ($h\upsilon$) of PVA-PAAm:CuNW Nanocomposites respectively with thickness of 90 µm.**

**Table (4.1): The values of energy gap of the allowed indirect transition of PVA-PAAm:CuNW Nanocomposites with thickness of 120, 90 µm.**

| Samples | Allowed indirect transition (eV) | |
|---|---|---|
| | thickness of 120 µm | thickness of 90 µm. |
| PVA-PAAm | 4.10 | 4.12 |
| PVA-PAAm-0.5%CuNW | 3.70 | 3.75 |
| PVA-PAAm-1.0%CuNW | 3.25 | 3.27 |
| PVA-PAAm-2.0%CuNW | 3.00 | 3.00 |

## 4.4 Dispersion Parameters

Dispersion parameters were studied and diagnosed using Wemple DiDomenico model with two different thicknesses. The quantities of $E_o$, $E_d$, $E_g$, $n_o$, $\varepsilon_\infty$, $M_{-1}$, $M_{-3}$ were calculated from the equations (2.23 - 2.27). From drawing the graphic relationship between $(n^2-1)^{-1}$ and $(h\upsilon)^2$ as shown in figures (4.25 and 4.26). The calculated values were listed in Table (4.2 and 4.3) showing a decrease in their values with the increasing of CuNW concentrations at films with a thickness of 120 µm. At films with a thickness of 90 µm, it can seen that as CuNW increases, $E_o$ and $E_g$ decrease, while the other parameters increase. The value of the energy gap with the thicknesses (120, 90) µm estimated by Wemple–DiDomenico was comparable with the value of the optical energy gap obtained from Tauc relation. The results agree with the results of the previous researchers [49].

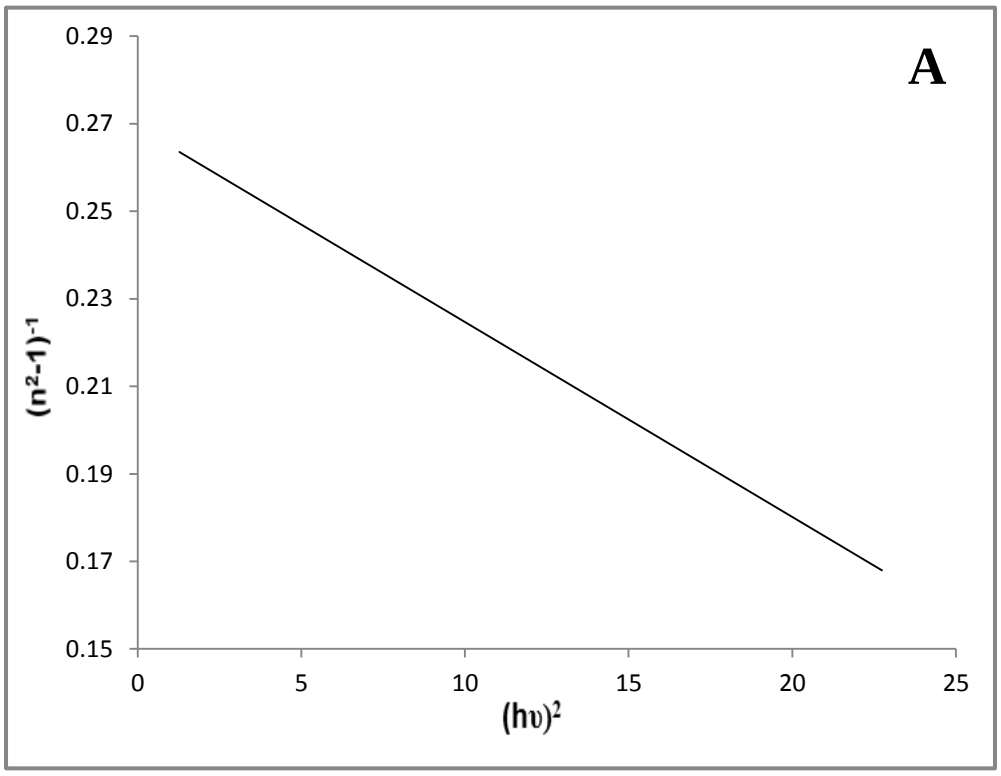
A
0.29
0.27
0.25
0.23
0.21
0.19
0.17
0.15
$(n^2-1)^{-1}$
0
5
10
15
20
25
$(h\upsilon)^2$

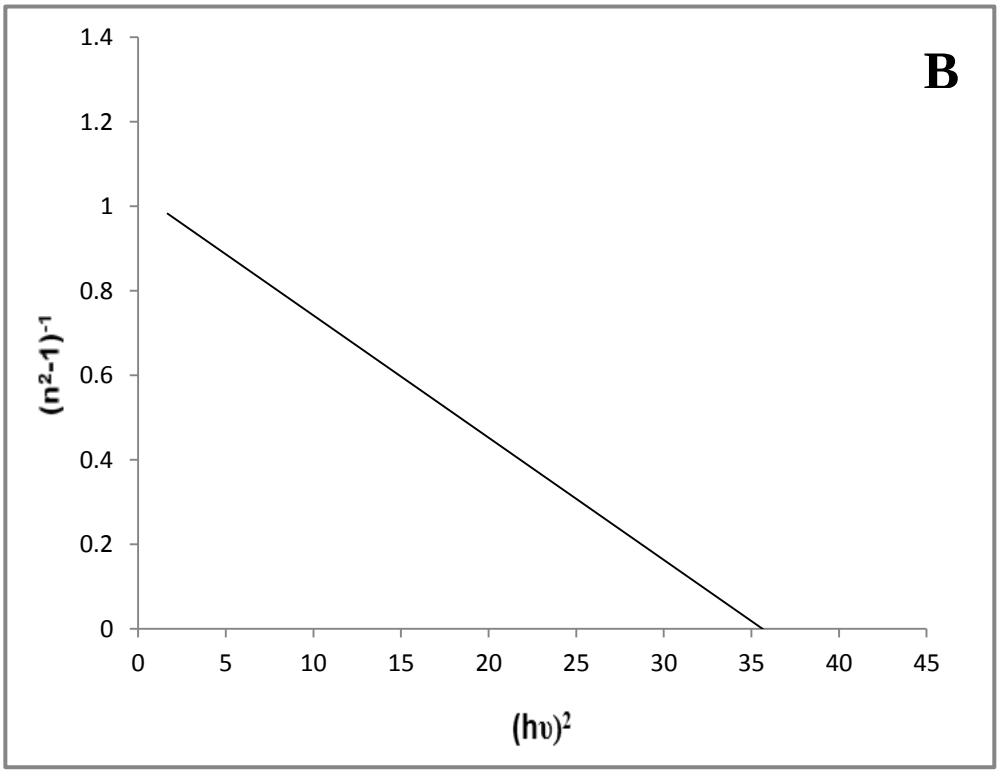
B
1.4
1.2
1
0.8
0.6
0.4
0.2
0
$(n^2-1)^{-1}$
0
5
10
15
20
25
30
35
40
45
$(h\upsilon)^2$

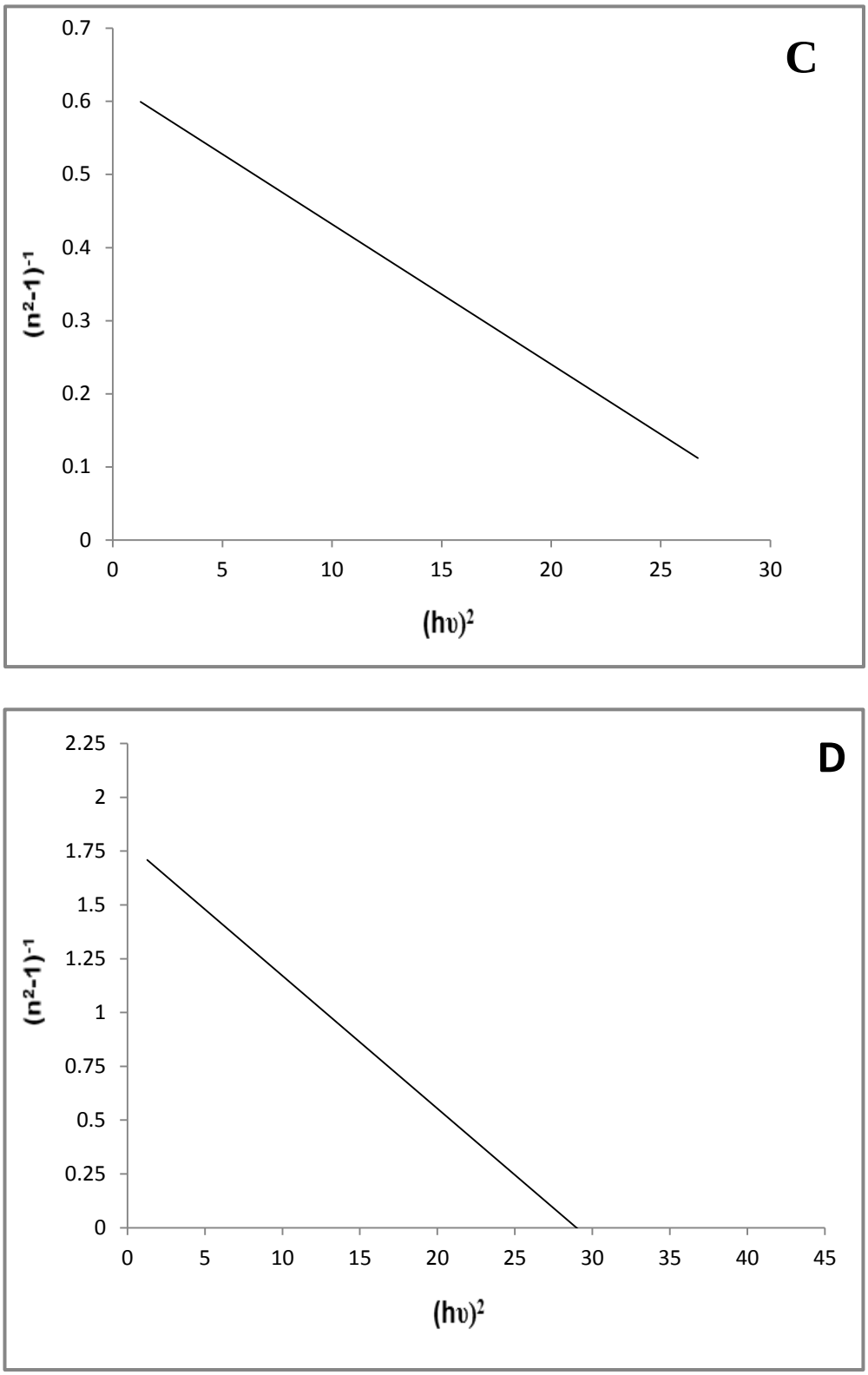


**Figure(4.25): Plot of $(n^2 -1)^{-1}$ vs $(h\upsilon)^2$ of PVA-PAAm with various content of CuNW: (A) 0 wt.% (B) 0.5 wt.% (C) 1 wt.% and (D) 2 wt.% with thickness of 120 µm.**

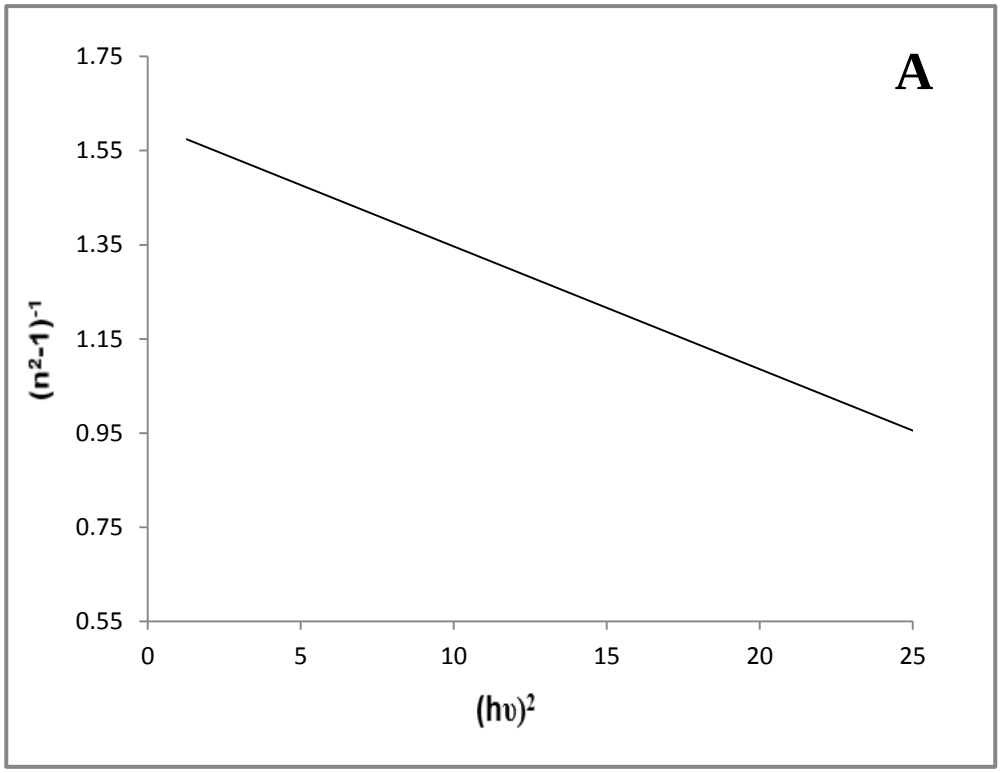
A
1.75
1.55
1.35
1.15
0.95
0.75
0.55
$(n^2-1)^{-1}$
0
5
10
15
20
25
$(h\upsilon)^2$

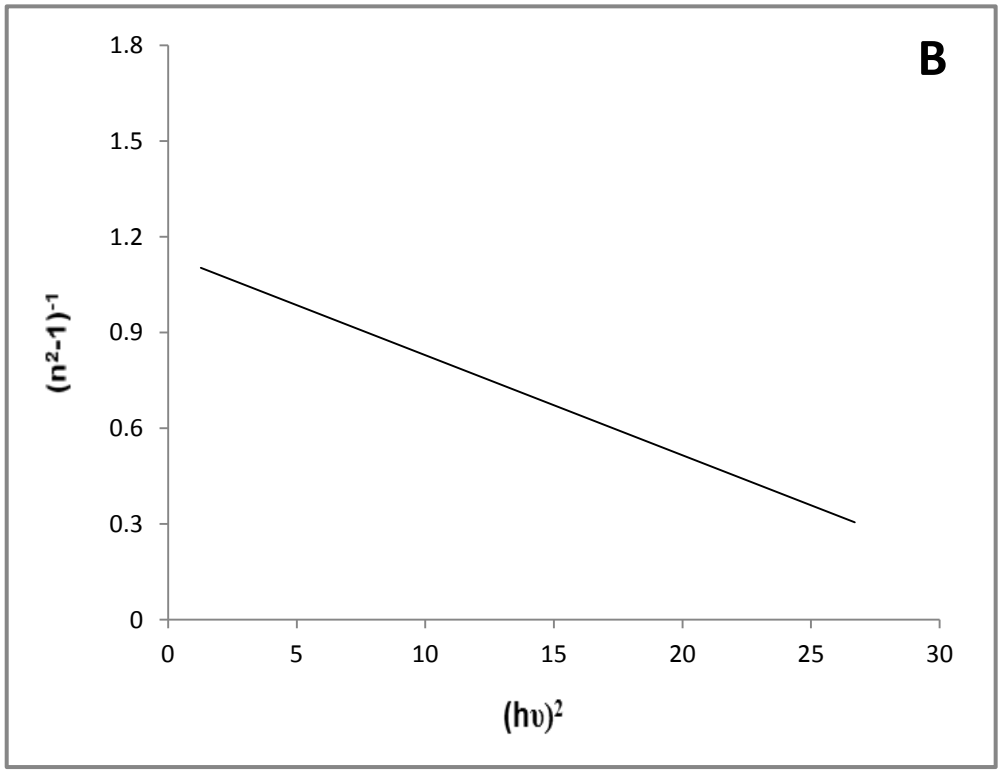
B
1.8
1.5
1.2
0.9
0.6
0.3
0
$(n^2-1)^{-1}$
0
5
10
15
20
25
30
$(h\upsilon)^2$

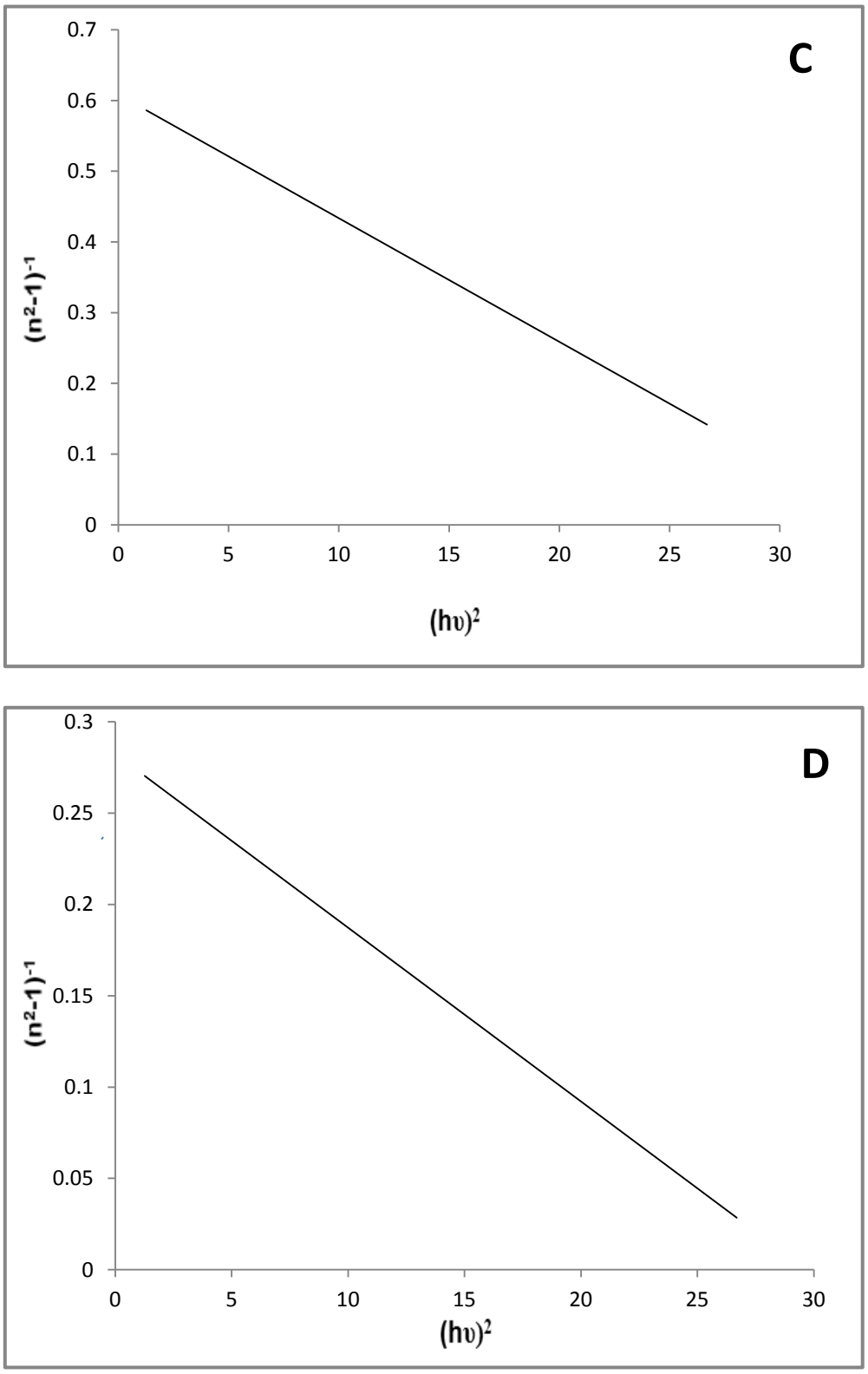


**Figure(4.26): Plot of $(n^2 -1)^{-1}$ vs $(h\upsilon)^2$ of PVA-PAAm with various content of CuNW: (A) 0 wt.% (B) 0.5 wt.% (C) 1 wt.% and (D) 2 wt.% with thickness of 90 µm.**

**Table(4.2): Dispersion parameters of PVA-PAAm:CuNW Nanocomposites with thickness of 120 µm.**

| parameter | PVA-PAAm | | | |
|---|---|---|---|---|
| | 0.0 wt.% CuNW | 0.5 wt.% CuNW | 1.0 wt.% CuNW | 2.0 wt.% CuNW |
| $E_o$ | 7.88 | 5.94 | 5.78 | 5.24 |
| $E_d$ | 29.18 | 5.94 | 9.25 | 2.99 |
| $E_g$ | 3.94 | 2.97 | 2.89 | 2.62 |
| $n^2(0)$ | 4.70 | 2.00 | 2.60 | 1.57 |
| $n_o(0)$ | 2.17 | 1.41 | 1.61 | 1.25 |
| $\varepsilon_\infty$ | 4.70 | 2.00 | 2.60 | 1.57 |
| $M_{-1}$ | 3.70 | 1.00 | 1.60 | 0.57 |
| $M_{-3}$ | 0.06 | 0.03 | 0.04 | 0.02 |

**Table(4.3): Dispersion parameters of PVA-PAAm:CuNW Nanocomposites with thickness of 90 µm.**

| parameter | PVA-PAAm | | | |
|---|---|---|---|---|
| | 0.0 wt.% CuNW | 0.5 wt.% CuNW | 1.0 wt.% CuNW | 2.0 wt.% CuNW |
| $E_o$ | 7.91 | 5.96 | 5.80 | 5.50 |
| $E_d$ | 4.85 | 5.18 | 9.51 | 19.66 |
| $E_g$ | 3.95 | 2.98 | 2.90 | 2.57 |
| $n^2(0)$ | 1.61 | 1.86 | 2.63 | 4.57 |
| $n_o(0)$ | 1.27 | 1.36 | 1.62 | 2.13 |
| $\varepsilon_\infty$ | 1.61 | 1.86 | 2.63 | 4.57 |
| $M_{-1}$ | 0.61 | 0.86 | 1.63 | 3.57 |
| $M_{-3}$ | 0.009 | 0.02 | 0.04 | 0.01 |

# Chapter five

## Conclusions and Future Works

## 5.1 Conclusions

The summarized results from this work are the following:

1. It was found through the study that the PVA-PAAm:CuNW nanocomposites appears a continuous change in its physical properties (morphology and structural, optical, and dispersion parameters) as a result of the CuNW additive.
2. The used method successfully fabricated new nanocomposites with homogeneous and fine dispersion as presented by an optical microscope. When comparing the two thicknesses (120, 90) µm, it can be found that the films with a thickness of 120 µm have more distribution and fewer aggregates than films with a thickness of 90 µm.
3. Scanning electron microscopy was used to investigate the surface morphology of samples and the dispersion of CuNW in the polymers matrix. The films exhibit uniform morphology revealing a rather soft surface. It concludes that increasing the ratio of CuNW in a polymer matrix for the PVA-PAAm:CuNW nanocomposites led to changes in the morphology of the surface and increase the roughness. When comparing the two thicknesses (120, 90) µm, it can seen that the surface roughness decreases with the increase of the film thickness.
4. Fourier transform infrared spectroscopy showed a shift in some bands and change in the intensities of other bands compared to the PVA-PAAm blend film. The decrease in transmittance can also be observed with an increase in the proportion of CuNW. When comparing the two thicknesses (120, 90) µm, the results showed that the change in film thickness had a slight effect.

5. The absorbance, absorption coefficient, refractive index, extinction coefficient, optical conductivity, and dielectric constant (real, imaginary) of PVA-PAAm:CuNW nanocomposites increases with the increase of the concentrations of CuNW, while the transmittance decreased.
6. The energy gap of indirect transition (allowed) of PVA-PAAm:CuNW nanocomposites decreases with the increase of the concentrations of CuNW, which decreased from 4.10 eV to 3.00 eV with thickness of 120 μm and from 4.12 eV to 3.00 eV with thickness of 90 μm, make these films appropriate for solar cell applications. When comparing the two thicknesses (120 and 90) μm the change in films thickness had a slight effect on the optical properties.
7. From the Wemple–DiDomenico model, the dispersion parameters were determined and found that the parameters were decreased with the increase of CuNW content at films with a thickness of 120 μm. At the films with a thickness of 90 μm, it can seen that as CuNW increases, $E_o$ and $E_g$ decrease, while the other parameters increases. The value of the energy gap with the thicknesses 120 and 90 μm obtained from Wemple–DiDomenico was comparable with the value of the optical energy gap obtained from Tauc relation, the films appropriate optical communications and in the design of optical devices.
8. The results showed that the change of films thickness had a slight effect on the structural and optical properties.

## 5.2 Future Works

1. Studying the thermal and mechanical properties of PVA-PAAm: CuNW nanocomposites.

2. Studying the effect of radiation on some physical properties of PVA-PAAm:CuNW nanocomposites.

3.Studying the electrical properties of PVA-PAAm:CuNW nanocomposites.

4. Studying of pressure and humidity sensors applications of the PVA-PAAm:CuNW nanocomposites.

# *References*

## Refrences

[1] A. P. Mouritz and A. G. Gibson, “Fire Properties of Polymer Composite Materials”, Solid Mechanics and Its Applications, Vol. 143, pp.1-18, (2007).

[2] P. U. Asogwa, “Effect of deposition medium on the optical and solid state properties of annealed MnO2 thin films”, J. of optoelectronics and biomedical materials, Vol. 2, pp.109-117, (2010).

[3] J. E. Mark, “Physical properties of polymers handbook”, Springe, Vol. 107, p.825, (2007).

[4] S. Logothetidis, “Nanostructured Materials and Their Applications”, NanoScience and Technology, pp.1-23, (2012).

[5] M. Köhler and W. Fritzsche, “Nanotechnology an Introduction to Nano structuring Techniques”, 2nd Ed, Completely Revised, (2008).

[6] A. T. Bell, “The Impact of Nanoscience on Heterogeneous Catalysis”, Sci., Vol. 299, No. 5613, pp.1688-1691, (2003).

[7] K. A. Shenoy, “Effects Of Multi-Wall Carbon Nanotubes On The Mechanical Properties Of Polymeric Nanocomposites”, M.Sc. Thesis, Department of Mechanical Engineering and the Faculty of the Graduate School of Wichita State University, (2008).

[8] S. Mustafa, “Engineering Chemistry”, Library of Arab society for pub. and dis, Jordan, (2008).

[9] A. C. Long and M. J. Clifford, “Composite forming mechanisms and materials characterization”, Composites forming technologies, pp.1-21, (2007).

[10] A. Muheisin, “Study of electrical conductivity for amorphous and semi crystalline polymers filled with Lithium Fluoride Additive”, M. Sc. Thesis, University of Mustansiriah, College of Science, (2009).

[11] J. M. Schultz, “Polymer materials science”, Prentice Hall, (1974).

[12] R. Klein, “Laser Welding of Plastics”, materials, processes and industrial applications, John Wiley and Sons, (2012).

[13] S. Amin and M. Amin, “Thermoplastic Elastomeric (Tpe) Materials and Their Use in Outdoor Electrical Insulation”, Rev. Adv. Mater. Sci.,Vol. 29, pp.15-30, (2011).

[14] J. M. G. Cowie, “Polymers: Chemistry and Physics of Modern Materials”, Glasgow, (2007).

[15] J. J. Scobbo and L. A. Goettler, “Applications of polymer alloys and blends”, Kluwer Academic Publishers , (2003).

[16] C. Uzunpinar, “Effect of Dispersion of Swcntson the Viscoelastic and Final Properties of Epoxy Based Nanocomposites”, M. Sc. Thesis, Graduate Faculty of Auburn University, (2010).

[17] J. Robertson, “Realistic applications of CNTs”, Materials Today,Vol. 7, No.10, pp. 46-52, (2004).

[18] L. Bokobza, “Multiwall carbon nanotube elastomeric composites: a review”, Polymer, Vol. 48, No.17, pp. 4907-4920, (2007).

[19] C. Demerlis and D. Schoneker, “Review of the oral toxicity of polyvinyl alcohol (PVA) - PDF Free Download”, Food Chem. Toxicol, Vol. 41, No. 3, pp. 319–326, (2003).

[20] C. Ravindra, M. Sarswati, G. Sukanya, P. Shivalila, Y. Soumya, and K. Deepak, "Tensile and thermal properties of poly (vinyl) pyrrolidone/vanillin incorporated polyvinyl alcohol films", Res. J. Phys. Sci., Vol. 3, No. 8, pp. 1–6, (2015).

[21] k. Choo, Y. C. Ching, C. H. Chuah, S. Julai, and N. S. Liou, "Preparation and characterization of polyvinyl alcohol-chitosan composite films reinforced with cellulose nanofiber", Materials, Vol. 9, No. 8, p.644. (2016).

[22] I. Sakurada, "Polyvinyl Alcohol Fibers", Taylor & Francis, of International Fiber Science and Technology, Vol. 6, p. 472, (1985).

[23] H. F. Mark, J. I. Kroschwitz, N. M. Bikales, C. G. Overberger and G. Menges, "Encyclopedia of polymer science and engineering", John Wiley & Sons, Chichester, p.841, (1985).

[24] S. S. Chiad, S. F. Oboudi, K. H. Abass, and N. F. Habubi,"Characterization of Silver/Polyvinyl Alcohol (Ag/PVA) Films prepared by Casting Technique", Iraqi J. of Polymers, Vol. 16, No. 2, pp.10-18, (2012).

[25] H. S. Mansur, C. M. Sadahira, A. N. Souza, and A. A. Mansur, "FTIR spectroscopy characterization of poly (vinyl alcohol) hydrogel with different hydrolysis degree and chemically crosslinked with glutaraldehyde", Materials Science and Engineering: C, Vol. 28, No. 4, pp.539-548, (2008).

[26] A. Gautam and S. Ram, "Preparation and thermomechanical properties of Ag-PVA nanocomposite films", Mater. Chem. Phys., vol. 119, No. 1–2, pp. 266–271 , (2010).

[27] P. K. Verma, P. S. Sardar, S. Ghosh, and M. Biswas, “Conducting Nanocomposites of Polyacrylamide With Acetylene Black and Polyaniline”, Polymer Composites, Vol. 30, No. 4, pp. 490-496 (2009).

[28] H. V. Boenig, “Polyolefins: structure and properties” Elsevier Publishing Company, (1966).

[29] M. E. Zeynali, A. Rabii, and H. Baharvand, “Synthesis of Partially Hydrolyzed Polyacrylamide and Investigation of Solution Properties (Viscosity Behaviour)”, Iranian Polymer Journal,Vol.13, No. 6, pp.479-484, (2004).

[30] H. Dweik, W. Sultan, M. Sowwan, and S. Makharza, “Analysis characterization and some properties of polyacrylamide copper complexes”, International Journal of Polymeric Materials, Vol. 57, No. 3, pp.228-244, (2008).

[31] E. S. Hassan and S. K. Hassun, “The effects of the x-rays by different doses on some physical properties of polyacrylamide (PAAm)”, M.Sc. Thesis, Al-Mustansiriyah University, Iraq , (2007).

[32] R. D. Lentz, “Polyacrylamide and biopolymer effects on flocculation, aggregate stability, and water seepage in a silt loam”, Geoderma, Vol. 241, pp.289-294, (2015).

[33] S. Jewell, S. Kimball, “Mineral Commodity Summaries”, US Geological Survey: Reston, VA, USA, (2014).

[34] V. B. Nam and D. Lee, “Copper nanowires and their applications for flexible, transparent conducting films: a review”, Nanomaterials,Vol. 6, No. 3, p. 47, (2016).

[35] J. C. Yu, F. G. Zhao, W. Shao, C. W. Ge, and W. S. Li, “Shape-controllable and versatile synthesis of copper nanocrystals with amino acids as capping agents”, Nanoscale, Vol. 7, No. 19, pp.8811-8818, (2015).

[36] L. Xu, Y. Yang, Z. W. Hu, and S. H. Yu, “Comparison study on the stability of copper nanowires and their oxidation kinetics in gas and liquid”, ACS nano, Vol. 10, No. 3, pp.3823-3834, (2016).

[37] B. K. Park, S. Jeong, D. Kim, J. Moon, S. Lim and J. S. Kim, “Synthesis and size control of monodisperse copper nanoparticles by polyol method”, Journal of colloid and interface science, Vol. 311, No. 2, pp.417-424, (2007).

[38] J. W. Lee, J. Han, D. S. Lee, S. Bae, S. H. Lee, S. K. Lee, B. J. Moon, C. J. Choi, G. Wang and T. W. Kim, “2D Single-Crystalline Copper Nanoplates as a Conductive Filler for Electronic Ink Applications”, Small, Vol. 14, No. 8, p.1703312, (2018).

[39] Z. Liu and Y. Bando, “behaviour of copper nanorods”, Chemical physics letters, Vol. 378, pp.85–88, (2003).

[40] Y. Zhan, Y. Lu, C. Peng and J. Lou, “ Solvothermal synthesis and mechanical characterization of single crystalline copper nanorings”, Journal of crystal growth, Vol. 325, No. 1, pp.76–80, (2011).

[41] F. Cui, Y. Yu, L. T. Dou, J. W. Sun, Q. Yang, C. Schildknecht, K. Schierle-Arndt, P.D Yang, “Synthesis of ultrathin copper nanowires using tris(trimethylsilyl)silane for high-performance and low-haze transparent conductors”, Nano Lett, Vol. 15, No. 11, pp.7610–7615, (2015).

[42] S. Han, S. Hong, J. Ham, J. Yeo, J. Lee, , B. Kang, P. Lee, J. Kwon, S. S. Lee, M.Y. Yang, "Fast plasmonic laser nanowelding for a Cu-nanowire percolation network for flexible transparent conductors and stretchable electronics", Adv. Mater, Vol. 26, No. 33, pp.5808–5814, (2014).

[43] Y. L. Luo, L. L. Chen, F. Xu, and Q. S. Feng, "Fabrication and characterization of copper nanoparticles in PVA/PAAm IPNs and swelling of the resulting nanocomposites", Metals and Materials International, Vol. 18, No. 5, pp.899-908, (2012).

[44] A. Hashim, M. Husaien, J. H. Ghazi, and H. Hakim, "Characterization of (polyvinyl alcohol–polyacrylamide–pomegranate peel) composite so as biocomposites materials", Universal Journal of Physics and Application, Vol. 1, No. 3, pp.242-244, (2013).

[45] M. A. Habeeb, H. M. Mohssen, and R. G. Kadhim, "Effect of (CoO) Nanoparticles on Someoptical Properties of (PVA-PAAm) Composite", International Journal of Engineering Research, Vol. 3, No. 5, (2014).

[46] M. A. Habeeb, "Enhancement of Structural and Mechanical Properties for (PVA-PAAm) By Adding Titanium Nanoparticles", Australian Journal of Basic and Applied Sciences, Vol. 8, No. 17, pp.1-9, (2014).

[47] M. M. El-Toony, "Casting of Acrylamide/Poly (vinyl alcohol) Reinforced by Carbon Nano-Wire for Using into Proton Exchange Membrane Fuel Cell", Egyptian Journal of Chemistry, Vol. 60, No. 5, pp.779-791, (2017).

[48] X. Ren, Q. Zeng, J. Xu, W. Zhang, L. Xue, and K. Li, "The antifouling performance of biomimetic fish slime-like PVA/PAAm hydrogels modified coating in marine", Easy Chair, (2018).

[49] N. F. Habubi, K. H. Abass, C. S. Sami, D. M. Latif, J. N. Nidhal, and A. I. Al Baidhany, "Dispersion Parameters of Polyvinyl Alcohol Films doped with Fe", In Journal of Physics: Conference Series Vol. 1003, No. 1, p. 012094, (2018).

[50] S. M. A. Asadi, F. J. Hamood, K. H Abass, S. K. Mohammed, I. M. Hassan, and D. Latif, "The Effect of MGO Nanoparticles on Structure and optical Properties of PVA-PAAm Blend", Research Journal of Pharmacy and Technology, Vol. 12, No. 6, pp.2768-2771, (2019).

[51] S. El-Gamal and A. M. El Sayed, "Physical properties of the organic polymeric blend (PVA/PAM) modified with MgO nanofillers", Journal of Composite Materials, Vol. 53, No. 20, pp.2831-2847, (2019).

[52] H. M. Ragab and A. Rajeh, "Structural, thermal, optical and conductive properties of PAM/PVA polymer composite doped with Ag nanoparticles for electrochemical application", J. Mater. Sci. Mater. Electron, Vol. 31, No. 19, pp.16780–16792, (2020).

[53] O. K. Abdali and K. H Abass, "Effect of Silver Nano-Particles on Structural, Optical and Electrical Properties of Casted ( Polyvinyl alcohol / Polyacrylamide / Polyethylene oxide ) Composites for Antibacterial Applications", (2021).

[54] A. K. Al-Shammari and E. Al-Bermany, "New Fabricated (PAA-PVA/GO) and (PAAm-PVA/GO) Nanocomposites: Functional Groups and Graphene Nanosheets effect on the Morphology and Mechanical Properties", In Journal of Physics: Conference Series, Vol. 1973, No. 1, p. 012165, (2021).

[55] A. Telser, "Fundamentals of Light Microscopy and Electronic Imaging", Shock, Vol. 17, No. 5, p. 442, (2002).

[56] B. Jörgen, “in Mechanics of Solid Polymers”, (2015).

[57] A. Khursheed, “Scanning electron microscope optics and spectrometers”, World scientific, (2011).

[58] M. Dambarudhar, “A Detailed study on optical and physical properties of rice and its by-products”, Diss. Tezpur University, (2017).

[59] F. T. Infrared and A. Ftir, “What is FTEM ?”, Aust. Orienteer, No. 172, pp. 28–29, (2013).

[60] L. R. Faulknerand, A. J, “Bard Electrochemical methods: fundamentals and applications”, John Wiley and Sons, (2002).

[61] T. Theophanides, “Introduction to infrared spectroscopy”, Infrared Spectroscopy-Materials Science, Engineering and Technology, pp.1-10, (2012).

[62] D. I. Bower, “An introduction to polymer physics”, (2003).

[63] A. Abdulmitalib, “Studying in Electric and Optical Properties of Polymers with Application on Non crystal Films from Poly acrylic acid”, M.Sc. Thesis, Collage of Sci, University of Bassrah, (1981).

[64] R. T. Kivaisi, “Optical properties of obliquely evaporated aluminium films”, Thin Solid Films, Vol. 97, No. 2, pp. 153–163, (1982).

[65] G. K. Raheem, S. H. Ahmed, “Study Of Optical Properties Of (PEO-PEG) Blends”, Journal University of Kerbala, Vol. 12, No. 2, pp.163-174, (2016).

[66] M. Stamm, “Introduction to Physical Polymer Science”, pp.787-78, (2006).

[67] R. Berglund, P. Graham and R. Miller, “Applications of In-situ FT-IR in Pharmaceutical Process R and D”, spectroscopy-Springfield then Eugene-, Vol. 8, pp.31-31,(1993).

[68] L. A. Prystaj, “effect of carbon filler characteristics on the electrical properties of conductive polymer composites possessing segregated network microstructures”, M. Sc.E. Thesis, Georgia Institute of Technology , (2008).

[69] C. Kittel, “Introduction to solid state physics”, 5th Ed, Willy, New York, (1981).

[70] F. Yakuphanoglu and H. Erten, “Refractive index dispersion and analysis of the optical constants of an ionomer thin film”, Optica applicata, Vol. 35, No. 4, pp. 969–976, (2005).

[71] H. A. Macleod, “Thin Film Optical Filter”, McGraw-Hill, New York. (2001).

[72] O. G. Abdullah, B. K. Aziz, and S. A. Hussen, “Optical Characterization of Polyvinyl alcohol - Ammonium Nitrate Polymer Electrolytes Films”, Journal of Chemistry and Materials Research, Vol. 3, No. 9, pp.84-90, (2013).

[73] A. V. Vannikov, V. K. Matveev, V. P. Sichkar, and A. P. Tiutnev, “Radiation effects in polymers, Electrical properties,” Moscow Izd. Nauk, (1982).

[74] K. H. Abass and D. M. Latif. “The urbach energy and dispersion parameters dependence of substrate temperature of CdO thin films prepared by chemical spray pyrolysis”, International Journal of ChemTech Research, Vol. 9, No. 9, pp.332-338, (2016).

[75] J. I. Pankove, “Optical Process in Semiconductors”, Dover Publishing, Inc., New York, (1971).

[76] A. N. Donald, “Semiconductor physics and devices”, Irwin, University of New Mexico, USA, (1992).

[77] A. N. Alias, Z. M. Zabid, A. M. M. Ali, M. K. Harun, and M. Z. A. Yahya, "Optical Characterization and Properties of Polymeric Materials for Optoelectronic and Photonic Applications," Int. J. Appl. Sci. Technol., Vol. 3, No. 5, pp. 11–38, (2013).

[78] R. Naik, C. Kumar, R. Ganesan, and K. S. Sangunni, "Effect of Thickness on The Optical Properties Change in Bi / As 2S3 Bilayer Thin Films," Chem. Mater. Res., Vol. 6, No. 2, pp. 1–2, (2014).

[79] V. N. Suryawanshi, A. S. Varpe, M. D. Deshpande, "Band gap engineering in PbO nanostructured thin films by Mn doping", Thin Solid Films, Vol. 645, pp. 87-92. (2018).

[80] C. Mwolfe, N. Holouyak, and G. B. Stillman, "Physical Properties of Semiconductor", prentice Hall, New York, (1989).

[81] Y. N. Al-Jamal, "Solid State Physics", Al-Mosel University, (2nd Ed.), Arabic Version, (2000).

[82] T. Numai, "Fundamentals of semiconductor lasers: Second edition" , Springer Ser. Opt. Sci, Vol. 93, No.28 Augst, pp.55147, (2015).

[83] J. Pankove and D. Kiewit, "Optical Processes in Semiconductors", J. Electrochem. Soc, Vol. 119, No. 5, pp.156C, (1972).

[84] W. A Morais, B. D. Barros, I. M. Cavalcanti. F. H. Xavier N. S. Santos-Magalhães, and M. A. M. Maciel. "Coencapsulation of trans-Dehydrocrotonin and trans-Dehydrocrotonin: hydroxypropyl-β-cyclodextrin into Microparticles", Journal of the Brazilian Chemical Society, Vol. 28, pp.1494-1505, (2017).

[85] A. A. K. Zbala, A. O. M. Al-Ogaili, K. H. Abass, "Optical Properties and Dispersion Parameters of PAAm-PEG Polymer Blend Doped with Antimony (III) Oxide Nanoparticles", NeuroQuantology, Vol. 20, No.2, pp. 62-69. (2022).

[86] S. H. Wemple, "Refractive-Index Behavior of Amorphous Semiconductors and Glasses", Physical Review Journals B, Vol. 7, No. 8, p.3767, (1973).

[87] A. S. Hassanien and A. A. Akl, "Influence of Composition on Optical and Dispersion Parameters of Thermally Evaporated Non-Crystalline Cd50S50− xSex Thin Films", Journal of Alloys and Compounds, Vol. 648, pp.280-290, (2015).

[88] F. A. Jenkins, H. E. White,. "Fundamentals of Optics", Indian Journal of Physics, Vol. 25, pp. 265-266, (1957).

[89] F. S. Ahmed, N. Y. Ahmed, R. S. Ali, N. F Habubi, K. H. Abass, S. S, "Chiad Effects of substrate type on some optical and dispersion properties of sprayed CdO thin films, NeuroQuantology", Vol. 18, No. 3, pp. 56-65, (2020).

[90] F. Y. akuphanoglua, A. Cukurovalib, and I. Yilmazb, "Physica", B, Vol. 351, p.53, (2004).

[91] H. A. Khalid and H. H. Ana , "Reduction of Energy Gap in $ZrO_2$ Nanoparticles on Structural and Optical Properties of Casted PVA–PAAm Blend", Journal of Green Engineering. Vol.10, No.7, pp. 4166–4176, (2020).

[92] W. Hadi, "Effect of (TiC) Nanoparticles on Structural, Optical and Electrical Properties of (PVA-PAAm) Blends and their Applications" , M.Sc. thesis, Babylon University College of Education for Pure Sciences, (2017).

[93] Y. M. Yue, K. Xu, X. G. Liu, Q. Chen, X. Sheng, and P. X. Wang. "Preparation and characterization of interpenetration polymer network films based on poly (vinyl alcohol) and poly (acrylic acid) for drug delivery", Journal of applied polymer science, Vol. 108, No. 6, pp.3836-3842, (2008).

[94] A. Manjunath, T. Deepa, N. K. Supreetha, and M. Irfan, "Studies on AC Electrical Conductivity and Dielectric Properties of PVA/$NH_4NO_3$ Solid Polymer Electrolyte Films", Advances in Materials Physics and Chemistry, Vol. 5, pp.295-301, (2015).

[95] K. Abdali, "Structural, Morphological, and Gamma Ray Shielding (GRS) Characterization of HVCMC/PVP/PEG Polymer Blend Encapsulated with Silicon Dioxide Nanoparticles", Silicon, pp.1-6, (2022).

[96] K. Deshmukh, J. Ahmad, MB. Hägg. "Fabrication and characterization of polymer blends consisting of cationic polyallylamine and anionic polyvinyl alcohol", Ionics, Vol. 20, No. 7, pp.957–967, (2014).

[97] R. G .Kadhim, "Study of Some Optical Properties of Polystyrene-Copper Nanocomposite Films", World Scientific News, Vol. 30, p.14-25, (2016).

[98] M. Dahshan, "Introduction to Material Science and engineering", 2nd, McGraw Hill, New York, (2002).

[99] H. Hakim, N. Al- Garah and A . Hashim, "The Effect of Aluminum Oxide Nanoparticles on Optical Properties of (Polyvinyl alcohol-Polyethylene glycol) Blend", Journal of Industrial Engineering Research, Vol. 1, pp.94-98, (2015).

[100] K. Khurana, A. K. Patel and K. Das, "Refractive Indices Studies on PVA and PVP Blends", International Journal for Scientific Research & Development, Vol. 4, pp.984-985, (2016).

[101] O. Gh. Abdullah, "Influence of Barium Salt on Optical Behavior of PVA Based Solid Polymer Electrolytes", European Scientific Journal, Vol.10, No.33, (2014).

[102] J. J. Mathen, G. P. Joseph, J. Madhavan, "Improving the optical and dielectric properties of PVA matrix with nano-ZnSe: Synthesis and Characterization", International Journal of Engineering Development and Research, Vol. 4, No.3, pp.1088-1092, (2016).

[103] H. N. Najeeb, "Study of Some Electrical and Optical Properties for Thin Films Prepared from Polymeric Composites", M.Sc. thesis ,College of sciences, University of Babylon , (2011).

[104] G. A. AL-Dahash, H. N. Najeeb, A. Baqer, and R. Tiama, "The Effect of Bismuth Oxide Bi2O3 on Some Optical Properties of Poly vinyl Alcohol", British Journal of Science, Vol. 4, pp.117-124, (2012).

[105] K. H. Abass, A. Adil, and M. K. Mohammed, "Fabrication and Enhancement of SnS: Ag/Si Solar Cell Via Thermal Evaporation Technique", Journal of Engineering and Applied Sciences, Vol. 13, No. 4, pp.919-925, (2018).

[106] E. H. Hadi, D. A. Sabur, S. S. Chiad, and N. Fadhil, "Physical Properties of Nanostructured Li-Doped ZrO2 Thin Films", Journal of Green Engineering, Vol. 10, pp.8390-8400, (2020).

# الخلاصة

تم تحضير المتراكبات النانوية PVA-PAAm:CuNW بطريقة صب المحلول في سماك مختلفة (120,90 ) مايكرومتر ونسب وزنية مختلفة ( 0.5, 1, 2) من CuNW عند درجة حرارة 70 درجة مئوية. تم دراسة الخصائص المورفولوجيا و التركيبية والبصرية وايضا معاملات التفريق للمتراكبات النانوية. صور المجهر الضوئي بينت توزيع جيد لذرات CuNW داخل المخاليط البوليمرية لجميع اغشية المركبات النانوية. أظهر المجهر الإلكتروني الماسح (SEM) شكلاً موحدًا يكشف عن سطح ناعم نوعًا ما ، وأدت زيادة نسبة CuNW في مصفوفة بوليمر للمركبات النانوية PVA-PAAm:CuNW إلى تغييرات في مورفولوجيا السطح وزيادة الخشونة . بينما أظهرت الخصائص الهيكلية للتحليل الطيفي (FTIR) تغيرًا في موضع الذروة بالإضافة إلى تغيير في الشكل والكثافة مقارنة بمزيج PVA-PAAm. نتائج الخواص البصرية للمتراكبات النانوية PVA-PAAm:CuNW بينت زيادة الامتصاصية، معامل الامتصاص، معامل الخمود، معامل الانكسار، الموصلية البصرية، ثوابت العزل الحقيقي والخيالي للخليط البوليمر بزيادة تركيز CuNW بينما النفاذية وفجوات الطاقة البصرية غير المباشرة المسموح بها تنخفض. المتراكبات النانوية جميعها تمتلك امتصاصية عالية في المنطقة فوق البنفسجية. معاملات التفريق مثل: $E_o$, $E_d$, $n_o$, $\varepsilon_\alpha$, $M_{-1}$, $M_{-3}$ تم حسابها باستخدام عمليات Wemple–DiDomenico.كانت قيمة فجوة الطاقة المقدرة بواسطة Wemple–DiDomenico متقاربة مع قيمة فجوة الطاقة البصرية التي تم الحصول عليها من علاقة Tauc.

تم دراسة تأثير تغير السماك واظهرت النتائج ان تغير السماك كان له تأثير قليل على الخواص التركيبية و البصريه المدروسة.

جمهورية العراق
وزارة التعليم العالي والبحث العلمي
جامعة بابل – كلية التربية للعلوم الصرفة
قسم الفيزياء


# تأثير أسلاك النحاس النانوية على الخصائص التركيبة والبصرية لخليط PVA-PAAm

رسالة مقدمة
إلى مجلس كلية التربية للعلوم الصرفة في جامعة بابل وهي جزء من متطلبات
نيل درجة الماجستير في التربية / الفيزياء

من قبل
**زينب محمد جواد جواد كاظم**
بكالوريوس تربية علوم ( فيزياء)
جامعة بابل 2014 م

بإشراف
**أ.د. خالد حنين عباس**

١٤٤٣هـ ٢٠٢٢ م